

# Role of Protein Phosphatase 2A inhibition in modulation of VE- cadherin and Claudin-5 in human brain microvascular endothelial cells and the potential reversal by small molecule activators of PP2A (SMAPs)

A Thesis Submitted to Trinity College Dublin,  
The University of Dublin

In the fulfilment of the requirement  
For the Degree of  
Master of Science  
2021

By

**Sylwia Konieczna, B.Sc**

**Supervisor: Prof Paul Spiers**

Department of Pharmacology and Therapeutics, School of Medicine  
Trinity College Dublin



Coláiste na Tríonóide, Baile Átha Cliath  
Trinity College Dublin

Ollscoil Átha Cliath | The University of Dublin



## Declaration

I declare that this thesis has not been submitted as an exercise for a degree at this or any other university and it is entirely my own work.

I agree to deposit this thesis in the University's open access institutional repository or allow the Library to do so on my behalf, subject to Irish Copyright Legislation and Trinity College Library conditions of use and acknowledgement.

I consent to the examiner retaining a copy of the thesis beyond the examining period, should they so wish (EU GDPR May 2018).



---

Sylwia Konieczna

## Acknowledgements

Firstly, I would like to express my sincere gratitude to my supervisor, Prof Paul Spiers, from whom I've received a great deal of support and assistance throughout this research project and during the writing of this thesis. Your expertise and immense knowledge were invaluable in composing the research questions of this study. I could not have hoped for a better or more patient mentor.

I would also like to thank Dr Pierce Kavanagh, Mr Ken Scott, Dr Ismail Elgenaidi and Dr Bashir Mohamed for their valuable guidance and insightful comments throughout my study. I would also like to acknowledge Dr Margaret Lucitt, Ms Teresa Mulroy and all the staff of the Department of Pharmacology and Therapeutics.

I would like to thank my lab partner, Manos Lioudakis, who provided stimulating discussions as well as a happy distraction.

Last but not least, I would like to thank my partner Tom and mum for their wise counsel and unfailing support throughout my years of study.

## Table of Contents

<b>1. INTRODUCTION.....</b>	<b>1</b>
1.1 BLOOD-BRAIN BARRIER PHYSIOLOGY .....	2
1.2. STRUCTURE AND FUNCTION OF THE BBB .....	3
1.2.1 <i>Endothelial Cells</i> .....	4
1.2.2. <i>Pericytes</i> .....	6
1.2.3. <i>Astrocytes</i> .....	7
1.2.4. <i>Microglia</i> .....	8
1.3. TIGHT & ADHERENS JUNCTIONS .....	9
1.3.1 <i>Tight Junctions</i> .....	10
1.3.2 <i>Adherens Junctions</i> .....	14
1.3.3 <i>Gap junctions</i> .....	17
1.4 TRANSMEMBRANE MOVEMENT .....	18
1.4.1 <i>Transcellular transport route</i> .....	18
1.4.2 <i>Paracellular transport</i> .....	21
1.4.3 <i>Diapedesis</i> .....	23
1.4.4. <i>Traversing BBB for CNS drug delivery</i> .....	23
1.5 BLOOD-BRAIN BARRIER PATHOPHYSIOLOGY.....	26
1.5.1 <i>Junctional proteins in BBB pathologies</i> .....	27
1.5.2 <i>Blood-Brain Barrier Dysfunction in Disease</i> .....	28
1.6 PROTEIN PHOSPHATASES.....	33
1.6.1 PP2A .....	35
1.6.2 <i>Structural organization of PP2A</i> .....	35
1.6.3 <i>Post-translational modifications of PP2A</i> .....	38
1.6.4 <i>PP2A inhibitors</i> .....	40
1.6.4.6 <i>Other exogenous inhibitors</i> .....	44
1.6.5 <i>Activators of PP2A</i> .....	45
1.7 AIMS AND HYPOTHESIS OF THE PROJECT.....	49
<b>2. MATERIALS AND METHODS.....</b>	<b>51</b>
2.1 LIST OF CONSUMABLES .....	52

2.2 LIST OF EQUIPMENT .....	53
2.4 CELL CULTURE .....	55
2.5 CELL VIABILITY: MTT ASSAY.....	55
2.6 CELL VIABILITY: LDH ASSAY .....	55
2.7 SEMI-QUANTITATIVE REAL-TIME PCR.....	56
2.8 WESTERN BLOTTING .....	57
2.9 BRADFORD PROTEIN ASSAY .....	58
2.10 MRNA STABILITY ASSAY .....	59
2.11 TTP GENE KNOCKDOWN USING siRNA .....	59
2.12 TRANSFORMATION OF E. COLI .....	59
2.13 PLASMID ISOLATION.....	60
2.14 CELL TRANSFECTION .....	60
2.15 CELL FIXING AND STAINING .....	61
2.16 DATA AND STATISTICAL ANALYSIS .....	61
<b>3. RESULTS .....</b>	<b>62</b>
3.1 EFFECT OF SMAPs ON CELL VIABILITY.....	63
3.1.1 Cytotoxicity Screen.....	63
3.1.2 Effect of DBK-1154 and DBK-766 on cell viability .....	65
3.2 EFFECT OF OKADAIC ACID ON VE-CADHERIN AND CLAUDIN-5 EXPRESSION ALONE AND IN COMBINATION WITH SMAPs .....	66
3.3 EFFECT OF INFLAMMATORY CYTOKINES ON VE-CADHERIN AND CLAUDIN-5 EXPRESSION ALONE OR IN COMBINATION WITH SMAPs .....	68
3.4 INVESTIGATION OF THE EFFECT OF IFN $\gamma$ /TNF $\alpha$ ON PP2Ac.....	70
3.5 EFFECT OF INF $\gamma$ /TNF $\alpha$ ON VE-CADHERIN AND CLAUDIN-5 MRNA STABILITY IN HCMEC/D3 CELLS .....	72
3.6. OPTIMIZATION OF TRISTETRAPROLIN GENE KNOCKDOWN PROTOCOL USING siRNA.....	73
3.6 OPTIMIZATION OF THE DNA TRANSFECTION PROTOCOL.....	76
<b>4. DISCUSSION AND CONCLUSION.....</b>	<b>84</b>
4.1 FUTURE DIRECTIONS .....	92

**REFERENCES.....94**

**List of Figures**

Figure 1: Cerebrovascular barriers.....3

Figure 2: Cross-section of a capillary within the neurovascular unit. ....4

Figure 3: Structure of the BBB junctions. ....11

Figure 4: Transmembrane transport pathways of the BBB.....21

Figure 5: Inter-endothelial junctions localized at microvessels. ....22

Figure 6: Protein Phosphatases classification. ....34

Figure 7: The structure of PP2A. ....37

Figure 8: SMAPs' chemical structure. ....47

Figure 9: Effect of SMAP on cell viability.....64

Figure 10: Effect of DMSO and Dox on cell viability.....65

Figure 11: Effect of DBK-1154 and DBK-766 and cell viability.....66

Figure 12: Effect of OA alone and in combination with DBK-1154 or FTY-720 on VE-cadherin mRNA (A) and protein (B, D) expression and claudin-5 mRNA (C) expression.....67

Figure 13: Effect of IFN $\gamma$ /TNF $\alpha$  alone and in combination with DBK-1154 or FTY-720 on VE-cadherin mRNA (A) and protein (B,D) expression and claudin-5 mRNA (C) expression.....69

Figure 14: Effect of IFN $\gamma$ /TNF $\alpha$  on PP2Ac (A, C) and dmPP2Ac (B, D) protein abundance.....70

Figure 15: Effect of IFN $\gamma$ /TNF $\alpha$  on LCMT-1 (A, C) and PME-1 (B, D) protein abundance.....71

Figure 16: Effect of IFN $\gamma$ /TNF $\alpha$  on pPP2Ac protein abundance, represented as graph (A) and blot (B).....72

Figure 17: Effect of IFN $\gamma$ /TNF $\alpha$  on VE-cadherin (A) and claudin-5 (B) mRNA stability.....73

Figure 18: TTP knockdown protocol optimization graph (A) and representative blots (B). ....75

Figure 19: Effect of TTP siRNA transfection on TTP mRNA expression (A) and protein abundance (B, C) .....	76
Figure 20: Transfection optimization using a GFP plasmid and PolyFect transfection reagent. ....	78
Figure 21: Transfection of hCMEC/d3 cells with a CIP2A plasmid (pcCIP2A). ....	80
Figure 22: Transfection using 10 $\mu$ L PolyFect Transfection Reagent and 1 $\mu$ g PP2Ac plasmid (pcPP2Ac). ....	81
Figure 23: Transfection of hCMEC/d3 cells with a PP2Ac plasmid (pcPP2ac) using Lipofectamine 2000 (A) or TransIT-X2 (B).....	82
Figure 24: Transfection using varying volumes of PP2Ac plasmid DNA and PolyFect Transfection Reagent. ....	83

## List of Tables

Table 1: Consumables .....	52
Table 2: Equipment .....	53
Table 3: List of primers including gene identification numbers and sequence.....	57



## List of Abbreviations

<b>Abbreviation</b>	<b>Full name</b>
<b>AD</b>	Alzheimer's disease
<b>AJ</b>	Adherens junction
<b>Akt</b>	Protein kinase B
<b>APOE</b>	Apolipoprotein E
<b>ATP</b>	Adenosine triphosphate
<b>BBB</b>	Blood-brain barrier
<b>BDNF</b>	Brain derived neurotrophic factor
<b>BME</b>	2- $\beta$ -mercaptoethanol
<b>BMEC</b>	Brain microvascular endothelial cells
<b>cAMP</b>	Cyclic adenosine monophosphate
<b>CCM</b>	Cerebral cavernous malformation
<b>CIP2A</b>	Cancerous inhibitor of PP2A
<b>CML</b>	Chronic myelogenous leukemia
<b>CNS</b>	Central nervous system
<b>COVID-19</b>	Coronavirus infectious disease 2019
<b>CRPC</b>	Castration-resistant prostate cancer
<b>CSF</b>	Cerebrospinal fluid
<b>dmPP2Ac</b>	Demethylated PP2Ac
<b>DMSO</b>	Dimethyl sulphoxide
<b>DOX</b>	Doxorubicin
<b>E-cadherin</b>	Endothelial cadherin
<b>EAE</b>	Experimental autoimmune encephalomyelitis
<b>EDTA</b>	Ethylenediaminetetraacetic acid
<b>EGFR</b>	Epidermal growth factor receptor
<b>Erk</b>	Extracellular signal regulated kinase
<b>FBS</b>	Fetal bovine serum
<b>FDA</b>	Food and Drug Administration
<b>FGFR</b>	Fibroblast growth factor receptor

<b>GAPDH</b>	Glyceraldehyde 3-phosphate dehydrogenase
<b>GFAP</b>	Glial fibrillary acid protein
<b>GFP</b>	Green fluorescent protein
<b>GI</b>	Gastrointestinal
<b>GLUT</b>	Glucose transporter
<b>GPI</b>	Glycosylphosphatidylinositol
<b>HCC</b>	Hepatocellular carcinoma
<b>HCl</b>	Hydrochloric acid
<b>hCMEC/d3</b>	Human cerebral microvascular endothelial cells
<b>HEAT</b>	Huntington/elongation/A-subunit/TOR
<b>HRP</b>	Horseradish peroxidase
<b>IBA1</b>	Ionized calcium-binding adapter molecule 1
<b>IDUA</b>	$\alpha$ -L-iduronidase
<b>IFN<math>\gamma</math></b>	Interferon- $\gamma$
<b>IGF-1</b>	Insulin-like growth factor 1
<b>Jak2</b>	Janus kinase 2
<b>JAM</b>	Junctional adhesion molecule
<b>kDa</b>	Kilodalton
<b>LAT1</b>	Large amino acid transporter 1
<b>LDH</b>	Lactate dehydrogenase
<b>LDL</b>	Low-density lipoprotein
<b>LFA-1</b>	Lymphocyte function-associated antigen-1
<b>LRP-1</b>	Low density lipoprotein receptor-related protein 1
<b>MAPK</b>	Mitogen-activated protein kinase
<b>MAV-1</b>	Mouse adenovirus type-1
<b>MDR1</b>	Multidrug resistance protein 1
<b>MMP</b>	Matrix Metalloproteinase
<b>MS</b>	Multiple sclerosis
<b>mTORC1</b>	Mammalian target of rapamycin complex 1
<b>MTT</b>	3-(4,5-dimethylthiazol-2-yl)-2,5-diphenyltetrazolium bromide

<b>MUPP1</b>	Multi-PDZ domain protein 1
<b>N-cadherin</b>	Neural cadherin
<b>NaCl</b>	Sodium chloride
<b>NDRG2</b>	N-myc downstream-regulated gene 2
<b>NF-<math>\kappa</math>B</b>	Nuclear factor $\kappa$ -light-chain-enhancer of activated B cells
<b>NG2</b>	Neural/glial antigen 2
<b>NP40</b>	Nonyl phenoxyethoxyethanol
<b>NSCLC</b>	Non-small cell lung cancer
<b>NVU</b>	Neurovascular unit
<b>OA</b>	Okadaic acid
<b>P-gp</b>	P-glycoprotein
<b>p-tau</b>	Hyperphosphorylated-tau
<b>Pals1</b>	Proteins associated with Lin Seven 1
<b>PATJ</b>	PALS-1 associated TJ protein
<b>qPCR</b>	Quantitative polymerase chain reaction
<b>PD</b>	Parkinson's disease
<b>PDGFR-<math>\beta</math></b>	Platelet derived growth factor receptor- $\beta$
<b>PFA</b>	Paraformaldehyde
<b>PKA</b>	Protein kinase A
<b>PKC</b>	Protein kinase C
<b>PKR</b>	Protein Kinase R
<b>PME-1</b>	Protein phosphatase methylesterase 1
<b>PP2A</b>	Protein phosphatase 2A
<b>pPP2Ac</b>	Phosphorylated PP2Ac
<b>PSP</b>	Protein Serine/Threonine phosphatase
<b>PTP</b>	Protein Tyrosine phosphatase
<b>PTPA</b>	Phosphotyrosyl phosphatase activator
<b>PVDF</b>	Polyvinylidene fluoride
<b>RAGE</b>	Receptor for advanced glycation end products
<b>RIPA</b>	Radioimmunoprecipitation assay

<b>ROS</b>	Reactive oxygen species
<b>S100B</b>	S100 calcium-binding protein B
<b>SARS-CoV-2</b>	Severe acute respiratory syndrome coronavirus 2
<b>SDS-PAGE</b>	Sodium dodecyl sulphate-polyacrylamide gel electrophoresis
<b>Ser</b>	Serine
<b>SET</b>	Inhibitor 2 of PP2A
<b>SGLT</b>	Sodium dependent glucose transporter
<b>SMAPs</b>	Small molecule activators of PP2A
<b>TBS-T</b>	Tris-buffered saline-tween
<b>TEER</b>	Trans endothelial electrical resistance
<b>TGF- <math>\beta</math></b>	Transforming growth factor $\beta$
<b>Thr</b>	Threonine
<b>TJ</b>	Tight junction
<b>TNF<math>\alpha</math></b>	Tumour necrosis factor $\alpha$
<b>TTP</b>	Tristetraprolin
<b>Tyr</b>	Tyrosine
<b>VE-cadherin</b>	Vascular endothelial cadherin
<b>VE-PTP</b>	Vascular endothelial protein tyrosine phosphatase
<b>VEGF</b>	Vascular endothelial growth factor
<b>ZO</b>	Zonula occludens

## Summary of Methods and Results

Protein phosphatase 2A (PP2A) is a serine/threonine phosphatase which plays a key role in modulating signalling, metabolism and cell growth, and is implicated in various pathologies. There is conflicting evidence regarding the role of PP2A in regulating blood brain barrier function. This study investigates if okadaic acid and inflammation modulate VE-cadherin and claudin-5 through PP2A, and whether this can be reversed by novel small molecule activators of PP2A as a possible therapeutic intervention.

Human brain microvascular endothelial cells (hCMEC/d3) were exposed to IFN $\gamma$ /TNF $\alpha$  (10ng/mL each) or okadaic acid (OA, 10 nM; PP2A inhibitor) for 24 h. mRNA and protein abundance were determined using qPCR and western blotting, respectively. Data were analysed using one-way ANOVA ( $P < 0.05$ ) with post hoc analysis. IFN $\gamma$ /TNF $\alpha$  decreased claudin-5 and VE-cadherin mRNA expression by  $68 \pm 6 \%$  and  $54 \pm 8 \%$  respectively, and VE-cadherin protein by  $83 \pm 6 \%$ . Interestingly, OA decreased VE-cadherin mRNA and protein expression by  $80 \pm 5 \%$  and  $80 \pm 3 \%$ , respectively, but had no effect on claudin-5. PP2A activators FTY-720 (1  $\mu$ M) and DBK-1154 (1  $\mu$ M) did not alter the responses to OA or IFN $\gamma$ /TNF $\alpha$ . Additionally, IFN $\gamma$ /TNF $\alpha$  decreased demethylated PP2Ac and potentially increased phosphorylated PP2Ac. Furthermore, transfection experiments were carried out in order to overexpress PP2Ac, SET or CIP2A in hCMEC/d3 cells, however the protocol needs to be further optimized.

In conclusion, this study has shown IFN $\gamma$ /TNF $\alpha$  and OA to differentially modulate claudin-5 mRNA expression but to have similar effects on VE-cadherin. This indicates a role for PP2A in transcriptional regulation of VE-cadherin but not claudin-5. Importantly, the VE-cadherin response was insensitive to DBK-1154. The role of PP2A in modulating junctional proteins requires further investigation.



# Chapter 1

---

## 1. Introduction

## 1.1 Blood-Brain Barrier Physiology

The blood-brain barrier (BBB) is a term used to describe the unique structure and properties of the vasculature of the central nervous system (CNS). The microvasculature of the CNS differs from that in other organs as the cells that make up the vascular bed are in extremely close proximity, forming a physical barrier between the blood and the interstitial fluid bathing the neurons. This barrier helps to maintain homeostasis of the cells within the CNS, protecting them from xenobiotics and imbalances of ions in the blood as a result of physical exercise or food intake [1].

The discovery of a barrier which separates the brain and spinal cord from the rest of the body dates back over 100 years. The first experiments were performed by Paul Ehrlich, a German scientist who injected dyes such as Trypan blue into the peritoneum of animals and found that they did not reach the CNS [2]. Experiments by one of Ehrlich's students, Edwin Goldman, provided further evidence for the presence of brain barrier. Goldman injected the dye directly into the cerebrospinal fluid of the brain, and showed that the staining did not spread to the rest of the body [3]. The concept of the blood-brain barrier has been extensively researched since.

The blood-brain barrier is most evident at 1) the endothelium of parenchymal microvessels, 2) the epithelium of the choroid plexus and 3) the arachnoid epithelium (Figure 1). Endothelial cells forming the parenchymal microvessel barrier are the most important site for transport of molecules between the blood and the CNS, due to the vast surface area and their proximity to neurons (8-25  $\mu\text{m}$ ) [1, 4]. Tight junctions (TJs) are present at each of the three barrier locations, restricting ions and solutes circulating in the blood from moving into the brain. Maintaining the correct ionic microenvironment around the



neurons is critical for synaptic signalling, and hence for reliable neuronal function [5]. Because of tight junctions, only gaseous molecules such as oxygen and carbon dioxide and small lipophilic compounds, including some CNS drugs, can penetrate the barrier in absence of active transport [6].

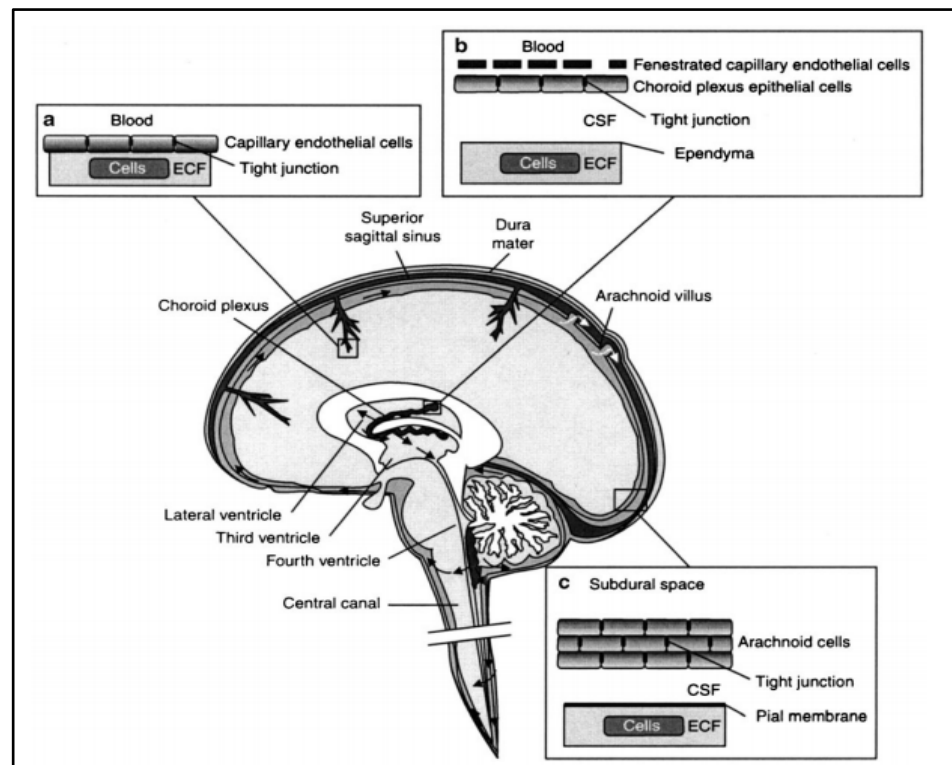


**Figure 1: Cerebrovascular barriers.**

The brain is protected from the blood primarily at three sites; a) microvascular endothelial cells, which create a selective barrier due to the formation of tight junctions between neighbouring cells, b) the choroid plexuses in the brain's ventricles and c) the arachnoid cells, a multi-layered epithelium which only allows for cerebrospinal fluid to move into the blood and out of the brain. Image taken from Abbot *et al.*, 2010 [1].

## 1.2. Structure and function of the BBB

The neurovascular unit (NVU) is a unique structure in the brain composed of closely associated vascular and perivascular cells, which make up a functional and anatomical unit. It regulates blood flow through the

cerebral vasculature. The three main cell types which make up the NVU are endothelial cells, pericytes and astrocytes (Figure 2) [7]. Endothelial cells and pericytes are surrounded by a basement membrane, a 30 to 40 nm thick matrix in close contact with the end-feet processes of astrocytes, which enclose cerebral microvessels [8]. Certain cells, such as microglia, as well as nerve terminals, are in close proximity to endothelial cells and release cytokines and vasoactive agents, which can regulate BBB permeability and tight junction assembly [6, 9].

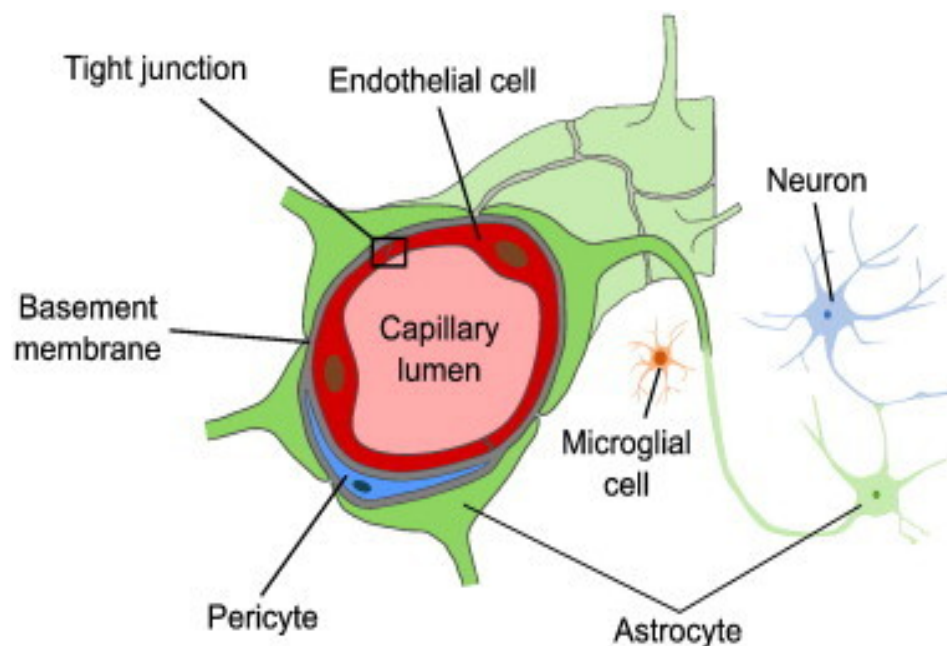


**Figure 2: Cross-section of a capillary within the neurovascular unit.**

Endothelial cells form tight junctions creating a physical barrier between the blood and brain. Pericytes surround the endothelial cells. Astrocyte endfeet surround the capillaries and microglia are the immune cells resident in the brain. Image taken from Heye *et al.*, 2014 [10].

### 1.2.1 Endothelial Cells

A single layer of endothelial cells, called the endothelium, is found lining the interior surface of the heart chambers, blood vessels and lymphatic vessels. In humans, the endothelium covers a surface of about 6,000

square meters [11]. The cell surface markers originally used to characterise endothelial cells were angiotensin-converting enzyme, Von Willebrand factor and Weibel-Palade bodies [12]. This list has now been updated and includes nearly 60 proteins, which can be used to confirm the purity and authenticity of endothelial cell cultures [13]. Endothelial cells are flat, with an elongated nucleus at the centre of the cell. Brain microvascular endothelial cells can be distinguished from other types of endothelial cells by higher metabolic activity and thus more mitochondria, few or no pinocytotic vesicles, and polarized expression of peptide and ion transporters [14].

Endothelial cells are the main anatomical unit of the vascular blood-brain barrier, as they limit paracellular and transcellular transport mechanisms, protecting the brain [15]. Brain microvascular endothelial cells (BMECs) are encased in a basement membrane, rich in extracellular matrix proteins, growth factors, cytokines and enzymes [16]. They interact with extracellular matrix proteins such as collagen, laminin and perlecan through integrin receptors, which links the basement membrane to the cytoskeleton of endothelial cells [17]. Adherens and tight junctions form between neighbouring endothelial cells and contribute to the physical barrier property of these cells. Endothelial cells also play a role in selective transport due to ion channels, transporters, receptors, and metabolite-degrading enzymes present in their membranes. These work together to deliver nutrients such as electrolytes, glucose, amino acids and nucleosides to the brain and efflux metabolite waste products and solutes from the brain to the blood [18, 19].

Brain microvascular endothelial cells are also involved in activation and adhesion of platelets. Platelets circulate throughout the body without interacting with the vasculature due to prostacyclin, nitric oxide and adenosine generated by the endothelium, which act as adhesion inhibitors [20]. These anti-adhesion molecules are downregulated during

periods of cellular stress, such as inflammation, enabling platelets to attach. Furthermore, platelet activation by chemical stimuli, vascular injury or altered blood flow allows them to directly interact with endothelial cells or leukocytes attached to the vessel wall [14, 20].

Brain microvascular endothelial cells appear to play a neuroprotective role through the secretion of neurotrophins, such as vascular endothelial growth factor (VEGF) necessary for angiogenesis, brain-derived neurotrophic factor (BDNF) essential for neuronal survival and insulin-like growth factor 1 (IGF-1), which plays a role in nervous system development and neurotransmission [21-24].

### 1.2.2. Pericytes

Pericytes are mural cells that surround small-diameter blood vessels. They are embedded within the vascular basement membrane and are situated between endothelial cells and astrocyte endfeet processes [25, 26]. While no pericyte-specific markers have been identified to date, the markers characteristic for pericytes include platelet-derived growth factor receptor- $\beta$  (PDGFR- $\beta$ ), neural/glial antigen 2 (NG2) and desmin [27-29].

The vasculature of the CNS is particularly rich in pericytes, with an endothelial cell to pericyte ratio of between 1:1 and 1:3, which accounts for about 30 % of the endothelial cells' abluminal surface [25, 30]. However, the percentage of pericyte coverage is organ specific, with most coverage in the brain, less in lungs and least in muscle, which is positively correlated with barrier properties [31]. Pericytes have key roles in the formation, maturation and maintenance of the blood-brain barrier [31-33]. The importance of pericytes has been illustrated by *in vitro* studies performed on mice deficient in pericytes. The mutant animals had increased brain vessel permeability as a result of upregulated endothelial transcytosis, demonstrating that pericyte deficiency influences

endothelium function [33, 34]. Interestingly, pericytes have multipotential neural stem cell capability, being able to differentiate into other cell types found in the neurovascular unit, such as neurons and glial cells [35, 36].

Pericytes communicate directly with other pericytes and endothelial cells through gap junction CX43 hemichannels and peg-and-socket contacts formed by N-cadherin [37, 38]. Several signalling pathways have been identified in pericyte-endothelial crosstalk. They include PDGF- $\beta$ /PDGFR- $\beta$  signalling involved in pericyte recruitment, angiopoietin-tie receptor signalling, essential for blood vessel maturation and transforming growth factor- $\beta$  (TGF- $\beta$ ) and Notch signalling, which plays a role in pericyte differentiation [39].

### 1.2.3. Astrocytes

Astrocytes are star-shaped glial cells, originating from radial glial cells [40]. Glial fibrillary acid protein (GFAP), N-myc downstream-regulated gene 2 (NDRG2) and S100 calcium-binding protein B (S100B) are used to identify astrocytes, however, not all of these proteins are expressed by all astrocyte subpopulations, making their identification somewhat difficult [41]. There are two main subtypes of astrocytes; fibrous and protoplasmic. Fibrous astrocytes are made up of multiple long fibre-like processes and are found within the white matter. Protoplasmic astrocytes are resident in the grey matter and resemble a sphere composed of branches extending from the centre [42, 43]. The processes of protoplasmic astrocytes can surround synapses, whereas fibrous astrocytes make contact with the nodes of Ranvier of neurons. A single astrocyte's processes can make contact with several neurons and up to 140,000 synapses [44]. Both types of astrocytes interact with the vasculature, covering up to 99 % of a vessel's abluminal surface [45, 46].

In the neurovascular unit, astrocytes are positioned between endothelial cells and neurons. Astrocytes play a role in the induction and maintenance of barrier properties, such as tight junction formation and expression of transporters by endothelial cells. This is supported by *in vitro* work showing that the formation of tight junctions between endothelial cells is induced upon co-culture with astrocytes and pericytes [47]. Furthermore, astrocytes secrete apolipoprotein E (APOE), which signals to pericytes and suppresses their production of matrix metalloproteinase 9 (MMP-9), preventing blood-brain barrier breakdown [48].

The position of astrocytes within the neurovascular unit enables them to recognise and dynamically respond to both vascular and neuronal activity. They release molecular mediators such as nitric oxide, prostaglandins and arachidonic acid that regulate the diameter of blood vessels in the CNS [49]. Astrocytes also release chemical factors, such as endothelin-1 and glutamate which regulate endothelial permeability [50].

In response to injury and neuroinflammation, astrocytes are activated and become pro-inflammatory, termed A1 or trophic, termed A2. A1 astrocytes release pro-inflammatory factors such as reactive oxygen species (ROS), TNF $\alpha$  and IL-1 $\beta$  as well as toxic factors which damage neurons [51]. A2 astrocytes have the opposite effect on neurons as they aid synapse repair and neuron growth and survival, making their role very important following trauma or during ischemic conditions [52, 53].

#### 1.2.4. Microglia

Microglia are specialized macrophage-like cells found in the CNS. CD11b and ionized calcium-binding adapter molecule 1 (IBA1) are cell surface markers used to identify microglia; however, they are also expressed by macrophages [54]. Microglia are highly motile and plastic cells [55]. When

resting, they have a unique ramified shape, characterised by branching processes and a small cell body. Microglia become activated during disease, whereby their nucleus enlarges, the processes shorten, they become phagocytic and release various cytokines [56].

Microglia are the first and main type of cell to provide immune defence in the brain and spinal cord. When active, they can take on different phenotypes. 'Classical' M1 microglia are induced following activation by  $\text{TNF}\alpha$  and  $\text{IFN}\gamma$  leading to the generation of a pro-inflammatory phenotype, whereas the 'alternative' M2 phenotype is induced upon activation via IL-4 and IL-13 contributing to an anti-inflammatory phenotype [57]. Microglia activation is now identified as an early indicator of neuroinflammation [56].

### 1.3. Tight & Adherens Junctions

The organs of multicellular organisms are compartmentalized by endothelial and epithelial cell layers. Adherens junctions (AJs) maintain cell to cell contact, providing structural support to the monolayer and aid the formation of tight junctions [58]. Tight junctions generate polarity by regulating the movement of ions, water and proteins between cells at sites of cell-cell contact [59]. Degradation of junctional proteins is a major feature of physiological and pathological barrier remodelling, which leads to increased permeability [60]. Post-translational modifications of junctional proteins often contribute to blood-brain barrier dysfunctions as a result of protein degradation and redistribution/internalization. The post-translational modifications of junctional proteins include phosphorylation, glycosylation, acetylation, methylation and palmitoylation; with phosphorylation sites present on most junctional proteins making it the most important post-translational modification [60].

### 1.3.1 Tight Junctions

Tight junctions are intramembrane multiprotein complexes that link adjacent cells in endothelial and epithelial monolayers. Tight junctions provide a highly selective barrier, limiting the transport of molecules, but they also play roles in cell proliferation, migration, differentiation, gene expression and signal transduction [61-63]. Dysregulation of the function and structure of tight junctions is linked to many diseases, including acquired and hereditary inflammatory diseases such as multiple sclerosis, cancer, cystic fibrosis and vision loss [64].

There are three distinct families of integral membrane proteins localizing at tight junctions; occludin [65], claudin [66] and junctional adhesion molecule (JAM) [67]. Other proteins which localize at tight junctions form a framework that connects transmembrane proteins to the actin cytoskeleton. These proteins include zonula occludens (ZO) -1, -2 and -3, proteins associated with lin seven 1 (Pals1) and multi-PDZ domain protein 1 (MUPP1) [68].

The integral membrane proteins form dimers with their counterparts present on the surface of neighbouring endothelial cells, while cytoplasmic proteins link them to the actin cytoskeleton (Figure 3) [18]. These dimers make up strands of tight junctions within a plasma membrane, completely blocking the intercellular space at each meeting point [69]. This blockade results in high trans endothelial electrical resistance (TEER) of the blood-brain barrier [70]. The amount and complexity of the tight junction strand network is cell type dependent, contributing to differences in permeability of different tissue types [71]. Tight junctions are dynamic structures: they are sensitive to factors circulating in the CNS that have the ability to regulate paracellular pathway properties on a minute-to-minute basis [1].



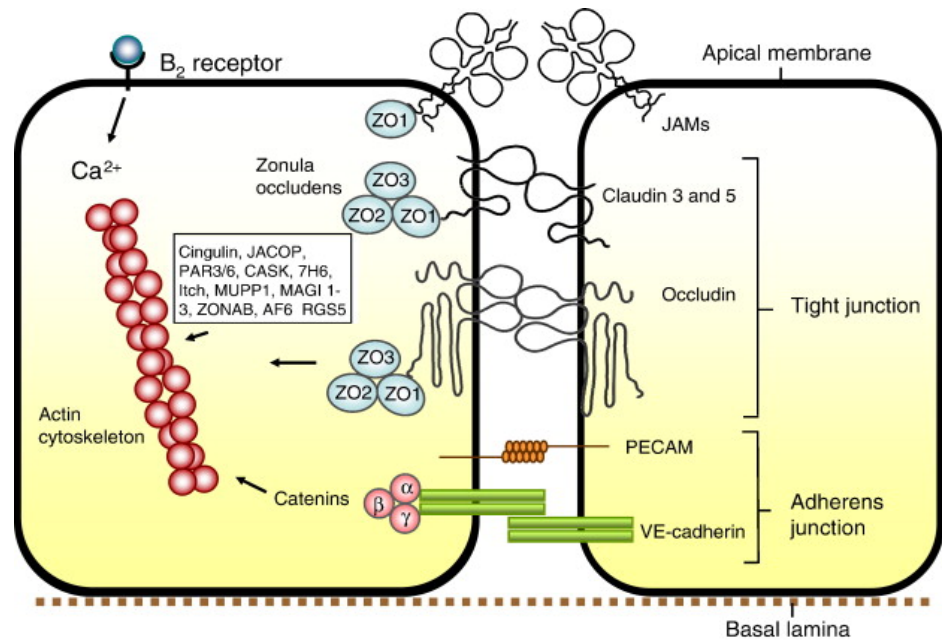


**Figure 3: Structure of the BBB junctions.**

Occludin, claudin-3 and -5 and JAMs comprise the tight junctions, whereas VE-cadherin and PECAM make up the adherens junctions. Tight junction proteins are linked to the scaffolding proteins ZO-1, -2 and -3 which are connected to the actin cytoskeleton via cingulin and other proteins. Catenins  $\beta$ ,  $\alpha$  and  $\gamma$  link VE-cadherin to the actin cytoskeleton. Image taken from Abbot *et al.*, 2010 [1].

#### 1.3.1.1 Claudins

Claudins are transmembrane proteins whose name is derived from the Latin *claudere*, meaning 'to close' [72]. Claudins are 20-27 kDa proteins that span the bilayer four times and have two extracellular loop domains with N- and C-terminal ends oriented towards the cytoplasm [73]. PDZ binding motifs at the C-terminal allow claudin to directly interact with cytoplasmic tight junction proteins such as ZO-1, -2 and -3, PALS-1 associated TJ protein (PATJ) and MUPP-1. ZO-1 and ZO-2 stabilise and regulate the junction by indirectly linking claudin to the actin cytoskeleton via cingulin [74].

To date, 24 claudins have been identified [75]. They can be divided into groups. Claudins 1, 3, 5, 11, 14 and 19 are the barrier forming claudins, which reduce paracellular permeability. Other claudins have the opposite effect, as they form channels across the tight junctions, enhancing paracellular permeability. The channel forming claudins either allow the passage of cations (claudin 2, 10b and 15) or anions (claudin 10a and 17). The functions of other claudins are inconsistent or unknown [76]. Some claudins are also tissue-specific, for example claudin-11 has only been seen in oligodendrocytes and Sertoli cells [73], while claudin-5 is primarily expressed by vascular endothelial cells [77].

Claudin is now believed to be the main protein constituting the tight junction strands [69, 78]. A selective loss in claudin-3 from tight junctions is seen in glioblastoma multiforme and experimental allergic encephalomyelitis, and is associated with decreased barrier integrity [79]. Similarly, genetically modified mice lacking claudin-5 have a highly permeable blood-brain barrier and die shortly after birth [80]. These studies suggest that both claudin-3 and -5 are essential for normal blood-brain barrier function. Importantly, the integrity of the barrier is not regulated solely by the expression of junctional proteins, but also by how these proteins are organized and interact with each other [81].

Paracellular permeability is also regulated through the phosphorylation of junctional proteins, including claudin. The cellular effect of claudin phosphorylation depends on whether the claudin belongs to the barrier forming or channel forming type. Generally, phosphorylation of channel forming claudins helps retain them at the tight junction, whereas phosphorylation of barrier forming claudins is detrimental for barrier function. For example, phosphorylation of claudin-16, a channel forming claudin, by protein kinase A (PKA) results in it localizing to the tight junction along with ZO-1 while its dephosphorylation leads to its translocation into the lysosome and degradation [82]. However, the

opposite effect is seen in regard to the barrier forming claudin-3, which, when phosphorylated by the same kinase, results in disruption of the tight junction [83]. Similarly, phosphorylation of claudin-5 by Rho kinase and claudin-1 by mitogen-activated protein kinase (MAPK) results in diminished barrier integrity [84, 85]. Following this logic, it could be assumed that dephosphorylation of the barrier forming claudins by a phosphatase such as the serine/threonine phosphatase PP2A, would be beneficial for barrier function. However, it remains to be determined if PP2A can regulate claudin-5 phosphorylation in brain microvascular endothelial cells.

#### 1.3.1.2 Occludins

Occludin is a 65 kDa integral membrane protein associated with tight junctions. Occludin has four membrane-spanning segments, two intracellular domains and two extracellular loops. Each of these domains have different regulatory features and functions. For example, the C terminus is essential for occludin dimerization, binding to ZO-1 and signalling, while the transmembrane domain is essential for membrane apposition and fusion events [86]. Occludin was the first tight junction protein to be identified and was thought to be a crucial barrier-forming component of the tight junction. However, a number of studies including mutation and gene knockout analyses show that occludin is not essential for the development of tight junction strands, although its overexpression increases transendothelial resistance in epithelial cells [87-90]. Even though occludin is not necessary in tight junction barrier formation, mice lacking occludin demonstrated growth retardation, chronic inflammation, brain calcifications and other histological abnormalities [88]. This suggests a role for occludin in maintaining tight junction stability and barrier function.

Occludin is regulated by post-translational modifications, including phosphorylation. However, there are conflicting data regarding the effect

of phosphorylation of occludin on barrier function. A study by Sakakibara *et al.*, 1997 showed phosphorylation of serine and threonine residues to cause selective localization at tight junctions [91]. Consistent with this, another group showed that when occludin is dephosphorylated in response to inflammation, specifically in experimental autoimmune encephalomyelitis, the experimental mouse model of multiple sclerosis, this coincided with increased barrier permeability [92]. Contrary to these studies, Antonetti *et al.*, 1999 showed that phosphorylation of occludin and ZO-1 is associated with increased endothelial permeability [93], while DeMaio *et al.*, 2006 linked phosphorylation of occludin to disruption of tight junctions and barrier compromise [94].

#### 1.3.1.3 Junctional adhesion molecules (JAMs)

JAMs belong to the immunoglobulin superfamily of cell adhesion receptors. To date, 3 JAM isoforms have been identified; JAM-A, -B and -C. They all contain two extracellular immunoglobulin-like domains, a single membrane spanning domain and a 40-48 amino acid long cytoplasmic tail [95]. JAMs are found in endothelial and epithelial cells, in which they cluster at tight junctions; however, they are also present in cells lacking tight junctions, such as leukocytes and platelets [96].

JAMs can make homophilic interactions with other JAMs expressed on adjacent cells. They can also make heterophilic interactions with other membrane proteins, like ZO-1 and -2 expressed by the same cell, as well as neighbouring cells [97, 98]. JAMs present on the surface of vascular endothelial cells can interact with JAMs and lymphocyte function-associated antigen 1 (LFA-1) on the surface of leukocytes circulating in the blood, which plays a role in diapedesis [99, 100].

#### 1.3.2 Adherens Junctions

The formation of tight junctions requires the existence of adherens junctions. Adjacent cells establish adherens junctions by the homophilic

interactions between the transmembrane proteins vascular endothelial cadherin (VE-cadherin) and epithelial cadherin (E-Cadherin) present in CNS endothelial and choroid plexus epithelial cells [101].

#### 1.3.2.1 Cadherins

Cadherins belong to a family of calcium-dependent adhesion molecules, hence their name. The classical cadherins are grouped based on their localization; E-cadherin is found in the epithelium/endothelium, N-cadherin in neurons, M-cadherin in skeletal muscle, P-cadherin in the placenta and R-cadherin is expressed in the retina. All of these cadherins weigh between 100 and 130 kDa and have a similar structure, containing an extracellular domain with five repeats of around 110 amino acids, which contain the calcium-binding motif [102]. VE-cadherin and N-cadherin are both present on the surface of endothelial cells; however, only VE-cadherin clusters at adherens junctions [103].

VE-cadherin is the most important adhesive component of adherens junctions, with an essential role in the formation and regulation of endothelial cell junctions [104]. *Cis* and *trans* associations mediate homophilic adhesion of VE-cadherins. VE-cadherin molecules on the surface of the same cell interact laterally through *cis*-associations, forming *cis*-dimers, which can then form adhesive bonds with other VE-cadherin *cis*-dimers on opposing cells through *trans*-associations, resulting in antiparallel tetramers. Importantly, VE-cadherin dimers dissociate into monomers in the absence of calcium [105, 106].

The C-terminal cytoplasmic domain of VE-cadherin associates with p120-catenin,  $\beta$ -catenin and plakoglobin ( $\gamma$ -catenin), providing the organization of adherens junctions [107]. It regulates cytoskeletal remodelling via indirect interactions with actin-binding proteins, such as vinculin, eplin,  $\alpha$ -catenin and  $\alpha$ -actinin. The clustering of VE-cadherin, and its association

with Tiam, vinculin and the cerebral cavernous malformations (CCM) proteins complex regulates the stability of adherens junctions [108].

VE-cadherin is the earliest specific marker of endothelial cells, detectable at a very early stage of vascular development in the embryo [109]. It plays a role during embryogenesis, contributing to the maturation and remodelling of vessels [110]. VE-cadherin is also important for the maintenance of vascular homeostasis, as demonstrated in a study in which functional blocking antibodies raised against VE-cadherin led to a redistribution of VE-cadherin from intercellular junctions to the cell surface, resulting in increased permeability in lungs and heart [111]. Furthermore, mice lacking VE-cadherin are lethal at an early embryonic stage due to defective vascularization and impaired angiogenesis, highlighting VE-cadherin's importance in vascular morphogenesis [112].

N-cadherin doesn't localize to adherens junctions; however, its deletion from endothelial cells also results in embryonic lethality because of severe vascular defects. Interestingly, VE-cadherin and p120 are downregulated in cells lacking N-cadherin, indicating that N-cadherin modulates angiogenesis through regulation of VE-cadherin expression [113]. Although the mechanism is poorly understood, N-cadherin might induce VE-cadherin expression through interaction with fibroblast growth factor receptor (FGFR), which reduces VE-cadherin internalization and increases cell-cell adhesion [114, 115]. Importantly, VE-cadherin can also regulate N-Cadherin's expression, although in a different manner, by excluding it from cell-cell junctions [103].

Crosstalk between VE-cadherin and other junctional proteins is essential for the proper functioning of cell-cell junctions. For example, VE-cadherin clustering at endothelial junctions, along with high cell confluency, have the ability to induce upregulated transcription of claudin-5, the principal claudin present at the blood-brain barrier. Mechanistically, VE-cadherin

clustering triggers phosphorylation of the FoxO1 transcription factor leading to transcriptional inhibition of claudin-5 [116]. This study demonstrates the link between adherens and tight junctions on endothelial cells, and the importance of VE-cadherin in regulating paracellular permeability.

Post-translational modification of VE-cadherin and proteins which associate and interact with it can modulate the integrity of adherens junctions, and thus vascular permeability. For example, the association of vascular endothelial protein tyrosine phosphatase (VE-PTP) with VE-cadherin increases barrier integrity and reduces the permeability of a cell monolayer [117]. In an *in vivo* study, phosphorylation of Tyr<sup>685</sup> of VE-cadherin led to impaired barrier function. Furthermore, TNF $\alpha$  increases barrier permeability via phosphorylation of tyrosine residues in VE-cadherin [118, 119]. Tyrosine phosphorylation of VE-cadherin, although at a different residue (Tyr<sup>731</sup>) is needed for lymphocytes to migrate from blood into tissue. In this case, the phosphorylation event is initiated by lymphocyte binding, or activation of ICAM-1, an endothelial adhesion receptor [120]. Very little is known about phosphorylation of serine/threonine residues with respect to VE-cadherin, although a study by Yan *et al.*, 2013 suggests it has a similar barrier-disruptive effect as tyrosine phosphorylation [121]. Nevertheless, our current knowledge on the role of serine/threonine phosphatase PP2A in VE-cadherin phosphorylation requires extending.

### 1.3.3 Gap junctions

Gap junctions are another type of junction associated with the blood-brain barrier. They are formed by connexins and the connexin-like proteins, innexins and pannexins. Connexins are tetra-transmembrane proteins which form hemichannels, also called connexons, composed of six connexin subunits [122]. Connexins 37, 40 and 43, named after their respective molecular weights, are specifically expressed in vascular

endothelial cells [123, 124]. Gap junctions bring together connexons located on adjacent cells, while leaving a 2-nm gap, for which they were named 'gap' junctions [125]. These junctions help in communication between cells, and allow for the passage of ions, small molecules and second messengers [60]. Normal functioning of gap junctions is vital for tissue growth, development and homeostasis [126, 127].

## 1.4 Transmembrane movement

The transport of regulatory molecules and nutrients into the brain across the endothelium is achieved through active and passive transport (Figure 4). Two routes regulate the passage of fluid, solutes, and proteins across the endothelium; the transcellular route and paracellular route. Macromolecules are transported by transcytosis via transcellular transport, while small solutes (up to 3 nm radius) cross the endothelium by inter-endothelial junctions via the paracellular route [128, 129]. In the BBB, unlike all other endothelia, the physical barrier formed by tight junctions between endothelial cells forces most molecules to move via the transcellular route [58].

### 1.4.1 Transcellular transport route

Macromolecules such as albumin, insulin, hormones, and lipids are transported across the endothelium via transcellular transport. This transport mechanism is usually unidirectional, with macromolecules travelling from the apical to basolateral surface of the cells. Types of transcellular transport routes present at the blood-brain barrier include diffusion (Figure 4a), vesicle-mediated transcytosis, carrier-mediated transport and energy-dependent transport [130].

#### 1.4.1.1 Vesicle-mediated transcytosis

Transcytosis is a bidirectional process of transport of cargo across the cell cytoplasm, which involves three distinct steps; endocytosis, intracellular



vesicle transport and exocytosis. Endocytosis may be receptor-mediated or charge dependent/adsorptive. The second step, intracellular vesicle trafficking, can be mediated via three distinct types of vesicles in brain endothelial cells: 1) macropinocytotic vesicles, 2) clathrin coated pits which facilitate receptor-mediated transcytosis, and 3) caveolae which participate in both receptor trafficking and adsorptive-mediated endocytosis [131]. In the final step of transcytosis, the vesicle fuses with the target membrane, releasing the cargo into the extracellular space.

Charge dependent/adsorptive endocytosis (Figure 4e) is triggered through an electrostatic interaction between the negatively charged cell membrane surface and a positively charged protein or micro-molecule [132]. Cationic lipids, albumin, polymers and nanoparticles, which are positively charged, are internalized through adsorptive transcytosis [133, 134]. Receptor-mediated endocytosis (Figure 4d) is initiated by the binding of a ligand to a specific receptor located on the luminal side of a cell, and is well documented for all endothelial cells. Some of the essential compounds that are taken into the cell by their specific receptors include transferrin, insulin, thiamine, biotin, folic acid and vitamin B12 [135, 136].

#### 1.4.1.2 Carrier-mediated transport

Carrier-mediated transport (Figure 4c) utilizes transport proteins, also called transporters, which enable solutes such as amino acids, fatty acids, carbohydrates, nucleotides and vitamins to cross the blood-brain barrier [137]. Carrier-mediated transport can take place via diffusion facilitated by a transporter, or by active transport. Glucose is a great example, as it can be transported across the cell membrane by facilitated diffusion through glucose transporters (GLUT) but also by active transport via sodium dependent glucose transporters (SGLTs) [138].

#### 1.4.1.3 Energy-dependent transport

ATP-binding cassette (ABC) transporters use ATP as an energy source to transport substrates across the cell membrane [139]. ABC transporters are ubiquitously expressed, although they are most abundant at barriers and in excretory and absorption tissues [140]. In brain endothelial cells, they are primarily localized on the luminal side, extruding metabolic waste products, xenobiotics, drugs and nucleosides from the brain into the bloodstream (Figure 4f) [141]. P-glycoprotein, also known as multidrug resistance protein 1 (MDR1) or ABCB1, is the most important ABC transporter in the CNS, with a role in pharmacoresistance and neuroprotection. Studies have shown that dysfunction of P-glycoprotein or its downregulation contribute to Alzheimer's disease through an accumulation of amyloid- $\beta$  within the brain [142, 143].

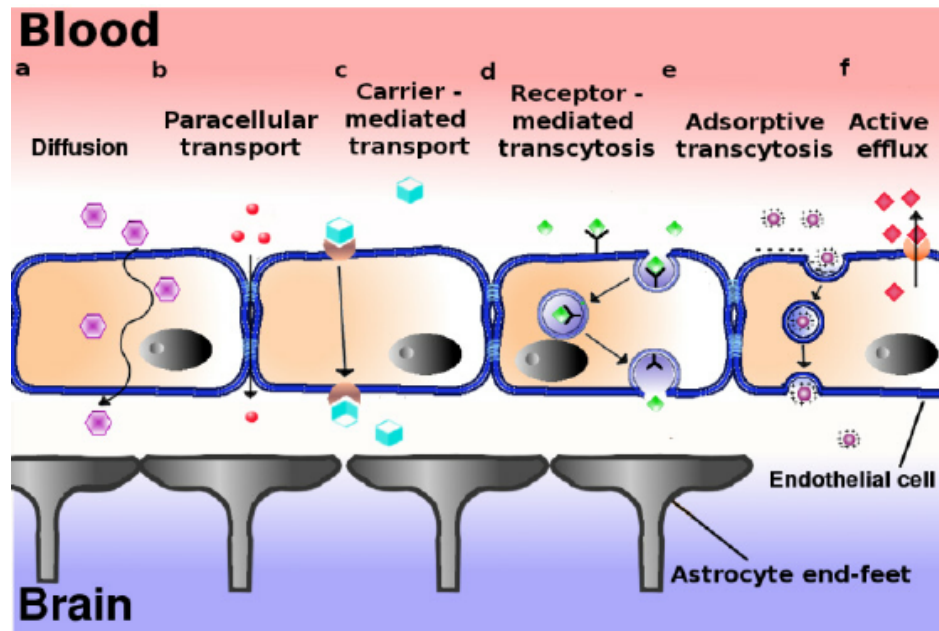


**Figure 4: Transmembrane transport pathways of the BBB.**

The main routes of transport of molecules across endothelial cells of the brain are a) diffusion down a concentration gradient, b) paracellular transport of gases and small lipophilic molecules, c) carrier-mediated transport of substrates including glucose and amino acids, d) receptor-mediated transcytosis of nutrients and signalling and regulatory molecules, e) adsorptive transcytosis of positively charged molecules and f) active efflux of drugs and waste products. Figure taken from Georgieva *et al.*, 2014 [144].

#### 1.4.2 Paracellular transport

Paracellular permeability of the endothelium is controlled by the inter-endothelial junctions; adherens, tight and gap junctions (Figure 4b) [145]. They allow the passage of small gaseous molecules such as oxygen and carbon dioxide, and small lipophilic agents such as ethanol and barbiturates [6]. The junction types present vary in different vascular beds. For example, tight and adherens junctions are intermingled in small arterioles, whereas in venules the inter-endothelial junctions present are mainly adherens junctions with only small areas of concentrated tight junctions on the apical side of the intercellular cleft (Figure 5). The architectural integrity of endothelial cells is primarily maintained by VE-

cadherin at adherens junctions, while tight junctions provide a secondary line of support with the exception of the vasculature of the brain where they are enriched [146, 147]. The integrity of adherens junctions is critical for the maintenance of paracellular permeability and their disruption results in fluid accumulation in the interstitium, which is often seen in pathologies such as inflammation and cerebral cavernous malformation [148, 149].

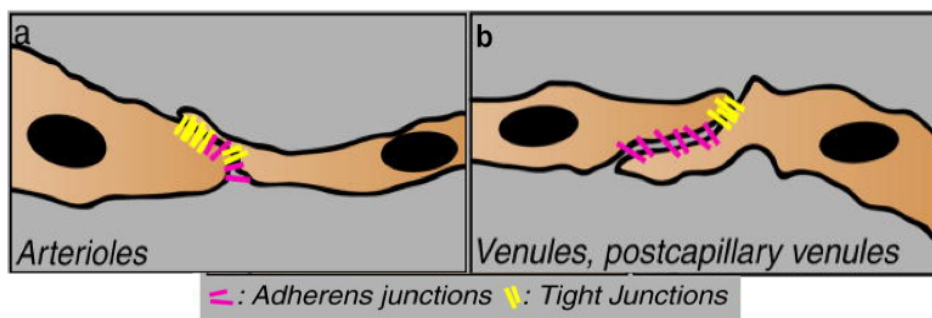


**Figure 5: Inter-endothelial junctions localized at microvessels.**

Tight junctions and adherens junctions are intermingled in arterioles (a). In venules (b), the transport between blood and tissues is primarily limited by adherens junctions, with a small area at the apical side only occupied by tight junctions. Figure taken from Dejana *et al.*, 2009 [146].

External stimuli can either increase or decrease paracellular permeability. The expression of certain mediators or cytokine secretion can weaken junctional adhesions, leading to leaking vessel walls. This can happen through the phosphorylation of junctional proteins, often leading to their internalization and junction destabilization [145]. The duration of the increase in permeability depends on the mediator responsible for the effect. For example, inflammatory cytokines and proangiogenic mediators such as kinin cleavage products and VEGF result in a sustained 'leaky' barrier, whereas thrombin, histamine and bradykinin elicit a transient and reversible increase in permeability [150].

### 1.4.3 Diapedesis

During an immune insult, immune cells are recruited to sites of inflammation. To do so, they travel from the blood across the endothelium and into the inflamed tissue, through a process named diapedesis [151]. Leukocytes traverse the endothelium of vessels by the paracellular and transcellular routes. There is conflicting data relating which route is predominantly used, and which is physiologically more important. However, transcellular diapedesis seems to be dominant in cells that possess very tight cell-cell junctions, such as those found at the blood-brain barrier [152, 153].

During transcellular diapedesis, the membrane of endothelial cells and leukocytes fuses, creating a channel between the basal and apical sides of the endothelium. The leukocytes then use that channel to cross the endothelium, without disturbing cellular junctions [154]. Leukocytes travelling via the paracellular route need to destabilize endothelial cell contacts, which are mediated by VE-cadherin. *In vivo*, VE-cadherin blocking antibodies lead to an increase in vascular permeability and accelerated immune cell extravasation [155]. Furthermore, replacing VE-cadherin by a fusion of VE-cadherin bound to the scaffolding protein,  $\alpha$ -catenin, resulted in an *in vivo* model resistant to the permeability-inducing effect of VEGF and leukocyte extravasation [152].

### 1.4.4. Traversing BBB for CNS drug delivery

Poor CNS access of most drugs is a result of the highly selective barrier formed by the cells of the neurovascular unit, which isolates the brain and spinal cord from the blood vessels [156]. Tight junctions located in the endothelium, low endosomal and pinocytic transport and the lack of fenestrations makes the diffusion of water soluble molecules across the blood-brain barrier very difficult [58, 157]. For a drug to be able to gain access into the CNS it needs to be sufficiently lipid soluble and have a

molecular weight of no more than 180 Da [158, 159]. Lipid solubility is the most important property that decides a drug's BBB permeability; however, other factors such as cerebral blood flow, plasma protein binding and the drug's affinity for its transport protein also control their permeability [160]. Only a small number of molecules meet these criteria, but even the ones that do are not guaranteed entry into the CNS [161]. Additionally, efflux pumps, such as P-gp, actively expel harmful molecules and therapeutics back into the blood [162]. As a result of these obstacles imposed by the blood-brain barrier, 98 % of small molecules and all drugs with a large molecular weight are unable to enter the CNS [163].

Due to the abovementioned limitations in drug delivery across the blood-brain barrier, there are few effective therapies available for the treatment of CNS diseases. Approaches used to bypass the blood-brain barrier to increase drug delivery to the CNS are divided into the classes: surgical and pharmacological. Surgical strategies are mostly very invasive and include transcranial delivery, trans-nasal delivery, convection enhanced delivery and osmotic BBB disruption. Pharmacological approaches include synthesis of a pro-drug, drug modification and utilizing specific receptor or carrier-mediated transport systems [164].

#### 1.4.4.1 Osmotic BBB disruption

The concept of osmotic blood-brain barrier disruption was started with a 1972 study by Rapoport *et al.*, in which concentrated solutions applied to the cerebral cortex of a rabbit led to blood-brain barrier opening, demonstrated by CNS tissue staining by a dye circulating in the bloodstream [165]. Shortly thereafter the authors published another study, showing that the increase in blood-brain barrier permeability caused by hypertonic solutions is due to the shrinkage of cerebrovascular endothelial cells which leads to opening of the tight junctions [166].

The procedure of osmotic BBB disruption has been used in preclinical and clinical studies for the treatment of brain tumours, although it's not a standard practice due to the need for repeated hospitalization and often general anaesthesia [167]. Still, osmotic BBB disruption has gained the interest of many research groups as drug delivery increases 10 to 100 times when using this method compared to delivering the drug without an osmotic agent [168]. Furthermore, neurocognitive function of patients who underwent the procedure is not declined, although adverse effects such as seizures and brain herniation have been documented [169].

#### 1.4.4.2. Receptor-mediated transcytosis

Receptor-mediated transcytosis is a method of delivering drugs to the brain that requires the generation of a drug chemically linked to a ligand which targets a specific receptor. The ligand can be either an endogenous protein, a mimetic peptide ligand or an antibody which targets the receptor [170]. The targets located in brain endothelial cells which have gained the most interest are the insulin, transferrin and low-density lipoprotein (LDL) receptors [171].

Transferrin is the protein responsible for delivering iron into the brain. Multiple animal studies have shown that drugs conjugated to transferrin or to an anti-transferrin receptor antibody have a much higher ability to cross the blood-brain barrier [172-174]. Similar findings were reported for the insulin receptor. Furthermore, the insulin receptor was the first receptor to be used to deliver drugs to the brain via the receptor-mediated transcytosis approach in a clinical study, aimed at patients with mucopolysaccharidosis type I (MPSI), a genetic disorder caused by a mutation in the gene encoding the  $\alpha$ -L-iduronidase (IDUA) lysosomal enzyme. In that study, human IDUA was fused to an insulin receptor monoclonal antibody, enabling the insulin receptor to act as a Trojan horse to ferry the enzyme into the brain [175]. 11 MPSI pediatric patients with cognitive impairment were treated with the IgG-IDUA fusion protein

for 52 weeks. Some adverse effects such as transient hypoglycaemia and reactions at the infusion site were reported, however, the positive effects of the therapy which include cognitive and somatic stabilization or improvement, make this novel approach clinically significant [176].

#### 1.4.4.3 Carrier-mediated transcytosis

Some drugs can gain access into the cell utilizing naturally occurring transport proteins. One such transporter is the large amino acid transporter 1 (LAT1), responsible for transporting large amino acids, neurotherapeutics and thyroid hormones in and out of the brain [177]. LAT1-mediated drug delivery is an enticing approach as LAT1 is overexpressed not only on brain capillary endothelial cells, but also in many cancers, including glioblastoma [178]. In a 2017 study, glioblastoma bearing mice treated with a LAT1-selective drug carrier had a 60 % increase in survival [179]. These findings demonstrate the enormous potential of carrier-mediated transcytosis as a drug delivery mechanism.

### 1.5 Blood-Brain Barrier Pathophysiology

Transient opening of the blood-brain barrier is a standard process, allowing factors essential for normal functioning of the CNS to reach it. The endothelium, astrocytes and nerve terminals tightly regulate barrier permeability through mediators such as glutamate, aspartate, endothelin-1, ATP, nitric oxide, IL-1 $\beta$  and TNF $\alpha$ . Agents circulating in the blood, such as serotonin, histamine, bradykinin and substance P can also modulate blood-brain barrier permeability [50, 180]. However, prolonged opening of the endothelial tight junctions at the blood-brain barrier, along with other pathological changes including enhanced transcytosis, pore formation, and changes in nutrient and water transport lead to loss of barrier integrity. This is a critical step in the development and progression of many CNS diseases [181]



Neuroinflammation is localized within the brain or spinal cord and is generally mediated through the production of cytokines (IL-1 $\beta$ , IL-6, TNF $\alpha$ ), chemokines (CCL2, CCL5, CXCL1), ROS and other inflammatory mediators (nitric oxide and prostaglandins). These are released by microglia, astrocytes and endothelial cells, as well as peripherally derived immune cells [182, 183]. Pathological neuroinflammation coincides with microglia activation and cytokine and chemokine production, which can manifest edema, increased blood-brain barrier permeability and breakdown [8, 184].

#### 1.5.1 Junctional proteins in BBB pathologies

The integrity of tight junctions and adherens junctions is essential for protection of the brain during inflammation and infection [185]. The structure and function of these junctions is modulated by many cytokines and chemokines. For example, increased production of CCL2 as a result of neuroinflammation induces VE-cadherin and  $\beta$ -catenin phosphorylation, leading to their dissociation from the adherens junctions and weakening of the blood-brain barrier [186]. Claudin-5 is also downregulated in neuroinflammation, although through a different mechanism involving IL-1 $\beta$ -mediated inhibition of claudin-5 transcription in brain endothelial cells [187]. TNF $\alpha$  and IFN $\gamma$  also decrease trans endothelial electrical resistance, which is associated with increased internalisation of occludin, JAM-1, and claudin-1 and -4, all of which contribute to decreased BBB function [188, 189]. Interestingly, peripheral inflammation also appears to alter blood-brain barrier function as injection of formalin,  $\lambda$ -carrageenan and complete Freund's adjuvant into a hind paw of a rat caused an increase in blood-brain barrier permeability and altered abundance of junctional proteins. More specifically, occludin was found downregulated, ZO-1 was upregulated, while the expression of claudin-1 remained unchanged compared to the control group. This

study shows that inflammation localized outside the CNS can have a detrimental effect on the blood-brain barrier [190].

### 1.5.2 Blood-Brain Barrier Dysfunction in Disease

The blood-brain barrier is a highly dynamic anatomical boundary, with the ability to quickly react to physiological stressors such as inflammation, trauma, hypoxia and pain [191]. Therapeutic targeting of the blood-brain barrier is crucial in many clinical settings, as a dysfunctional blood-brain barrier can not only aggravate, but also initiate a plethora of pathologies and diseases, including Alzheimer's disease [192], multiple sclerosis [193], Parkinson's disease [194], epilepsy [195] and cerebral malaria [196], many of which are covered in detail in several excellent reviews [137, 197, 198]. As such, this overview summarizes the effect of some CNS diseases on the blood-brain barrier and the junctional proteins localised at the BBB, and where possible, a link is made between the specific CNS disease and neuroinflammation and/or PP2A.

#### 1.5.2.1 Multiple Sclerosis

Multiple sclerosis is the most common type of neurological autoimmune progressive condition in adults in Ireland [199]. In multiple sclerosis, auto-reactive immune cells attack myelin sheath lining the nerve fibres, resulting in an array of symptoms including visual impairment due to optic nerve inflammation, fatigue, muscle spasms and weakness [200].

Not surprisingly, increased blood-brain barrier permeability has been documented in patients with multiple sclerosis [193], with data from post-mortem samples showing abnormal localization of the tight junction proteins JAM-A, occludin and ZO-1 [201]. In keeping with this, when human brain microvascular endothelial cells are exposed to serum from patients with relapse-remitting multiple sclerosis, transendothelial electrical resistance and claudin-5 protein expression are decreased. [202]. The downregulation of junctional proteins seen in multiple

sclerosis is most likely mediated by IFN $\gamma$ , TNF $\alpha$  and IL-1 $\beta$  and the chemokine monocyte chemoattractant protein-1 [203, 204].

#### 1.5.2.2 Alzheimer's disease

Alzheimer's disease (AD) is the most prevalent neurodegenerative disorder in the world, affecting nearly 25 million people. It is characterised by a gradual decline in certain cognitive domains, such as memory, personality and language [205]. The main pathological characteristics of AD are 1) neurofibrillary tangles which form due to the accumulation of hyperphosphorylated tau (p-tau) protein, 2) deposition of  $\beta$ -amyloid plaques on the surface of neurons, and 3) a deficiency in acetylcholine (Ach) [206]. Interestingly, the PP2A inhibitor SET is responsible for tau hyperphosphorylation, suggesting a role for PP2A in AD [207]. Furthermore, a sustained immune response is now also recognised as a feature of AD pathogenesis, as amyloid and tau pathologies are aggravated when they coincide with chronic neuroinflammation brought about by activated microglia [208].

Blood-brain barrier dysfunction plays a role in the pathogenesis of Alzheimer's disease. The transport proteins RAGE (receptor for advanced glycation end products) and LRP-1 (low density lipoprotein receptor-related protein 1) present on the cells of the neurovascular unit are responsible for the influx and efflux of  $\beta$ -amyloid to and from the brain, respectively [209]. Not surprisingly, increased expression of RAGE receptors on astrocytes and neurons, and a decreased expression of LRP-1 receptors on endothelial cells has been reported in AD, leading to the formation of  $\beta$ -amyloid plaques [210, 211]. Furthermore, decreased abundance of claudin-5 and occludin has been documented in post-mortem samples from patients with AD, highlighting the importance of junctional proteins in maintaining an intact blood-brain barrier [212].

### 1.5.2.3 Parkinson's disease

Parkinson's disease (PD) is another progressive neurological disorder that mainly affects the motor system. The most common symptoms include tremors, muscle stiffness and slowness of movement; however, patients may also experience cognitive and psychological problems [213]. Pathophysiologically, the characteristic features of Parkinson's disease are the loss of dopamine-containing neurons in the substantia nigra region of the brain and a widespread accumulation of  $\alpha$ -synuclein into clumps termed Lewy bodies [214]. As with MS and AD, increased permeability of the blood-brain barrier has been documented in Parkinson's disease. Although the mechanism is still unclear, a reduced expression of the tight junction proteins ZO-1 and occludin was discovered in animal models of Parkinson's disease [194, 215].

Neuroinflammation also plays a role in the pathogenesis of Parkinson's disease. Microglia resident in the brain are found activated in PD. They take on the pro-inflammatory phenotype and produce  $\text{TNF}\alpha$ , IL-16, ROS, reactive nitrogen species (RNS) and inducible nitric oxide synthase (iNOS) [216, 217]. Furthermore, a study utilizing an animal model of chronic PD found the number of anti-inflammatory microglia to diminish and pro-inflammatory microglia to increase gradually as the disease progresses, which might play a role in the degeneration of dopaminergic neurons [218]. Other factors which contribute to the neuroinflammation recognized during Parkinson's disease are the dysfunction of astrocytes and CNS infiltration of cytotoxic T cells [219, 220]

### 1.5.2.4 Ischemic Stroke

Stroke is the second top cause of death globally, and a primary cause of long-term disability [221]. Various factors including hypertension, diabetes mellitus and smoking can increase the risk of having a stroke [222]. The two types of brain stroke are haemorrhagic stroke, which

happens as a result of vessel rupture, and ischemic stroke which is due to vessel blockage or occlusion. Ischemic strokes are much more prevalent, accounting for over 80 % of all strokes [223]. An ischemic stroke is characterised by a reduced blood supply to the affected brain region that leads to reduced delivery of oxygen and essential nutrients such as glucose [224].

Breakdown of the blood-brain barrier and increased paracellular permeability are a hallmark of ischemic stroke pathology. The characteristics of BBB disruption are activation of matrix metalloproteinases (MMPs), which are associated with barrier opening and edema formation, degradation of integrins, which bind cells to the extracellular matrix, and the disruption of cell-cell junctions [225]. Decreased expression of occludin, claudin-5, ZO-1 and VE-cadherin has been documented following ischemic stroke [226-228].

#### 1.5.2.5 Viral infections

The functional and structural architecture of the CNS can be disrupted during viral infections.

Viral infections usually downregulate the expression of junctional proteins, disrupting the blood-brain barrier and therefore facilitate viral entry into the CNS. For example, mouse adenovirus type 1 (MAV-1) targets brain endothelial cells, leading to reduced expression of claudin-5, occludin and ZO-2, loss of transendothelial electrical resistance and barrier breakdown [229]. Similar alterations in the expression of tight junction proteins are seen in West Nile virus infections, where claudin-1 and JAM-1 are downregulated or Human T-Lymphotropic Virus (HTLV-1) infected cells, where the expression of ZO-1 and occludin is reduced [230, 231].

Interestingly, severe acute respiratory syndrome coronavirus 2 (SARS-CoV-2), the virus responsible for the current outbreak of coronavirus infectious disease 2019 (COVID-19) might also be able to gain access into the CNS. Typical symptoms of COVID-19 include fever and cough, however some patients also suffer from gastrointestinal (GI) and neurologic symptoms [232, 233]. Although there is no consensus among the scientific community as to how this respiratory disease cause neurologic manifestations, a recent article suggests the mechanism involves the virus travelling to the CNS from an infected GI tract via the vasculature, vagal nerve or the lymphatic system [234]. Another article proposes seizures associated with a severe COVID-19 infection are due to blood-brain barrier breakdown as a result of pro-inflammatory cytokines and possible neurotropism of the virus [235]. This mechanism is highly probable, as early studies on human coronaviruses show they are neuroinvasive and neurotropic, with viral RNA present in post-mortem brain samples [236]. Additionally, *in vitro* studies show human coronaviruses can infect human microglia and astrocytes [237]; however this may not be true in relation to SARS-CoV-2 as analysis of cerebrospinal fluid and MRI testing of a patient with COVID-19-related encephalopathy showed the virus is unable to cross the blood-brain barrier [238]. Interestingly, PP2A, a hugely important member of the protein serine/threonine phosphatases family, has been suggested to play a role in SARS-CoV-2 pathogenesis. A surface coronavirus spike (S) glycoprotein responsible for membrane fusion and receptor-recognition has been shown to contain a PP2A-B56-binding motif which might recruit PP2A, disrupting the hosts' PP2A-mediated pro-inflammatory responses. This interaction between SARS-CoV-2 and PP2A could be a potential target for the development of a new therapeutic approach against COVID-19 [239].

## 1.6 Protein Phosphatases

Proteins transiently shift from a dephosphorylated to a phosphorylated state and vice versa, depending on the cell's physiological needs. Protein phosphorylation is coordinated by kinases, which add a phosphate group onto proteins and phosphatases, which remove the phosphate groups [240]. Human cells possess genes encoding around 500 different protein kinases, but only about 250 phosphatases to counterbalance their action [241, 242].

Protein phosphatases are classified based upon their dephosphorylation sites into three major classes: tyrosine, serine-threonine and dual-specificity phosphatases [243]. Most of the phosphorylation events within a cell happen on the serine residues (86.4 %), followed by threonine (11.8 %) and tyrosine (1.8 %) [244]. Protein serine/threonine phosphatases (PSP) are further broken down into phosphoprotein, metal dependent and aspartate-based phosphatases. Protein tyrosine phosphatases (PTP) are grouped into three classes based on their gene sequence and structure, with some classes further divided into sub-families (Figure 6) [240].

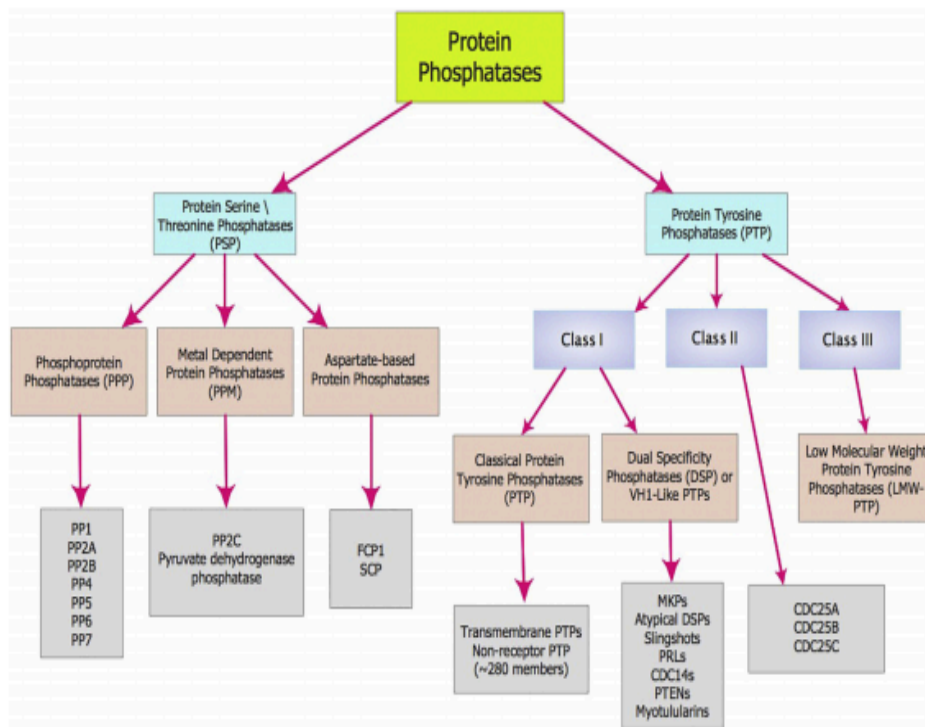


**Figure 6: Protein Phosphatases classification.**

Overview of the protein serine/threonine phosphatase (PSP) and protein tyrosine phosphatase (PTP) families. Image taken from Elgenaidi & Spiers, 2019 [245].

Protein kinases have been studied much more extensively than protein phosphatases, especially regarding drug development and human diseases. For example, in 2016 there were 45 times more papers on PubMed that studied the role of serine/threonine protein kinases in cancer compared to serine/threonine phosphatases in cancer. The reason why phosphatases are less studied than kinases might have to do with their structure, making them more difficult to work with, as most phosphatases, including PP2A, are multimers, while many kinases, like Erk (extracellular signal regulated kinase) and PKC (protein kinase C) are monomers [246]. Despite this, protein phosphatases are starting to emerge as drug targets not only in cancer [247], but also in cardiovascular disease [248] and neurodegenerative disease [249].



### 1.6.1 PP2A

Within the Ser/Thr phosphatase subfamily, protein phosphatase 2A (PP2A) is a key member which accounts for over 50 % of protein Ser/Thr phosphatase activity and 1 % of total protein mass within most cells [250, 251]. PP2A plays a prominent role in cell cycle, metabolism, growth, apoptosis, and signal transduction. It is also crucial for the regulation of a variety of targets in both non-excitabile and excitable cell types, including regulatory enzymes, transcription factors, cytoskeletal proteins, ion channels and transporters [252-254]. Importantly, dysfunction of the PP2A system is linked to a plethora of human diseases, including heart disease [248], neurodegenerative disorders [255], asthma [256], cancer [257] and diabetes [258]. Interestingly, PP2A also limits inflammatory responses by negatively modulating signalling pathways, such as the NF- $\kappa$ B and MAPK signalling pathways. For example, PP2A activates tristetraprolin (TTP), a zinc-finger mRNA binding protein, which negatively regulates inflammation by decreasing mRNA stability of many pro-inflammatory transcripts [259, 260]. This suggests that PP2A activation might be an effective treatment for inflammation-mediated disorders [261].

### 1.6.2 Structural organization of PP2A

The typical mammalian PP2A holoenzyme is a heterotrimer composed of a regulatory B subunit, a catalytic C subunit and a structural (aka scaffolding) A subunit (Figure 7). However, a third of all PP2A found inside the cell is only made up of the catalytic and scaffolding subunits, and is referred to as the 'core dimer' [262].

The globe-shaped catalytic subunit (PP2Ac) is ubiquitously expressed, however its highest expression is documented in the brain and heart [240]. The catalytic subunit has two isoforms, C $\alpha$  and C $\beta$ . Both isoforms are 35 kDa in size and share 97 % sequence homology; however C $\alpha$  is 10

times more abundant than C $\beta$  in most cells [263, 264]. They are also differently localized within the cell, with C $\alpha$  found mostly in the membrane and C $\beta$  within the nucleus and cytoplasm. The  $\alpha$  and  $\beta$  subunits are encoded by two different genes. Each gene is composed of six introns and seven exons, with exon 1 and 7 encoding the amino acid sequence which plays a role in regulation, and the sequence encoded by exons 2 to 6 encoding amino acids associated with catalysis and substrate binding [240]. Both isoforms have a conserved <sup>304</sup>TPDYFL<sup>309</sup> motif located in their C-terminal tail. Methylation and phosphorylation on Tyr and Thr residues of this motif regulate binding of the B subunit to the PP2A core dimer [265].

The scaffolding subunit (PP2Aa) also has two isoforms, A $\alpha$  and A $\beta$ . They are both ~65 kDa, share 87 % sequence homology and are mostly found in the cytoplasm [266]. The A $\alpha$  isoform is found within the core dimer/holoenzyme of 90 % of PP2A complexes within most cells, and binds to the catalytic and regulatory subunits stronger than A $\beta$  isoform [267]. The scaffolding subunit is horseshoe-shaped due to 15 HEAT (Huntington/elongation/A-subunit/TOR) tandem repeats which interact with each other [268]. The HEAT repeats are also essential for holoenzyme assembly, as the catalytic subunit binds to 4 HEAT repeats, creating the core dimer, which then binds to a specific regulatory subunit (of which there are > 15 subunits), forming the heterotrimeric PP2A holoenzyme complex [266] (Figure 7).

The regulatory subunit (PP2Ab) has four families: B (aka PR55/B55), B' (PR61/B56), B'' (PR130/PR72/PR48) and B''' (PR110/PR93), each of which has multiple isoforms and splice variants. The B' family is the biggest, with at least eight isoforms, which share a core domain and have key roles in cell cycle and signalling, due to their ability to dephosphorylate Erk and Akt [266]. Although regulatory subunits are conserved within their respective families, there is little sequence overlap between families

[251]. Different regulatory subunit classes use different mechanisms to bind to the core dimer. For example, B' family isoforms bind to both scaffolding and catalytic subunits, while the B family isoforms only bind to the HEAT repeats of the scaffolding subunit [245]. The regulatory subunit plays a crucial role in establishing substrate specificity and the subcellular localization of PP2A [269].

PP2A can form 96 unique holoenzyme complexes as a result of multiple isoforms of each of the catalytic, scaffolding and regulatory subunits [265]. The ability of PP2A to dephosphorylate a plethora of substrates and modulate a variety of cellular functions is due to this ability to form multiple holoenzymes, as well as being able to be regulated through the actions of activators, inhibitors and post-translational modifications [250, 270].

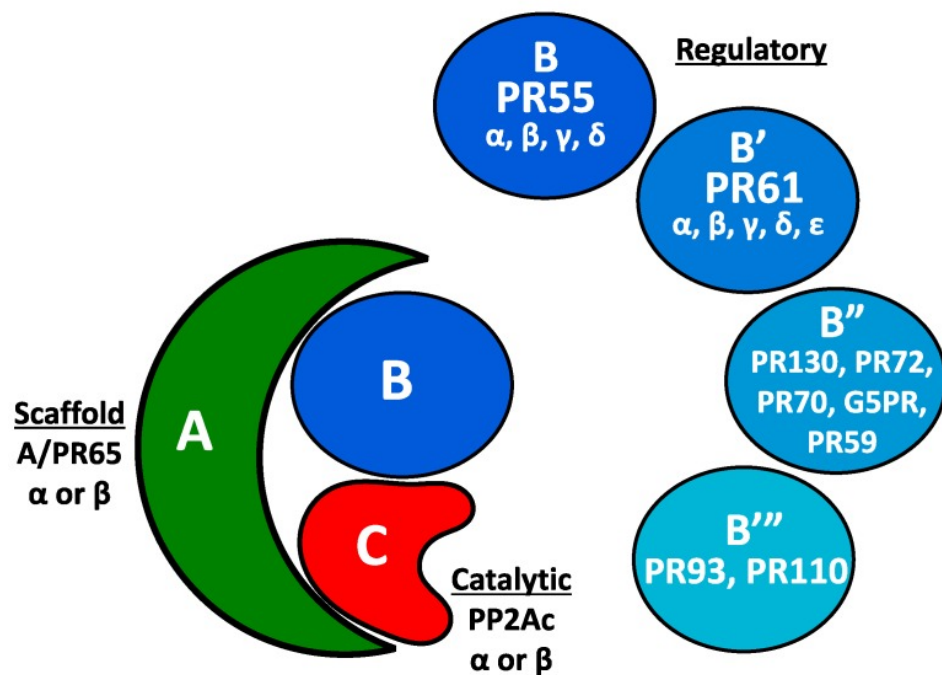


**Figure 7: The structure of PP2A.**

PP2A holoenzyme consist of the scaffolding (A), catalytic (C) and regulatory (B) subunits, each of which has many possible isoforms. Figure taken from Thompson & Williams, 2018 [271].

### 1.6.3 Post-translational modifications of PP2A

As mentioned above, PP2A's hetero-multimeric composition, substrate specificity and catalytic activity are regulated by post-translational modifications. The two major modifications are phosphorylation and methylation, which occur mostly on the catalytic subunit, although the regulatory subunit is also subject to post-translational modification [272].

#### 1.6.3.1 PP2A phosphorylation

Several tyrosine kinases including epidermal growth factor receptor (EGFR), insulin receptors, p60v-src and p56lck kinase can phosphorylate PP2Ac *in vitro* [273]. Tyrosine phosphorylation of PP2Ac occurs on Tyr<sup>307</sup>, which leads to a transient deactivation of phosphatase activity, possibly through enhanced binding of the endogenous inhibitors of PP2A – CIP2A and SET [274]. This phosphorylation event is enhanced in the presence of IL-1 and TNF $\alpha$ , insulin and epidermal growth factor, and the exogenous PP2A inhibitor, okadaic acid. PP2Ac can also be phosphorylated by an autophosphorylation-activated protein kinase on threonine residues [275]. As with tyrosine phosphorylation of PP2Ac, threonine phosphorylation leads to inactivation of phosphatase activity, which can be regained through auto-dephosphorylation [273, 276]. Furthermore, phosphorylation of PP2Ac on threonine residues plays a role in assembly of the trimeric holoenzyme. In a study by Longin *et al.*, mutation of Thr<sup>304</sup> to a non-phosphorylatable mutant showed all possible PP2A complexes can still be formed, whereas binding of the B subunits was prevented in phosphorylation-mimicking mutants, showing that PP2A phosphorylation can regulate holoenzyme assembly and functional specificity [277].

In contrast, less is known about the dephosphorylation of PP2A. In an early study by Chen *et al.*, it was suggested that PP2A undergoes dephosphorylation through an auto-dephosphorylation mechanism [273, 278]. This was based on data showing okadaic acid to prevent

dephosphorylation of PP2Ac; however, this should be viewed with caution as the concentration of okadaic acid used was sufficient to inhibit other Ser/Thr phosphatases [279].

PP2Ac isn't the only subunit that is subject to phosphorylation. There are three phosphorylation sites on the scaffolding subunit; Ser<sup>303</sup>, Ser<sup>314</sup> and Thr<sup>268</sup>. PP2Aa phosphorylation results in inhibition of the interaction between the scaffolding and catalytic subunits and disruption of PP2A-mediated signalling [280]. The regulatory subunit can also be phosphorylated, although with a different outcome than scaffolding subunit phosphorylation. *In vitro* and *in vivo* studies show that protein kinase R (PKR) and protein kinase A (PKA) phosphorylate B56 $\alpha$  and B56 $\delta$ , respectively, which manifests as an increase in PP2A activity [281, 282]. Likewise, the B'' regulatory subunit family is also phosphorylated by PKA at Ser<sup>60</sup> and Ser<sup>573</sup>, which broadens substrate specificity of the holoenzyme [283].

#### 1.6.3.2 PP2A methylation

The catalytic subunit of PP2A is methylated and demethylated by methyltransferase and methylesterase enzymes, respectively [284]. PP2A methylation is believed to increase PP2A holoenzyme activity, although early studies showed it had no effect [285, 286]. PP2Ac methylation is carried out by leucine carboxyl methyltransferase 1 (LCMT1), an enzyme which exclusively catalyses the methylation of Leu<sup>309</sup> on the <sup>304</sup>TPDYFL<sup>309</sup> motif on the C-terminal tail of PP2Ac [286, 287]. PP2Ac methylation plays a role in holoenzyme assembly as it is necessary for B subunit binding [284]. This is supported by a study showing LCMT1 knockdown was associated with B subunit degradation and apoptotic cell death [277]. However, it should be pointed out that B' and B'' subunits can bind to unmethylated PP2Ac [284]. As a side note, LCMT1 deregulation and a

disturbance of PP2A methylation/demethylation is linked to the pathogenesis of Alzheimer's disease [288].

PP2A demethylation is carried out by protein phosphatase methylesterase 1 (PME1), which directly binds to the active site of the catalytic subunit and removes the methyl group as well as manganese ions, essential for phosphatase activity, thus rendering PP2A inactive [289]. Interestingly, PP2A's phosphatase activity can be restored by phosphotyrosyl phosphatase activator (PTPA) via several different mechanisms. PTPA can facilitate the detachment of PME1 from PP2A, allowing the enzyme to function normally again [290]. PTPA can also promote PP2A activation by increasing its methylation by LCMT1 or by increasing its dephosphorylation by tyrosine phosphatase 1B [291, 292]. Alternatively, it has been proposed that PTPA facilitates re-binding of the regulatory subunit by inducing a conformational change in PP2Ac [293, 294].

#### 1.6.4 PP2A inhibitors

The activity of PP2A can be hindered by several endogenous and exogenous inhibitors. An overexpression of the endogenous inhibitors is generally associated with cancer; however, some have been assigned a tumour suppressive function [295]. The exogenous inhibitors of PP2A are natural compounds mostly derived from aquatic invertebrates, insects, and microorganisms. PP2A inhibitors have generated much interest due to their potential use in cancer and as a tool for investigating PP2A's function [296].

##### 1.6.4.1 SET

Inhibitor 2 of PP2A, also known as SET, is a 39 kDa protein principally located in the nucleus. It was first isolated from a patient with acute undifferentiated leukaemia [297] and its overexpression is now regarded

as a sign of aggressive disease [298]. Upregulated SET is also found in other human tumours, including breast, colorectal and head and neck squamous cell carcinoma, as well in Alzheimer's disease [207, 299-301]. SET plays a key role in a variety of cellular processes, including transcriptional activation, cell differentiation and proliferation [301, 302].

SET strongly and selectively inhibits PP2A, but has little, if any, effect on protein phosphatase 1, 2B and 2C [303]. SET directly binds to the catalytic subunit of PP2A through its amino and carboxy termini, leading to an inhibition of PP2A's phosphatase activity [304]. A recent study showed SET can also bind to the scaffolding subunit of PP2A, although the mechanism remains enigmatic [305].

SET's activity is regulated through posttranslational modifications, for example, phosphorylation at Ser<sup>171</sup> decreases SET's inhibitory activity, while phosphorylation at Ser<sup>9</sup> and Ser<sup>24</sup> activates SET [297, 306]. Compounds that target PP2A inhibitors have recently gained a lot of interest. For example, the FDA approved drug Fingolimod (aka FTY-720) which causes SET to dissociate from PP2Ac through a mechanism which likely involves SET phosphorylation at Ser<sup>171</sup> is used to treat multiple sclerosis and lately to treat cancer [307, 308]. A recent *in vitro* study has also shown that SET depletion increases the sensitivity of cancerous cells to drug treatment, highlighting the potential of therapies that target SET. Surprisingly, such drug response was not seen in cells lacking another inhibitor of PP2A, CIP2A [309].

#### 1.6.4.2 CIP2A

Cancerous inhibitor of PP2A (CIP2A) is a 90 kDa protein, whose overexpression is reported in many cancers including breast, lung and gastric cancers, and as with SET, it's associated with disease aggressivity and poor prognosis [310-312]. CIP2A forms homodimers that can directly

interact with the B56  $\alpha$  and  $\gamma$  isoforms of the regulatory subunit of PP2A, which are believed to be the key tumour suppressors of the B subunit family. Interestingly, inhibiting the expression of these PP2Ab isoforms or inhibiting CIP2A dimer formation, destabilizes CIP2A in human HeLa cells [313].

CIP2A can also indirectly inhibit PP2A's function by interacting with other proteins. For example, CIP2A can interact with the oncogenic transcription factor c-Myc, inhibiting PP2A from dephosphorylating it. This in turn prevents proteolytic degradation of c-Myc, leading to malignant cellular growth [314]. CIP2A also supports tumour growth by indirectly inhibiting PP2A activity towards mTORC1. mTORC1 is a protein complex that negatively regulates autophagy, a process of degrading and recycling cytosolic components, which is important for the survival of cancer cells. By inhibiting PP2A activity in an allosteric manner, CIP2A aids phosphorylation and stabilization of mTORC1 substrates, inhibiting autophagy and therefore promoting malignant cell growth [315, 316].

Interestingly, a recent study by Liu *et al.*, has suggested a link between the two inhibitors of PP2A, CIP2A and SET. They identified a feedforward loop consisting of pErk/pElk-1/CIP2A/PP2A, and showed that inhibition of SET using TD19, a novel SET/PP2A interaction inhibitor interrupts this loop resulting in restoration of PP2A activity [317].

#### 1.6.4.3 Alpha-4 ( $\alpha$ 4)

Alpha-4 is a 52 kDa phosphoprotein expressed in a variety of cell types, including immune cells such as B and T cells, but also non-immune cells such as those found in the brain and liver [318]. From a structural perspective, amino acids 94 to 202, which are in the middle region of the alpha-4 protein, directly bind to the catalytic subunit of PP2A. It is generally believed that this interaction inhibits PP2A activity [319, 320],



however, more recent studies suggest alpha-4 to have a regulatory rather than inhibitory effect on PP2A. For example, a 2007 study has shown an overexpression of alpha-4 resulting in increased PP2A activity [321] and another study demonstrated alpha-4 deletion resulting in loss of all PP2A complexes, as well as loss of PP4 and PP6. The mechanism here is related to the role of alpha-4 in modulating the assembly and maintenance of the PP2A holoenzyme by protecting it from proteasomal degradation during periods of cellular stress [322].

#### 1.6.4.4 Inhibitor 1 of PP2A (I1<sup>PP2A</sup>)

I1<sup>PP2A</sup> is a 28 kDa protein, first purified and characterised along with the better known PP2A inhibitor I2<sup>PP2A</sup>/SET. Both of these proteins exhibit PP2A-specific inhibitory activity and have little, if any, effect on the other phosphatases [303]. I1<sup>PP2A</sup> is known by many names, including ANP32A, MAPM and PHAP1 [323]. Unlike SET, I1<sup>PP2A</sup> has been assigned a tumour suppressive role as its inactivation is associated with tumour evolution and progression [295]. Other functional roles have also been assigned to I1<sup>PP2A</sup>, such as participating in cell-mediated cytotoxicity and HLA class II-mediated intracellular signalling [324, 325].

#### 1.6.4.5 Okadaic acid

Pharmacological inhibition of PP2A has traditionally been achieved by utilizing naturally occurring compounds, which are often toxins. One such compound is okadaic acid (OA). This toxin strongly inhibits PP2A (IC<sub>50</sub> 0.1 nM), as well as PP1 (IC<sub>50</sub> 15nM), 4, 5 and 2B to a lesser extent [326, 327]. OA is a cytotoxic polyether first isolated in 1981 from a black sponge [328]; however, it has since been shown that the sponge doesn't produce it. Instead it acquires it through feeding on algal dinoflagellates in the genera *Dinophysis* and *Prorocentrum* [329]. Overgrowth of these algae is a major public health concern, as they accumulate in fish and shellfish that feed on them [330]. Ingestion of seafood contaminated with okadaic

acid leads to diarrhoeic shellfish poisoning, a syndrome characterised by diarrhoea, vomiting and nausea [331].

The toxic effects of okadaic acid have been extensively studied in the last few decades. OA administered orally can enter the bloodstream and is distributed to organs within minutes. OA can be found in intestinal tissue and organs 24 hours after oral administration, and in the intestines up to four weeks after oral exposure, demonstrating that it is slowly eliminated by the body [332]. When applied topically, OA acts as a potent tumour promoter [333]. On a cellular level, the most reported cytotoxic effect of OA is the induction of apoptosis and alterations of the cell cycle [334]. OA also targets the cytoskeleton and morphological changes such as actin microfilament reorganization, cell rounding and loss of focal adhesion are seen in cells exposed to OA [335].

The effect of okadaic acid on junctional proteins has also gained interest recently. In intestinal epithelial cells, OA upregulates the channel-forming claudins, claudin-4 and -2, downregulates ZO-1 and therefore decreases barrier integrity [336]. E-cadherin-mediated cell-cell adhesion is also disrupted upon exposure of cells to OA [337]. However, there is some controversy regarding the effect of OA on junctional proteins, as a 2002 study showed that OA induces the recruitment of occludin, claudin-1 and ZO-1 to tight junctions, positively regulating tight junction assembly [338].

#### 1.6.4.6 Other exogenous inhibitors

Although PP2A is known to be a tumour suppressor, some studies utilize PP2A inhibitors as anti-cancer tools. Senescent tumour cells often contribute to treatment-resistant cancers as conventional anti-cancer treatments and radiotherapy are aimed at actively dividing cells. In such a scenario, inhibition of PP2A induces mitosis and helps overcome cell senescence, making the tumour cells susceptible to treatment [339, 340].

For example, LB-100, a novel inhibitor of PP2A, inhibits the proliferation of human tumour cell lines and increases the anti-tumour effect of co-administered drugs without increasing their toxicity [341, 342]. LB-100 has been shown to effectively sensitize glioblastoma xenograft mouse models to the actions of chemotherapeutics and radiotherapeutics, by inducing aberrant cell cycle progression and decreasing cell's ability to repair DNA breaks [339, 343]. These studies show that the role of PP2A in regulating the cell cycle is much more complex and multi-faceted than previously thought, as both PP2A inhibitors and activators can be used to treat cancer.

#### 1.6.5 Activators of PP2A

Given the well-established role of PP2A as a tumour suppressor it is not surprising that re-activation of PP2A using natural and synthetic compounds is emerging as a therapeutic approach in cancer [344].

##### 1.6.5.1 FTY-720

FTY-720, also known as fingolimod, is an oral sphingosine analogue with anticancer and immunosuppressive properties. FTY-720 is the synthetic version of a metabolite isolated from the fungus *Isaria sinclairii* [345]. The drug isn't toxic or tumorigenic in animals and has high oral bioavailability [346]. FTY-720 is phosphorylated by sphingosine kinase 2 to its active form FTY-720-P and binds to sphingosine-1-phosphate receptors, regulating their role in lymphocyte trafficking and migration [347, 348]. FTY-720-P has the ability to prevent immune cells from leaving the lymph nodes, and this immunosuppressive activity is used in patients with relapsing multiple sclerosis [349].

FTY-720-P's anticancer activity is due to its ability to re-activate PP2A by disrupting the interaction between PP2A and its endogenous inhibitor,

SET. By disrupting PP2A inhibition, FTY-720-P leads to an inhibition of survival factors mediated by Jak2, Akt and Erk1/2, resulting in apoptosis [350]. A study examining the effect of FTY-720 on two types of leukaemia has shown the drug induces apoptosis of CD34+/CD19+ leukaemia progenitor cells, but not normal or bone marrow CD34+/CD19+ cells, highlighting its therapeutic potential. Furthermore, *in vivo* FTY-720 treatment decreased leukemogenesis and prolonged survival without causing toxicity [351].

#### 1.6.5.2 Small molecule activators of PP2A (SMAPs)

SMAPs were developed by reengineering FDA-approved tricyclic neuroleptics used to treat multiple diseases of the nervous system, such as psychosis and depression [352]. Tricyclic neuroleptics are structurally similar to neurotransmitters and exert their anti-psychotic effect by binding to and blocking dopamine receptors in the brain. Due to weak affinity for other receptor, such as serotonin,  $\alpha$ -adrenergic and muscarinic receptors, these drugs result in side-effects, including neurotropic and muscle movement disorders [353]. While developing SMAPs, the neurotropic side effects of tricyclic neuroleptics were abrogated, and their antiproliferative properties were enhanced [354]. This was done by modifying the drugs' chemical structure, replacing a basic amine with a neutral polar functional group (Figure 8) [352]. A 2017 mouse study showed administration of high doses of the SMAPs DT-061 and DT-1154 for a week had no major adverse effects or impact on liver function, highlighting SMAPs' safety and therapeutic potential [355].

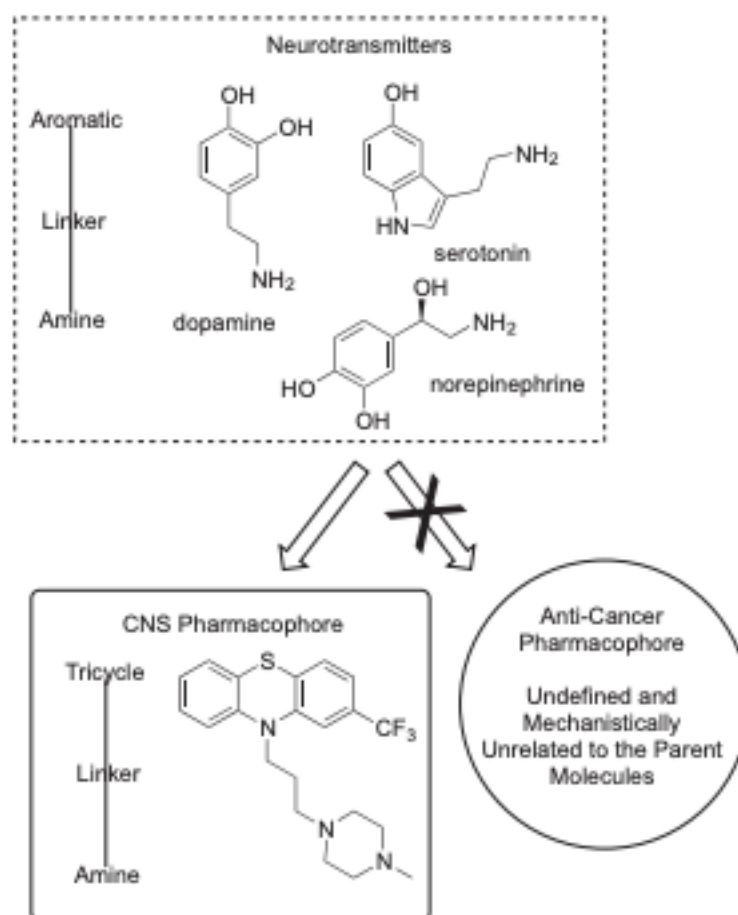


**Figure 8: SMAPs' chemical structure.**

The chemical structure of neurotransmitters (top) and tricyclic neuroleptics (bottom). While generating SMAPs, the CNS effects of tricyclic neuroleptics were eliminated by replacing the basic amine with a polar group. Figure taken from Kastrinsky *et al.*, 2015 [352].

A recent study has shown that SMAPS mediate their effect via PP2A activation. *In silico* docking modelling, hydroxyl radical footprint studies, photo-affinity labelling experiments and binding studies utilizing a tritiated version of SMAPs show that the drugs bind to the PP2A scaffolding subunit at the regulatory subunit binding domain, specifically the flexible HEAT repeat domains 5-8, which alters the conformation of the scaffolding subunit. Importantly, SMAPs are the first molecules with anticancer properties that directly bind and activate a tumour-suppressor protein [355].

A couple of groups have used SMAPs in the treatment of cancer and documented promising results. For example, Sangodkar *et al.*, used SMAPs in the treatment of KRAS-mutant lung cancer in murine models and showed that these drugs result in tumour growth inhibition and induction of apoptosis, possibly through a mechanism involving decreased MAPK signalling and pErk expression in the tumour [355]. SMAPs have also been used in the treatment of castration-resistant prostate cancer (CRPC), where they decreased tumour cell survival, inhibited colony formation and induced dephosphorylation of the androgen receptors, whose abnormal activation plays a key role in CRPC pathogenesis [356]. Dephosphorylation of the androgen receptor was shown to be PP2A-dependent, which is in agreement with previous studies showing PP2A to directly bind to and dephosphorylate androgen receptors [357].

#### 1.6.5.3 Forskolin

Forskolin is a diterpene isolated from the roots of *Coleus forskohlii*, a tropical plant found in India and Asia. It is used in traditional Indian medicine to treat heart conditions, asthma and high blood pressure [358]. Forskolin activates adenylyl cyclase, the enzyme responsible for converting ATP to cAMP [359]. Forskolin can also activate PP2A, most likely by decreasing its phosphorylation. Additionally, forskolin inhibits cell proliferation and induces changes in Akt and Erk signalling pathways [360]. A study on chronic myelogenous leukaemia (CML) showed treatment with forskolin induced apoptosis, inhibited tumorigenesis, decreased proliferation and disrupted colony formation of patient-derived leukemic cells. Furthermore, an animal study demonstrated that forskolin seriously impacted CML disease process, without causing toxicity [361].

#### 1.6.5.4 Erlotinib

Erlotinib is a drug approved for the treatment of non-small cell lung cancer (NSCLC) and pancreatic cancer. It competes with ATP for binding to the kinase domain of the epidermal growth factor receptor (EGFR), thus inhibiting its activity [362]. However, erlotinib can also bind to and inhibit CIP2A, which leads to PP2A re-activation and decreased phosphorylation of Akt. This mechanism, and not EGFR binding, is the predominant mediator of apoptosis in hepatocellular carcinoma (HCC) cells exposed to erlotinib [363]. Erlotinib also inhibits tumour cell proliferation and induces cell-cycle arrest and mitochondrial-mediated apoptosis in HCC [364].

### 1.7 Aims and Hypothesis of the Project

Junctional proteins, such as those present at the blood-brain barrier, are highly regulated through phosphorylation, hence fluctuations in the level of the serine/threonine phosphatase PP2A could modulate the expression of junctional proteins. The overall aim of this study was to investigate the effect of pro-inflammatory cytokines, and modulation of PP2A activity (pharmacological or via overexpression) on selected adherens and tight junctional proteins in a model of the blood-brain barrier.

The specific aims were to:

- 1) explore if PP2A modulates the expression of junctional proteins, by examining how inhibition of PP2A with okadaic acid or exposure to pro-inflammatory cytokines (IFN $\gamma$ /TNF $\alpha$ ) influences the expression of the adherens junction protein VE-cadherin and tight junction protein claudin-5 in human microvascular endothelial cells,
- 2) investigate if novel small molecule activators of PP2A can reverse any possible effects of okadaic acid or IFN $\gamma$ /TNF $\alpha$  have on VE-cadherin and claudin-5. This will establish if pharmacological activation of PP2A could

be developed as a therapeutic strategy to prevent/reverse the deleterious effects of inflammation on the blood brain barrier,

3) determine if IFN $\gamma$ /TNF $\alpha$  can modulate either the expression of PP2Ac or its post-translational modification, to gain a better mechanistic understanding of how inflammation modulates VE-cadherin and claudin-5 mRNA expression through PP2A,

4) establish if PP2Ac overexpression might prevent or reverse the effect of OA and IFN $\gamma$ /TNF $\alpha$  on VE-cadherin and claudin-5, and

5) determine if overexpression of the endogenous inhibitors of PP2Ac, SET or CIP2A, modulate VE-cadherin and claudin-5 expression in hCMEC/d3 cells.



# Chapter 2

---

## 2. Materials and Methods

## 2.1 List of Consumables

<b>Product</b>	<b>Manufacturer</b>
<b>6 well plates</b>	Sarstedt
<b>12 well plates</b>	Sarstedt
<b>96 well plates</b>	Sarstedt
<b>T-25 cell culture flasks, filter cap</b>	Nunc
<b>T-75 cell culture flasks, filter cap</b>	Nunc
<b>15 mL tubes</b>	Sarstedt
<b>50 mL tubes</b>	Sarstedt
<b>Cell scraper</b>	Fisher Scientific
<b>Cryogenic vials</b>	Corning
<b>Serological pipettes</b>	Corning
<b>MicroAmp Optical 8-Cap strip/cap</b>	Applied Biosciences
<b>PVDF membrane</b>	GE Healthcare

**Table 1: Consumables**

## 2.2 List of Equipment

<b>Equipment</b>	<b>Company, Model</b>
<b>Analytical balance</b>	Mettler, AE240
<b>Autoclave</b>	Dixon
<b>Fluorescence microscope</b>	EVOS fl
<b>Automated pipettes</b>	Gilson, Inc. (2 µL, 10 µL, 100 µL, 200 µL, 1000 µL, 5000 µL, Pipetman Ultra 8-channel (20-300 µL))
<b>Centrifuge</b>	Hettich Zentrifugen, EBA 12R/mikro 22R
<b>Digital imaging</b>	Fusion Fx imaging system, Vilber Lourmat
<b>Freezer (-80°C)</b>	Thermofischer Scientific , Revco Value Plus
<b>Gel electrophoresis system</b>	Bio-Rad, Mini-Protean
<b>Incubator (37°C, 5 % CO<sub>2</sub>, 95 % rh)</b>	HERAcell 240i
<b>Laminar flow hood</b>	Mason Technology, BioBan 48
<b>Luminometer</b>	Thermofischer Scientific, Fluoroskan AscentFL
<b>Microplate reader</b>	BioTek EL 808
<b>MX3000p, Real Time PCR machine</b>	Applied Biosystem
<b>Nanodrop 1000 Spectrophotometer</b>	Thermo Scientific
<b>Neubauer haemocytometer, improved</b>	BRAND GMBH + CO KG, Blaubrand <sup>®</sup>
<b>pH meter</b>	Mettler-Toledo Inc., MP320
<b>Thermocycler</b>	MJ Research Inc, PTC-100
<b>Heat Block</b>	ThermoScientific

**Table 2: Equipment**

### 2.3 Materials

Okadaic acid was purchased from Calbiochem (Carrigtwohill, Ireland) and FTY-720 was obtained from Cayman Chemical (Hamburg, Germany). SMAPs were obtained from Dr Michael Ohlmeyer (New York, USA). LDH Assay kit was purchased from Takara (cat. # MK401). TNF $\alpha$  and IFN $\gamma$  were purchased from Merck (Merck, Millipore). Anti-VE-cadherin (C-19, cat. # sc-6458), anti-PP2Ac (1D6, cat. # sc-80665), anti-CIP2A (4A9-1A2, cat. # sc-80662), anti-TTP (A8, cat. # sc-374305) and HRP-conjugated mouse anti- $\beta$ -actin (C4, cat. # sc-47778) antibodies as well as TTP siRNA (cat. # sc-36760) were procured from Santa Cruz Biotechnology (Santa Cruz, CA 95060, USA). Goat anti-mouse HRP-conjugated secondary antibody (cat. # P0447) was purchased from DAKO, Agilent Technologies (Cork, Ireland). The EZ-Run<sup>TM</sup> Pre-Stained Rec Protein Ladder was obtained from Fisher BioReagents (cat. # BP3603-500). DNA primers were obtained from IDT (Integrated DNA Technologies, Belgium), while ReverseAid (reverse transcription kit) and GoTaq (DNA polymerase) were purchased from Thermo Fisher (Dublin, Ireland) and Promega (Madison, USA) respectively. Actinomycin D was obtained from Sigma-Aldrich (cat. # A9415). One Shot<sup>TM</sup> TOP10 chemically competent *E.coli* cells (cat. # C4040-03) were bought from Invitrogen. Opti-mem reduced serum media (cat. # 31985062) was procured from Gibco. The pcDNA3.1\_CIP2aflag\_WT plasmid (pcCIP2A) was a gift from Prof J Westermarck (University of Turku, Finland). The pcDNA.3.1 empty vector was obtained from Dr Steven Grey (Trinity College Dublin, Ireland). The pCMV-6-PP2Ac $\alpha$  expression plasmid (pcPP2Ac; cat. # SC321401) and pCMV6-AC (pCMV6; cat. # PS100020) were procured from Origene (Maryland, USA). The pEGFP-c $\beta$ -PLCd1 plasmid (GFP) was a gift from Prof Stephen Ferguson (Ontario, Canada). The transfection reagents PolyFect, Lipofectamine 2000 and TransIT-X2 were purchased from Qiagen, Thermo Fisher Scientific and Mirus Bio, respectively. All other reagents were purchased from Sigma-Aldrich (Arklow, Ireland) unless otherwise specified.

## 2.4 Cell Culture

Human brain microvascular endothelial cells (hCMEC/d3) were obtained from Dr Matthew Campbell (Trinity College Dublin). The cells were cultured in EndoGRO-MV culture media (Merck, cat. # scme004) containing 5 % foetal bovine serum (FBS), supplemented with 100 U/mL penicillin, 100 mg/mL streptomycin and the growth supplements provided with the kit. Cells were maintained in a humidified atmosphere at 37°C and 5 % CO<sub>2</sub>. All experiments were carried out in media lacking serum. The cells were used up to passage 45.

## 2.5 Cell Viability: MTT Assay

hCMEC/d3s were seeded in 96-well plates and exposed to SMAPs (0-33 µM), dimethylsulphoxide (DMSO; 0.1 % v/v, solvent control for SMAPs), doxorubicin (DOX; 5 µM, positive control) or serum-free media for 24 h. After 22 h, MTT [3-(4,5-dimethylthiazol-2-yl)-2,5-diphenyltetrazolium bromide] (5 mg/mL) was added, and the cells incubated for a further 2 h. The culture media was then removed, and the purple formazan crystals dissolved in DMSO. Formazan production was quantified using spectrophotometry at a wavelength of 540 nm (BioTek, EL 808, Bedfordshire, UK).

## 2.6 Cell Viability: LDH Assay

hCMEC/d3s were seeded in 96-well plates and exposed to SMAPs (0-33 µM), DMSO (0.1 % v/v), DOX (5 µM) or serum-free media for 24 h. After 24 h, the culture plates were centrifuged at 250g for 10 minutes and the supernatants transferred into a clean 96-well plate. Solution C from the Lactate Dehydrogenase (LDH) assay kit (Takara) was then added to each well and incubated for 30 minutes at RT in the dark. Absorbance was read at 490 nm (BioTek, EL 808, Bedfordshire, UK) and percentage cell viability calculated following the kit's instructions. Triton-X100 (2 %) was used to determine maximum LDH release, which was defined as 100 % cell death.

## 2.7 Semi-Quantitative Real-Time PCR

hCMEC/d3 cells were grown in 6-well plates ( $4 \times 10^5$  cells per well) or 12-well plates ( $2 \times 10^5$  cells per well) and lysed in Tri Reagent™ (1 mL/  $4 \times 10^5$  cells; Sigma Aldrich). Following the addition of chloroform (200  $\mu$ L/1 mL Tri Reagent), incubation at RT for 10 minutes and centrifugation at 12,000 g for 15 minutes at 4°C, the mixture separated into three phases. The upper aqueous phase containing RNA was transferred to a fresh Eppendorf tube and isopropanol added to precipitate the RNA. The mixture was then centrifuged at 12,000 g for 10 minutes at 4°C, the supernatant discarded, and the RNA pellet sequentially washed with 75 % and 100 % ethanol. The RNA pellet was then resuspended in nuclease-free water and heated at 65°C for 5 minutes to dissolve. The RNA concentration was determined using a NanoDrop 1000 Spectrophotometer (Thermo Scientific). RNA samples were treated with DNase I (Sigma Aldrich) and reverse transcribed using random hexamers or OligoDTs (Invitrogen) and RevertAid reverse transcriptase (ThermoFisher, Dublin, Ireland). mRNA expression was analysed by semi-quantitative PCR (qPCR) using target specific primers (Table 1) with Sybr green chemistry and GoTaq DNA polymerase (Promega) on a Mx3000P qPCR system (Agilent Technology). Gene expression was quantified using the comparative Ct method [ $2^{-\Delta\Delta Ct}$ ]. For each primer set, a no template control was included. The validity of the primer sequences was verified by nucleotide search (Primer-BLAST; NCBI), while the specificity and size of the amplicons were checked using a dissociation curve and gel electrophoresis followed by UV trans-illumination (Fusion Fx imaging system, Vilber Lourmat).

Gene	NMID	Forward Sequence	Reverse Sequence
<b>PPP2CA</b>	NM_00 2715.2	TGAGCCTCAGCGAG CGG	GGCTCTTGACCTGGGAC T
<b>VE-cadherin</b>	NM_00 1795.4	ATACCAAGGTCCACTT C	GTGAGGATGCAGAGTAA
<b>Claudin-5</b>	NM_00 3277.4	AAGTGGTGTCACCTGA ACTG	CTTCCCAGACCTCTCAAT CTTC
<b>CIP2A</b>	NM_02 0890.2	CACTCTGGGAAGCCAT ACTAAA	CCTTGAACAACCTCCAATG CTAAA
<b>SET</b>	NM_00 112282 1.1	CTTGCCGAAGAAGGG AGAAA	CTCCTCACTGGCTTGTTT ATT
<b>TTP</b>	NM_00 3407.5	GGATCCGACCCTGATG AATATG	GAAACAGAGATGCGATT GAAGATG
<b>GAPDH</b>	NM_00 2046.5	CTCTGCTCCTCCTGTTC GAC	GCGCCCAATACGACCAA ATC
<b>GPI</b>	NM_00 132991 1.2	TCTATGCTCCCTCTGT GTTAGA	CTCCTCCGTGGCATCTTT ATT

**Table 3: List of primers including gene identification numbers and sequence**

### 2.8 Western Blotting

Cells were lifted from the culture plates using a cell scraper in the presence of a modified radioimmunoprecipitation assay (RIPA) buffer (Trizma Base 50 mM, NaCl 150 mM, EDTA 2 mM, and NP40 0.5 % v/v) supplemented with the protease inhibitor cocktail SIGMAFAST™ (Sigma-Aldrich) alone, or in combination with the phosphatase inhibitors sodium orthovanadate (2 mM) and sodium fluoride (5 mM) for the analysis of phospho-proteins. The cells were then transferred to an Eppendorf tube and lysed by freeze-thawing. The lysate was clarified by centrifugation at 400 g for 10 minutes and protein concentration quantified using the Bradford Assay [365]. Following standardisation, samples containing 15 µg of protein were boiled in lithium dodecyl sulphate (LDS) sample loading buffer (LDS 5 % v/v, glycerol 50 % v/v, Tris-HCl 1 M, bromophenol blue 2.5 mg, phenol red 2.5 mg and ficoll 400 5 % v/v) supplemented with 5 % v/v 2-β-mercaptoethanol (BME) for 30 seconds and chilled on ice for

3 minutes. The denatured samples were then subjected to sodium dodecyl sulphate-polyacrylamide gel electrophoresis (SDS-PAGE) using an 8 % gel; a molecular weight ladder was included to assess the relative molecular weight of the proteins. Following separation by electrophoresis, proteins were transferred onto a polyvinylidene fluoride (PVDF) membrane (Amersham) via semi-dry transfer (transfer buffer: Tris 50 mM, glycine 40 mM, methanol 20 % v/v, SDS 0.037 % w/v). The membranes were blocked in TBS-T (Tris 10 mM, NaCl 100 mM, HCl 1 M, and Tween-20 0.1 % v/v) containing 5 % w/v marvel prior to being probed overnight with the primary antibody (1:1000 dilution) at 4°C. The next day, membranes were washed in TBS-T and incubated at RT for 1 h with TBS-T + marvel containing the HRP-conjugated anti-mouse secondary antibody (1:1000). The protein bands were visualised following chemiluminescent detection (3.2 mL of 30 % hydrogen peroxide/6 mL of 250 mM Luminol, 90 mM 4-iodophenylboronic acid and 100 mM Tris-HCl) and captured on a Fusion Fx imaging system (Vilber Lourmat). Bio1D software was used for densitometric analysis of protein bands. Membranes were stripped (stripping buffer: 62.5 mM, pH 6.8 Tris-HCl, 2 % SDS and 0.83 mL BME) and re-probed with an HRP-conjugated  $\beta$ -actin antibody (dilution 1:2000).

## 2.9 Bradford Protein Assay

The protein concentration in cleared cellular lysates was quantified using the Bradford assay. Bovine serum albumin (cat. # A7888) dissolved in RIPA buffer was used to prepare standards ranging in concentration from 0 – 1500  $\mu$ g/mL. Standards (5  $\mu$ L) and unknown protein samples were added to a 96-well plate containing 250  $\mu$ L of Bradford Reagent (Sigma). The plate was incubated at RT for 15 minutes and the absorbance read at 595 nm. Protein concentration of the unknown samples was derived from the standard curve.



### 2.10 mRNA stability Assay

hCMEC/d3s were seeded ( $2 \times 10^5$  cells per well) in 12-well plates and allowed to attach overnight. The cells were treated with 10 ng/mL of IFN $\gamma$  and 10 ng/mL of TNF $\alpha$ . After 24 h, cells from one well (t=0) were lysed in Tri Reagent, and Actinomycin D (1mg/mL) was added to the remaining wells. Samples were collected at 1, 2, 4, 6 and 8 h time points following addition of Actinomycin D. RNA was isolated, reverse transcribed using Oligo dTs, and amplified by qPCR as described above, focussing on VE-cadherin and claudin-5 as the target transcripts. The average Ct value of each time point was normalized to the Ct average value of t=0 (cells not exposed to Actinomycin D), giving the  $\Delta$ Ct value. The relative abundance of each time point was calculated using the following formula  $2^{(-\Delta\text{CT})}$ . The mRNA decay rate was determined by a nonlinear regression curve fitting (one phase decay).

### 2.11 TTP gene knockdown using siRNA

hCMEC/d3s were seeded ( $3 \times 10^5$  cells per well) in 12-well plates in full cell culture media and allowed to attach overnight. The next day, full media was aspirated, and serum-free media was added to each well. TTP siRNA was mixed with TransIT-X2 transfection reagent (Mirus Bio) and opti-mem media (Gibco) and incubated for 30 minutes at RT to allow siRNA: transfection reagent complexes to develop. The mixture was added to the cells, which were cultured for 24 h before protein or mRNA was extracted as described above.

### 2.12 Transformation of *E. coli*

Competent TOP10 *E. coli* were thawed on ice for 30 minutes and mixed with either pcCIP2A, GFP, PP2A, DNA3.1 or CMV6 plasmids. The *E. coli* were heat-shocked for 30 s at 42°C and placed on ice. Brain heart infusion media (Sigma) was added to the mixture and incubated in a water bath at 37°C for 1 h. Transformed *E. coli* were plated onto Luria Broth (LB)-agar plates containing 50  $\mu$ g/mL of ampicillin. The next day, a single colony

was lifted from the plate and spread onto a fresh plate. This procedure was repeated once more before inoculating LB broth supplemented with 50 µg/mL of ampicillin. The culture was incubated in a water bath at 37°C for 4 h. After the incubation, a 500 µL aliquot of the culture was used to inoculate 40 mL of fresh LB broth in an Erlenmeyer flask, and incubated overnight at 37°C.

### 2.13 Plasmid isolation

The plasmids were isolated using the GenElute™ endotoxin-free plasmid midiprep kit (cat. # PLED35) following manufacturer's guidelines. In brief, *E. coli* were pelleted by centrifugation at 5,000 g for 10 minutes and the bacterial pellet resuspended in buffer provided by the kit. The cells were lysed in cell lysis buffer for 5 minutes. The solution was neutralized and spun as before to remove cell debris. The supernatant was transferred to a fresh tube and the endotoxin removal solution added. The mixture was sequentially chilled on ice, warmed in a water bath at 37°C and centrifuged. The clear upper phase was transferred to a fresh tube, and the endotoxin removal step repeated. Next, a DNA binding solution was added to the endotoxin free lysate and the mixture loaded onto a GenElute Binding Column. The column containing the plasmid DNA was washed with an ethanol solution. The DNA was eluted by adding endotoxin-free water to the column. The DNA concentration in the eluate was quantified using a nanodrop spectrophotometer. The plasmid solutions were stored at -20°C until needed.

### 2.14 Cell Transfection

hCMEC/d3s were seeded ( $2 \times 10^5$  cells per well) in 6-well plates 24 h before being transfected. Plasmid DNA was mixed with PolyFect (Qiagen), Lipofectamine 2000 (Thermo Fisher Scientific) or TransIT-X2 (Mirus Bio) transfection reagents and opti-mem media (Gibco), and incubated at RT for 30 minutes to allow the DNA:transfection reagent complexes to develop. The mixture was then added to cells cultured in EndoGRO®

media (Millipore) and the cells cultured for 72 h before mRNA or protein was isolated as described above.

### 2.15 Cell fixing and staining

hCMEC/d3s were seeded ( $2 \times 10^5$  cells per well) in 6-well plates and transfected with varying volumes of PolyFect transfection reagent (7.5, 10 or 12.5  $\mu\text{L}$ ) and GFP plasmid DNA (0.5, 1 or 1.5  $\mu\text{g}$ ), as described above. After being incubated with the transfection reagent:plasmid mixture for 72 h, the cells were washed 3 times with PBS and fixed with 3 % paraformaldehyde (PFA) at 37°C for 30 minutes. Following 3 PBS washes, Hoechst 33342 (Thermo Fisher Scientific) at 1:1000 dilution was added to the cells. After a 1 h incubation at 37°C the cells were washed 3 times with PBS. Images of the cells were captured on a cell imaging system (EVOS® FL) fitted with a GFP light cube.

### 2.16 Data and statistical analysis

All samples were randomly assigned to their respective groups using an online randomizer (GraphPad QuickCalcs: <https://www.graphpad.com/quickcalcs/randomize1.cfm>). PCR data were normalized to the geometric mean of the house-keeping genes GPI and GAPDH. Data from western blots were normalized to  $\beta$ -actin from the same blot. Statistical analysis of the western blots was only carried out between bands from the same blot and within the dynamic range of the imaging system. All data were normalised to the values obtained from the appropriate untreated controls and expressed as either a fold or percentage in order to set the Y-axis to 1 or 100 %. Data were analysed in Prism GraphPad software (GraphPad Prism version 7.0c: RRID:SCR\_002798) by global nonlinear regression, one-way ANOVA with post hoc analysis (Dunnett's, Bonferroni) or student t-test as appropriate. Post hoc analysis was only performed when ANOVA showed a statistically significant difference between group means (achieved  $P < 0.05$ ). Data are expressed as mean  $\pm$  S.E.M.

# Chapter 3

---

## 3. Results

### 3.1 Effect of SMAPs on cell viability

#### 3.1.1 Cytotoxicity Screen

In this study we aim to explore the concept of PP2A activation to prevent the effects of PP2A inhibition and inflammation. In order to establish a working concentration of the small molecule PP2A activators with minimal cytotoxicity, the effect of 0 - 33  $\mu$ M of the SMAPs on hCMEC/d3 cell viability was determined using an MTT assay (Figure 9). All of the active compounds caused a concentration dependent decrease in cell viability over the concentration range studied, with a similar maximum decrease in cell viability of  $\sim$  85 % at the highest concentration (33  $\mu$ M) compared to untreated cells. The drugs fell into 2 main populations, with DBK-1160 and DBK-1154 being the most cytotoxic, while FTY-720, NZ-8061, DBK-1532, DBK-1537, NZ-8065, DBK-794 and DBK-382 were less cytotoxic (Figure 9). By comparison, DBK-766, a non-functional SMAP analogue of DBK-1154, decreased cell viability by 27 % at a concentration of 33  $\mu$ M.

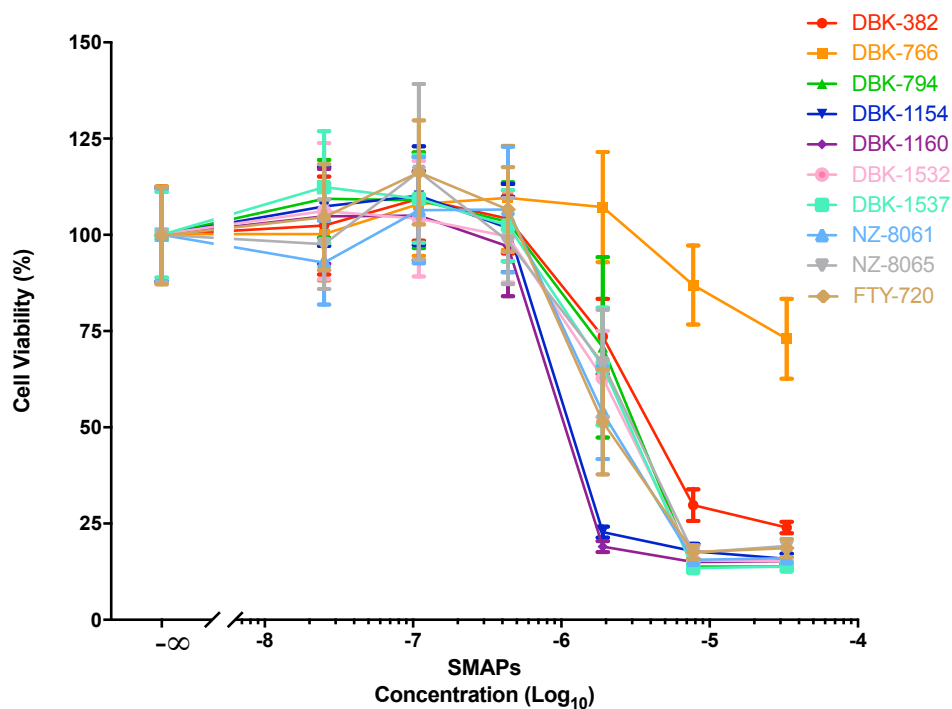


**Figure 9: Effect of SMAP on cell viability.**

hCMEC/d3 cells were exposed to SMAPS over concentrations ranging from 0 to 33  $\mu$ M for 24 h and the effect on cell viability determined using an MTT assay. Data are presented as mean  $\pm$  SEM (n=5).

As the SMAPs are insoluble in water, the polar aprotic solvent DMSO was used to reconstitute the drugs. Each SMAP was reconstituted at a concentration of 80  $\mu$ g/mL, diluted in serum-free media to acquire the appropriate concentration, which resulted in a maximum final DMSO concentration of 0.1 %. To rule out any confounding influence of DMSO, the effect of 0.1 % DMSO on hCMEC/d3 cells' viability was also tested and found to have no effect compared to cells exposed to culture media alone (Figure 10). Doxorubicin (5  $\mu$ M) was used as a positive control and was found to decrease cell viability by approximately 25 % compared to the untreated (Untx) group.

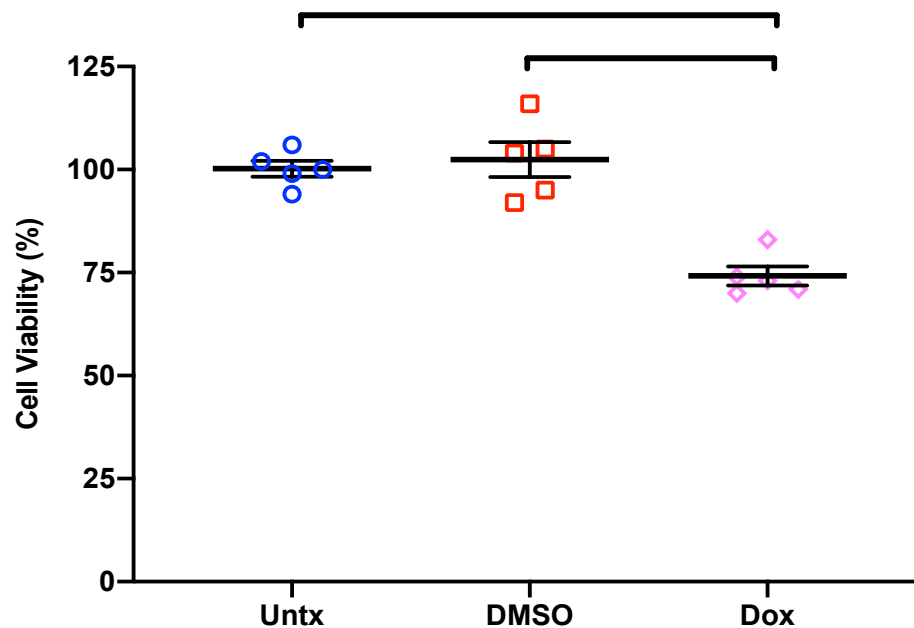


**Figure 10: Effect of DMSO and Dox on cell viability.**

hCMEC/d3 cells were exposed to DMSO (0.1 %, solvent control) and Doxorubicin (Dox, 5  $\mu$ M, positive control) for 24 h and cell viability assessed using an MTT assay. Data are presented as mean  $\pm$  SEM. Data were analysed using one-way ANOVA with post hoc analysis (Bonferroni).  $P < 0.05$  is indicated by horizontal bars ( $n=5$ ).

### 3.1.2 Effect of DBK-1154 and DBK-766 on cell viability

Through a collaboration with Dr Ohlmeyer we were provided a small library of novel SMAPs to investigate in our model, which were concurrently being investigated in cancer models by other groups. Based upon the cytotoxicity data above and communication from Dr Ohlmeyer relating to data from the cancer studies, all subsequent work focussed on DBK-1154 and its non-functional analogue DBK-766. To determine a working concentration of DBK-1154, MTT and LDH cytotoxicity assays were carried out over a more refined concentration range of 0 to 10  $\mu$ M. As in the screen, DBK-1154 caused a concentration dependent decrease in cell viability with an  $EC_{50}$  value of  $\sim 1.7 \mu$ M based upon data from both an MTT and LDH assay (Figure 11 A, B). Based on this, a working

concentration of 1  $\mu\text{M}$  was chosen for subsequent experiments. The inactive analogue DBK-766 had minimal effect on cell viability over this concentration range.

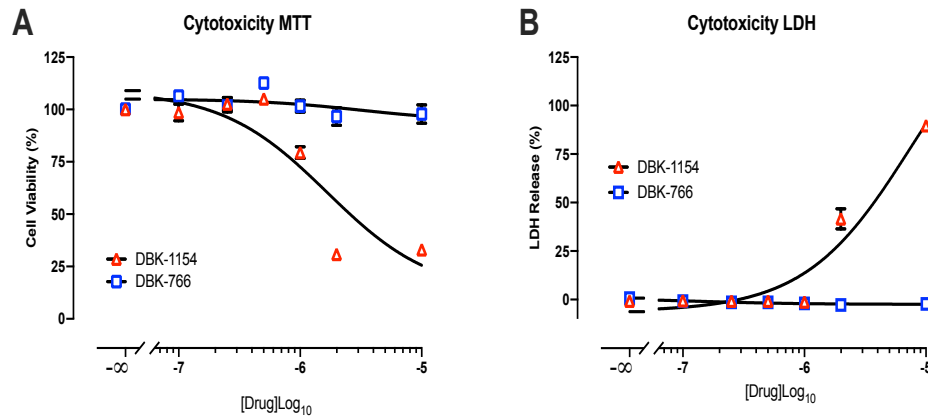


**Figure 11: Effect of DBK-1154 and DBK-766 and cell viability.**

hCMEC/d3 cells were exposed to DBK-1154 and DBK-766 at concentrations from 0 to 10  $\mu\text{M}$  for 24 h and cell viability determined using an MTT (A) and LDH (B) assay. Data are presented as mean  $\pm$  SEM ( $n=5$ ). Data were fit to a global nonlinear regression model and the  $\text{EC}_{50}$  value determined (GraphPad Prism, version 7.0c).

### 3.2 Effect of okadaic acid on VE-cadherin and claudin-5 expression alone and in combination with SMAPs

As previous work by our group (unpublished data) showed that OA decreased VE-cadherin protein abundance in brain microvascular endothelial cells, we chose to test if OA could also affect abundance of claudin-5 and whether the effect on VE-cadherin and claudin-5 could be altered by DBK-1154 or FTY-720 (PP2A activator). In hCMEC/d3 cells, OA (10 nM for 24 h) decreased VE-cadherin mRNA expression and protein abundance by  $79.9 \pm 4.8\%$  and  $80.6 \pm 3.4\%$  respectively, compared to untreated cells (Figure 12 A, B). However, OA had no effect on the expression of claudin-5 mRNA (Figure 12 C). Interestingly, DBK-1154 (1  $\mu\text{M}$ ) and FTY-720 (1  $\mu\text{M}$ ) were unable to prevent the decrease in VE-cadherin mRNA and protein caused by OA (Figure 12 A, B). DMSO (0.1 %)



did not alter VE-cadherin mRNA or protein expression, or claudin-5 mRNA levels (Figure 12 A-C).

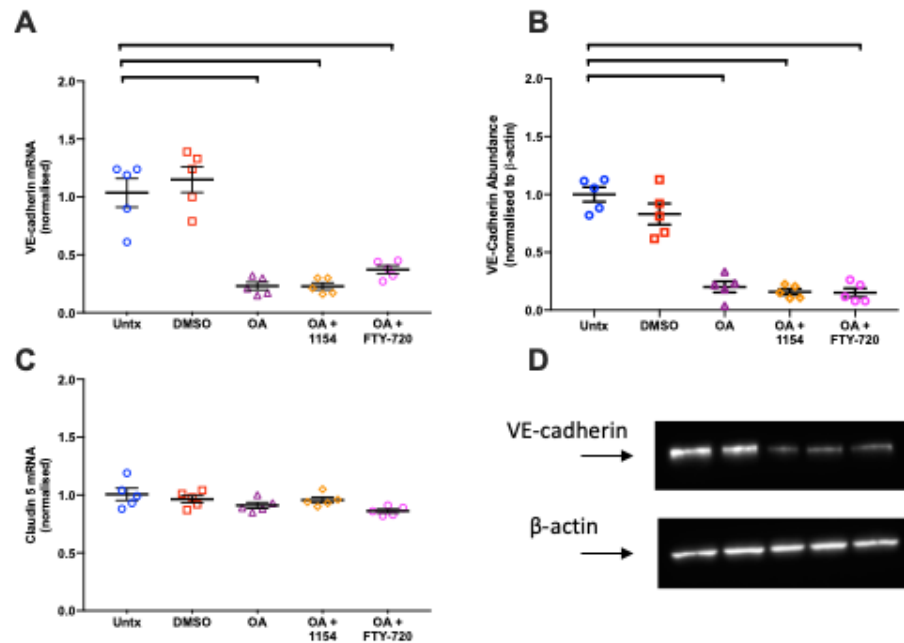


**Figure 12: Effect of OA alone and in combination with DBK-1154 or FTY-720 on VE-cadherin mRNA and protein expression and claudin-5 mRNA expression.**

hCMEC/d3 cells were exposed to DMSO (0.1 %, solvent control), OA (10 nM) and OA (10 nM) in combination with DBK-1154 (1 μM) or FTY-720 (1 μM) for 24 h. Relative mRNA expression of VE-cadherin (A) and Claudin-5 (C) was determined using semi quantitative RT-PCR-based SYBR green chemistry, normalised to the geometric mean of GAPDH and GPI. Protein abundance of VE-cadherin was determined using Western blot, normalised to the loading control β-actin (B, D). Data are presented as mean ± SEM (n=5) and were analysed using one-way ANOVA with post hoc analysis (Bonferroni). P < 0.05 is indicated by horizontal bars.

### 3.3 Effect of inflammatory cytokines on VE-cadherin and claudin-5 expression alone or in combination with SMAPs

PP2A is known to be involved in inflammatory responses, leading us to gain interest in investigating if inflammation can alter VE-cadherin and claudin-5 expression in our cell line, and whether this was affected by DBK-1154 or FTY-720, which would show PP2A's role in the mechanism. Exposure of hCMEC/d3 cells to IFN $\gamma$ /TNF $\alpha$  at 10ng/mL for 24 h decreased VE-cadherin mRNA and protein by  $54.2 \pm 7.5$  % and  $82.7 \pm 5.7$  % respectively, compared to untreated cells (Figure 13 A, B). A similar effect was seen on claudin-5, with a  $67.8 \pm 5.5$  % decrease in mRNA expression (Figure 13 C). DBK-1154 (1  $\mu$ M) and FTY-720 (1  $\mu$ M) did not alter IFN $\gamma$ /TNF $\alpha$ -mediated attenuation of VE-cadherin or claudin-5 expression compared to those exposed to IFN $\gamma$ /TNF $\alpha$  alone.

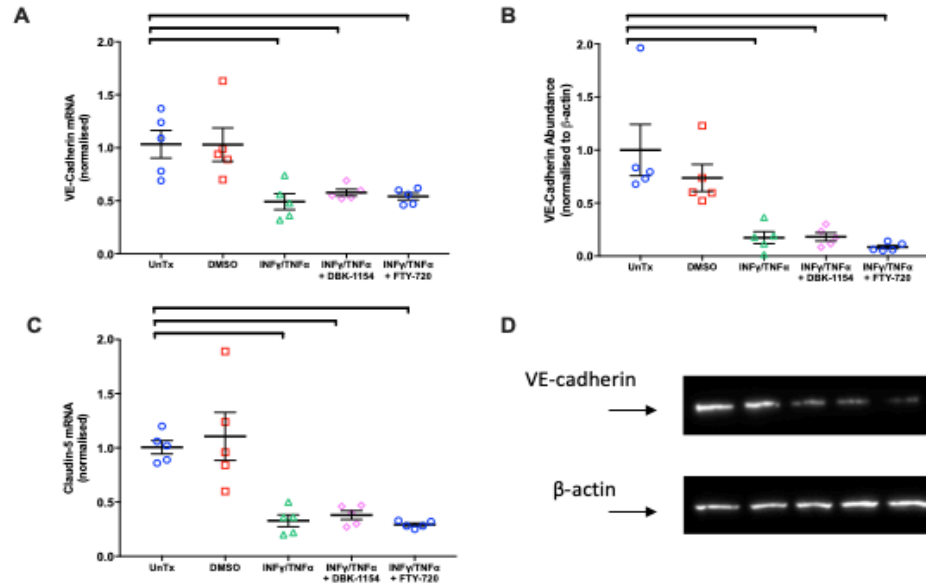


**Figure 13: Effect of IFN $\gamma$ /TNF $\alpha$  alone and in combination with DBK-1154 or FTY-720 on VE-cadherin mRNA and protein expression and claudin-5 mRNA expression.**

hCMEC/d3 cells were exposed to DMSO (0.1 %, solvent control), IFN $\gamma$ /TNF $\alpha$  (10 ng/mL each) alone and in combination with DBK-1154 (1  $\mu$ M) or FTY-720 (1  $\mu$ M) for 24 h. Relative mRNA expression of VE-cadherin (A) and Claudin-5 (C) was determined using semi quantitative RT-PCR-based SYBR green chemistry, normalised to the geometric mean of GAPDH and GPI. VE-cadherin protein abundance was determined using Western blot and normalised to the loading control  $\beta$ -actin (B, D). Data are presented as mean  $\pm$  SEM (n=5) and were analysed using one-way ANOVA with post hoc analysis (Bonferroni). P < 0.05 is indicated by horizontal bars.

### 3.4 Investigation of the effect of IFN $\gamma$ /TNF $\alpha$ on PP2Ac

In order to further explore if PP2A is involved in the downregulation of VE-cadherin and claudin-5 caused by IFN $\gamma$ /TNF $\alpha$  treatment, hCMEC/d3 cells were exposed to IFN $\gamma$ /TNF $\alpha$  at 10ng/mL for 24 h and the influence on PP2Ac expression and its methylation status examined. IFN $\gamma$ /TNF $\alpha$  did not affect the abundance of PP2Ac compared to untreated cells (Figure 14 A). However, IFN $\gamma$ /TNF $\alpha$  decreased the expression of demethylated PP2Ac (dmPP2Ac) by  $20.5 \pm 0.08 \%$  (Figure 14 B) compared to the untreated group.

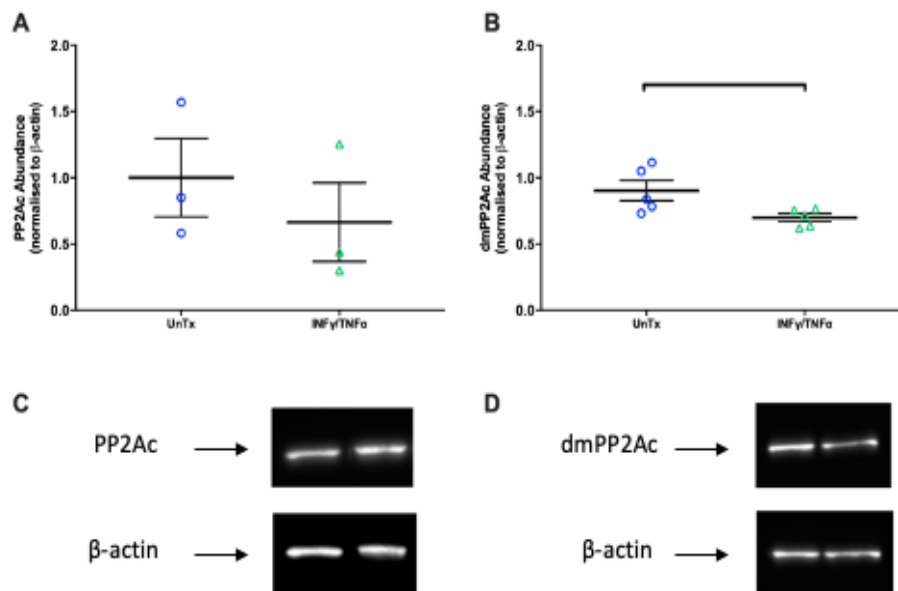


**Figure 14: Effect of IFN $\gamma$ /TNF $\alpha$  on PP2Ac and dmPP2Ac protein abundance.**

hCMEC/d3 cells were exposed to IFN $\gamma$ /TNF $\alpha$ , each at 10 ng/mL for 24 h. Protein abundance of PP2Ac (A, C) and dmPP2Ac (B, D) was determined using Western blot and normalised to the loading control  $\beta$ -actin. Data are presented as mean  $\pm$  SEM, n=3 (A) and n=5 (B). Data were analysed using an unpaired Student t test. P < 0.05 is indicated by horizontal bars.

Based on the above we decided to examine if IFN $\gamma$ /TNF $\alpha$  alters the expression of LCMT-1 and PME-1, which are responsible for methylation

and demethylation of PP2Ac, respectively. Unexpectedly, IFN $\gamma$ /TNF $\alpha$  did not alter the abundance of LCMT-1 (Figure 15 A) or PME-1 (Figure 15 B) compared to the untreated group.

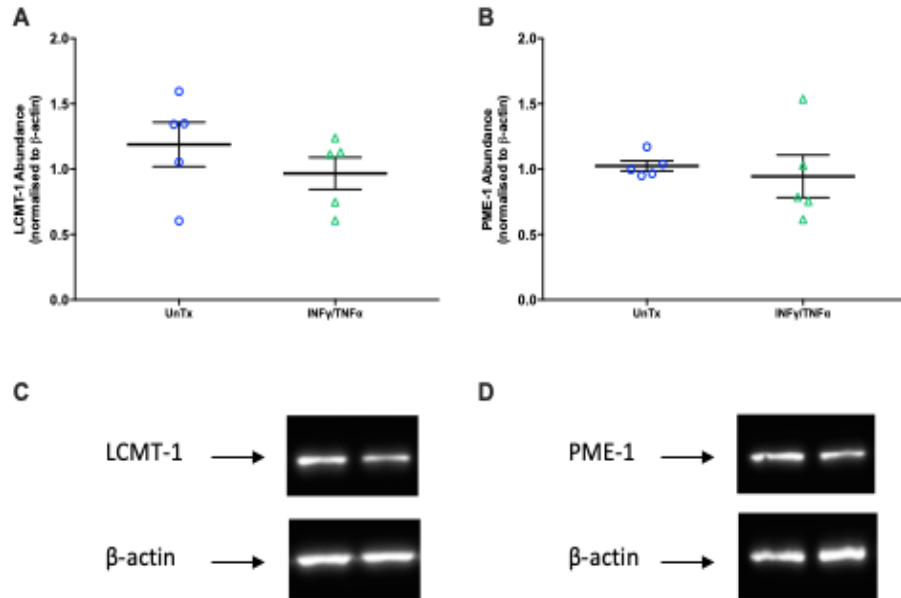


**Figure 15: Effect of IFN $\gamma$ /TNF $\alpha$  on LCMT-1 and PME-1 protein abundance.**

hCMEC/d3 cells were exposed to IFN $\gamma$ /TNF $\alpha$ , each at 10 ng/mL for 24 h. Protein abundance of LCMT-1 (A, C) and PME-1 (B, D) was determined using Western blot and normalised to the loading control  $\beta$ -actin. Data are presented as mean  $\pm$  SEM (n=5) and were analysed using an unpaired t test.

Next, we investigated if phosphorylation of PP2Ac is altered by IFN $\gamma$ /TNF $\alpha$ . Preliminary data based on two biological replicates showed that exposure of hCMEC/d3 to IFN $\gamma$ /TNF $\alpha$  at 10 ng/mL each for 24 h appear to increase the abundance of phosphorylated PP2Ac (pPP2Ac) by approximately 3 fold (Figure 16).

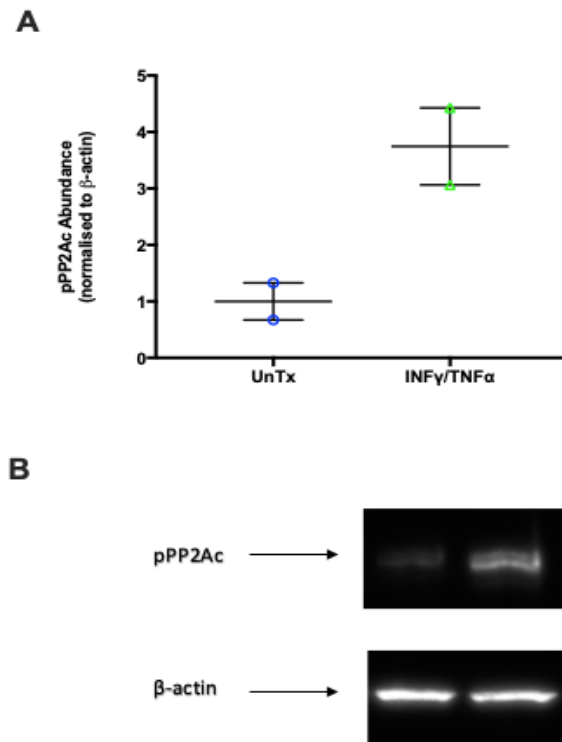


**Figure 16: Effect of IFN $\gamma$ /TNF $\alpha$  on pPP2Ac protein abundance.**

hCMEC/d3 cells were exposed to IFN $\gamma$ /TNF $\alpha$ , each at 10 ng/mL for 24 h. Protein abundance was determined by Western blot, normalised to the loading control  $\beta$ -actin. PP2Ac protein abundance is represented as a graph (A) and blot (B). Data are presented as mean  $\pm$  SEM (n=2).

### 3.5 Effect of IFN $\gamma$ /TNF $\alpha$ on VE-cadherin and claudin-5 mRNA stability in hCMEC/d3 cells

Previous studies show that inhibition of PP2A can alter mRNA expression of inflammatory cytokines through tristetraprolin (TTP) [366], a key mRNA destabilising protein. Interestingly, TTP can bind to claudin-1 3'-UTR and is associated with down regulation of claudin-1 mRNA [367]. Therefore, to better understand the mechanism involved in IFN $\gamma$ /TNF $\alpha$ -mediated downregulation of VE-cadherin and claudin-5 mRNA expression, their effect on mRNA stability and the role of TTP was investigated. hCMEC/d3 cells were exposed to IFN $\gamma$ /TNF $\alpha$  in the presence of Actinomycin D (1 mg/mL, transcription inhibitor) and mRNA samples

collected over an 8 h period. Compared to the control group, IFN $\gamma$ /TNF $\alpha$  did not alter the degradation rate of VE-cadherin mRNA over the 8 h period (control vs IFN $\gamma$ /TNF $\alpha$ :  $t_{1/2}$ , 2.1 vs 3.2 h; Figure 17 A). Similarly, IFN $\gamma$ /TNF $\alpha$  did not alter the half-life of claudin-5 mRNA (control vs IFN $\gamma$ /TNF $\alpha$ :  $t_{1/2}$ , 0.9 vs 1.3 h; Figure 17 B).

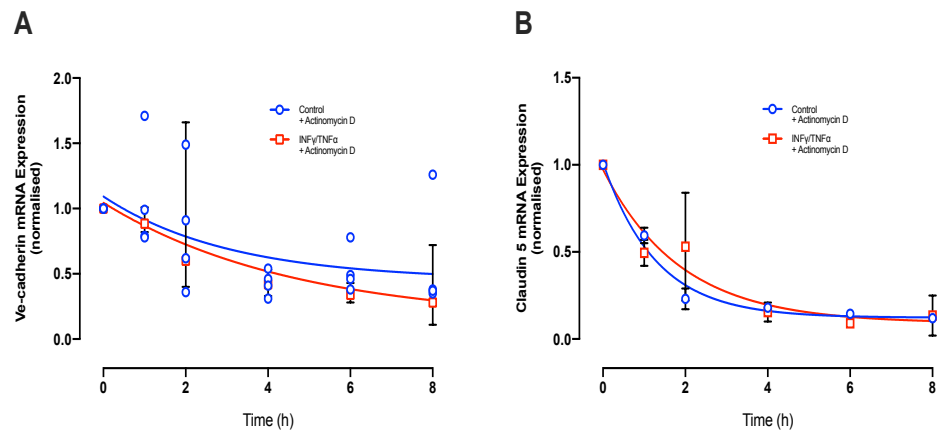


**Figure 17: Effect of IFN $\gamma$ /TNF $\alpha$  on VE-cadherin and claudin-5 mRNA stability.**

hCMEC/d3 cells were exposed to full cell culture media (control) or IFN $\gamma$ /TNF $\alpha$  (10 ng/mL each) at baseline ( $t=0$ ) and Actinomycin D (1 mg/ml) was immediately added. Samples were reserved at baseline and over the next 8 h for isolation of mRNA. Relative VE-cadherin (A) and Claudin-5 (B) mRNA expression was determined using semi quantitative RT-PCR-based SYBR green chemistry. The curves were fitted by non-linear regression (one phase decay),  $n=4$  (A) and  $n=2$  (B).

### 3.6 Optimization of tristetraprolin gene knockdown protocol using siRNA

While the mRNA stability protocol using Actinomycin D was being optimized, work on establishing a TTP knockdown protocol began. TTP binds to mRNA of pro-inflammatory mediators, including IFN $\gamma$  and TNF $\alpha$  leading to a removal of their poly-(A) tail [368, 369]. This in turn decreases mRNA stability and results in degradation of the target transcripts [370]. We were interested in investigating the effect of TTP knockdown alone

and in conjunction with IFN $\gamma$ /TNF $\alpha$  or OA treatment on VE-cadherin and claudin-5 mRNA and protein expression. To do that, a TTP siRNA knockdown protocol using TransIT-X2 (Mirus, Bio) as the transfection reagent needed to be optimized.

In a preliminary experiment, hCMEC/d3 cells were transfected with 10 or 25 nM of TTP siRNA (siTTP) in combination with either 5, 7.5 or 10  $\mu$ L of TransIT-X2 (TransIT) transfection reagent for 24 h. Transfection of the cells with 10 nM of TTP siRNA along with varying volumes of TransIT-X2 appeared to cause a modest increase in TTP mRNA abundance (Figure 18). In contrast, transfection of hCMEC/d3 cells with 25 nM of TTP siRNA appeared to decrease TTP abundance compared to mock transfected cells. This was most pronounced using 7.5  $\mu$ L of transfection reagent (Figure 18). To validate the knockdown, hCMEC/d3 cells were transfected with 7.5  $\mu$ L of transfection reagent alone (mock) or in combination with 25 nM scrambled siRNA (negative control) or TTP siRNA. Unfortunately, in follow up experiments to validate TTP knockdown on TTP mRNA and protein abundance, the protocol based upon the preliminary data did not alter TTP mRNA or protein abundance (Figure 19), suggesting further optimization is required.



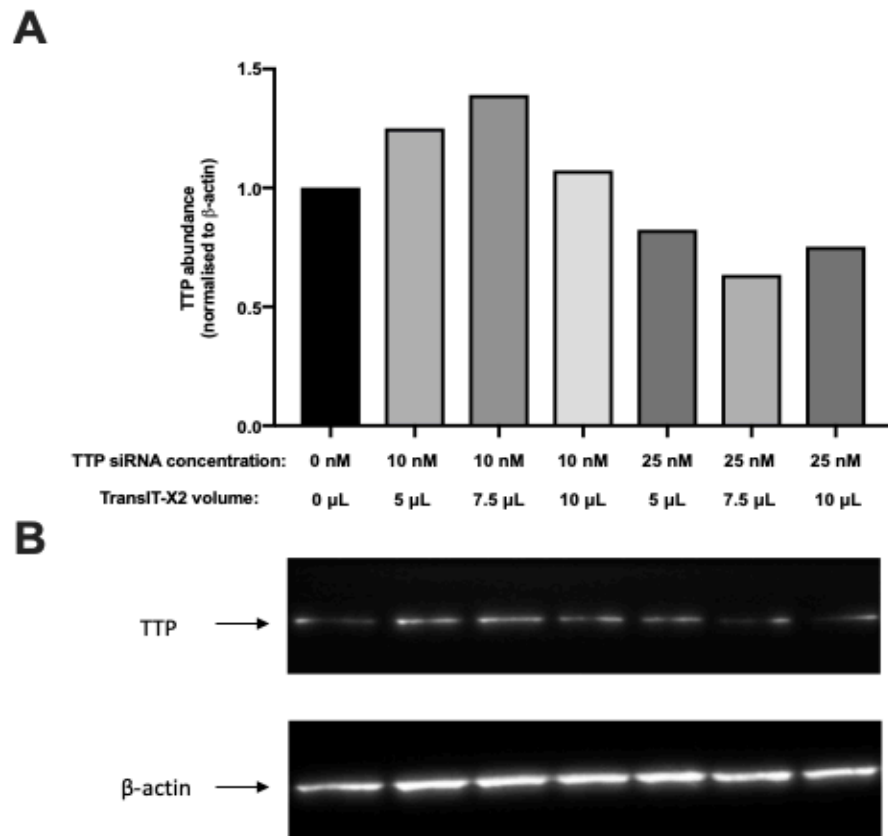


**Figure 18: TTP knockdown protocol optimization.**

hCMEC/d3 cells were exposed to 10 or 25 nM of TTP siRNA and varying volumes (5, 7.5 or 10 μL) of TransIT-X2 transfection reagent for 24 h, as indicated. Protein abundance was determined by Western blot, normalised to the loading control β-actin (n=1). TTP protein abundance is presented as a graph (A) and representative blot shown (B).

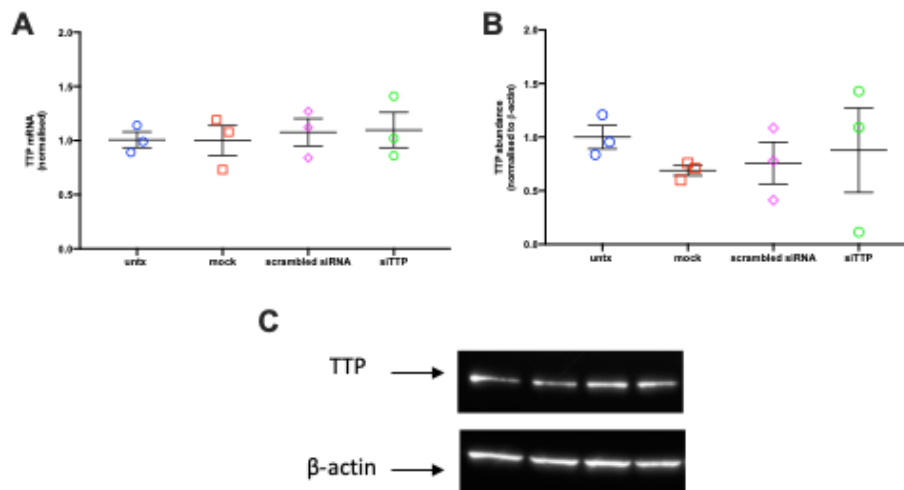


**Figure 19: Effect of TTP siRNA transfection on TTP mRNA expression and protein abundance.**

hCMEC/d3 cells were treated with 25 nM of TTP siRNA and 7.5  $\mu$ L of TransIT-X2 for 24 h. Relative TTP mRNA expression was determined using semi quantitative RT-PCR-based SYBR green chemistry, normalised to the geometric mean of GAPDH and GPI (A). TTP protein abundance was determined by Western blot, normalised to the loading control  $\beta$ -actin (B, C). Data are presented as mean  $\pm$  SEM (n=3). Data were analysed using one-way ANOVA.

### 3.7 Optimization of the DNA transfection protocol

To further investigate the idea that PP2A might be able to reverse the effect that OA and IFN $\gamma$ /TNF $\alpha$  have on VE-cadherin and claudin-5, PP2Ac was overexpressed by transfecting cells with a PP2Ac-containing plasmid. It would also be interesting to explore the effect of over expression of the endogenous inhibitors of PP2A, CIP2A and SET, on these junctional proteins. The first step towards overexpressing PP2Ac, CIP2A and SET was to establish a transfection protocol using a green fluorescent protein (GFP) plasmid. hCMEC/d3 cells were transfected with varying concentrations of the GFP plasmid (0.5, 1 or 1.5  $\mu$ g) in the presence of increasing volumes of PolyFect transfection reagent (7.5, 10 or 12.5  $\mu$ L) for 72 h. Following transfection, the cells were fixed with 3 % PFA and the nuclei stained with a Hoechst 33342 dye. The intensity of green

fluorescence was visually estimated with a fluorescence microscope (EVOS® FL) as a measure of transfection efficiency. It was found that transfection efficiency was highest using 12.5  $\mu\text{L}$  of PolyFect (Figure 20), irrespective of the amount of plasmid used. Regarding the latter, 1.0  $\mu\text{g}$  of plasmid gave an optimal fluorescence signal compared to either 0.5 or 1.5  $\mu\text{g}$  plasmid. Cells exposed to media only or mock transfected with 10  $\mu\text{L}$  of PolyFect alone showed no green fluorescence at 72 h. Based on these results 10  $\mu\text{L}$  of PolyFect and 1.0  $\mu\text{g}$  of plasmid DNA was chosen for subsequent work.

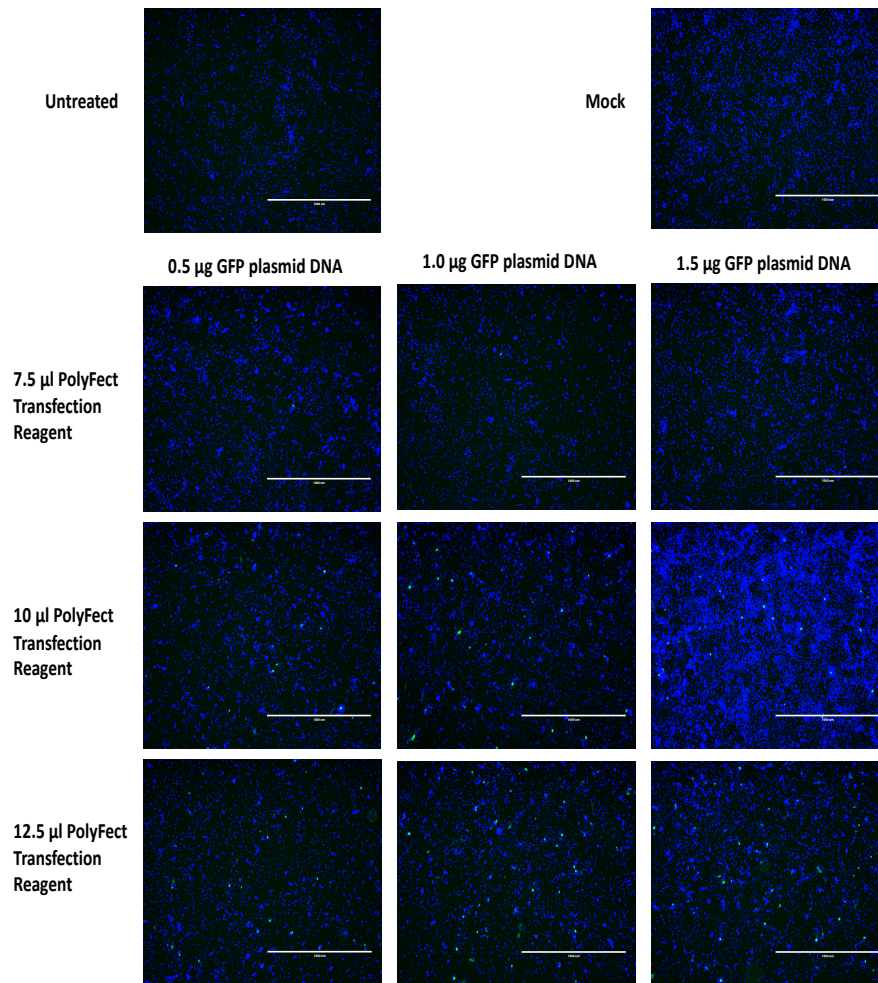


**Figure 20: Transfection optimization using a GFP plasmid and PolyFect transfection reagent.**

hCMEC/d3 cells were treated with varying volumes of PolyFect transfection reagent (7.5, 10 or 12.5  $\mu\text{L}$ ) and GFP plasmid DNA (0.5, 1 or 1.5  $\mu\text{g}$ ) for 72 h. Cells emitting green fluorescence were visualised using fluorescence microscopy (EVOS® FL) and deemed to have been successfully transfected with the GFP plasmid. Scale bar represents 1000  $\mu\text{m}$ . The nuclei were counter-stained with Hoechst (blue).

Next, hCMEC/d3 cells were transfected with 10  $\mu\text{L}$  of PolyFect and 1  $\mu\text{g}$  of CIP2A plasmid (pcCIP2A) or empty vector plasmid (pcDNA3.1) for 72 h, which augmented CIP2A mRNA expression by  $\sim 7$ -fold compared to the mock and empty vector transfected groups (Figure 21 A). Importantly, transfection with the empty plasmid did not increase CIP2A mRNA expression compared to the mock-transfected group. However, protein

analysis using Western blotting showed no increase in CIP2A abundance in the pcCIP2A transfected group compared to untreated, mock or pcDNA3.1 transfected cells, leading us to think that the protocol needs further optimizing. Mock transfection and transfection with pcDNA3.1 did not alter CIP2A expression in hCMEC/d3 cells compared to untreated cells.

Following consultation with past lab members, it was decided to use a mixture of 10  $\mu$ L of the PolyFect transfection reagent with 1  $\mu$ g of CIP2A plasmid, which was isolated from overnight culture of *E. coli* grown in a shaking incubator. Previous cultures were grown in an incubator at 37°C without shaking, which could lead to slower bacterial growth and therefore poor plasmid yield. Unfortunately, growing the bacteria in a shaking incubator did not increase transfection efficiency of hCMEC/d3 cells transfected with a CIP2A plasmid (Figure 21 B).

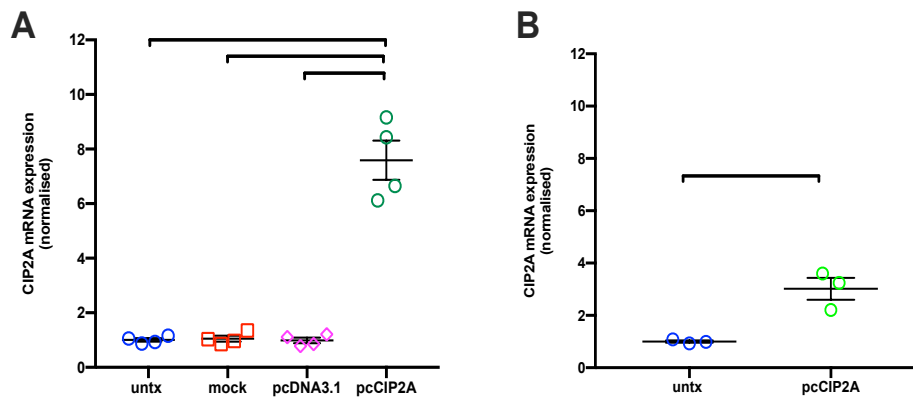


**Figure 21: Transfection of hCMEC/d3 cells with a CIP2A plasmid (pcCIP2A).**

hCMEC/d3 cells were treated with 10  $\mu$ L of PolyFect alone (mock) or in combination with 1  $\mu$ g pcDNA3.1 (control, empty vector plasmid) or pcCIP2A plasmid for 72 h. The pcCIP2A plasmid used for the transfections was isolated from a bacterial culture grown overnight in either a static (A) or shaking (B) incubator. Relative mRNA expression was determined using semi quantitative RT-PCR-based SYBR green chemistry, normalised to the geometric mean of GAPDH and GPI. Data are represented as mean  $\pm$  SEM and were analysed using one-way ANOVA with post hoc analysis (Bonferroni) (A) or a student t-test (B).  $P < 0.05$  is indicated by horizontal bars,  $n=4$  (A) and  $n=3$  (B).

To check if low transfection efficiency was due to the transfection protocol and not the CIP2A plasmid, hCMEC/d3 cells were transfected with 1  $\mu$ g of PP2Ac plasmid (pcPP2Ac) or empty vector plasmid (pcCMV6) for 72 h using 10  $\mu$ L of PolyFect. Similar to the outcome of the previous transfections with the CIP2A plasmid, transfection with the pcPP2Ac plasmid increased mRNA expression by  $\sim 5$  fold but had no effect on protein abundance (Figure 22).

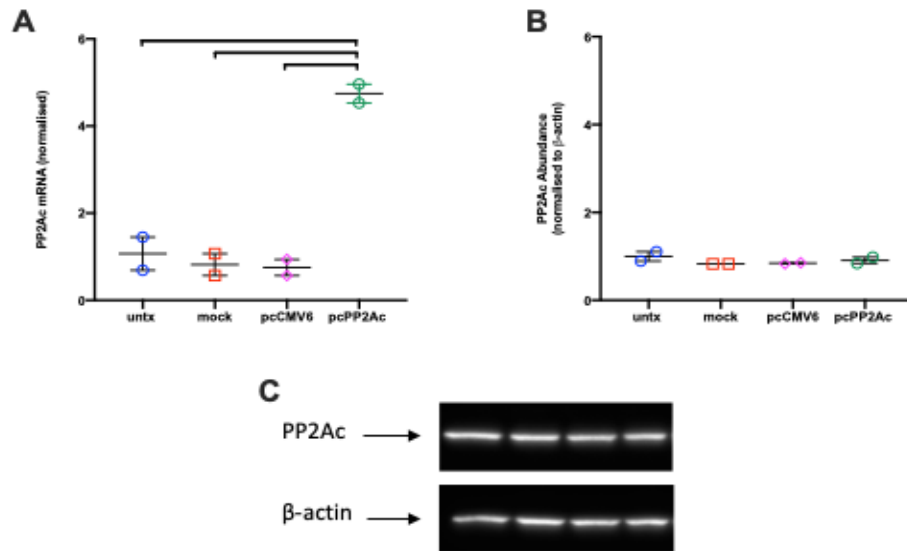


**Figure 22: Transfection using 10 µL PolyFect Transfection Reagent and 1 µg PP2Ac plasmid (pcPP2Ac).**

hCMEC/d3 cells were treated with 10 µL of PolyFect alone (mock) or in combination with 1 µg pcCMV6 (control, empty vector plasmid) or PP2Ac plasmid for 72 h. Relative mRNA expression was determined using semi quantitative RT-PCR-based SYBR green chemistry, normalised to the geometric mean of GAPDH and GPI (A). Protein abundance was determined by Western blot, normalised to the loading control β-actin (B, C). Data are represented as mean ± SEM (n=2). P < 0.05 is indicated by horizontal bars. Data were analysed using one-way ANOVA with post hoc analysis (Bonferroni).

As the data obtained using PolyFect were disappointing, an attempt was made to transfect hCMEC/d3 cells using alternative transfection reagents. Cells were transfected with 1 µg of PP2Ac plasmid and varying volumes of either Lipofectamine 2000 (0.5, 1, 2 or 3 µL) or TransIT-X2 (2, 3, 4 or 5 µL) transfection reagents. As per the manufacturer's protocols, the media containing the transfection reagent and plasmid DNA mixture was changed to fresh media after 6 h. mRNA was isolated after 72 h. No increase in PP2Ac mRNA was seen in any of the transfection groups using Lipofectamine 2000 (Figure 23 A) or TransIT-X2 (Figure 23 B) as the transfection reagent.

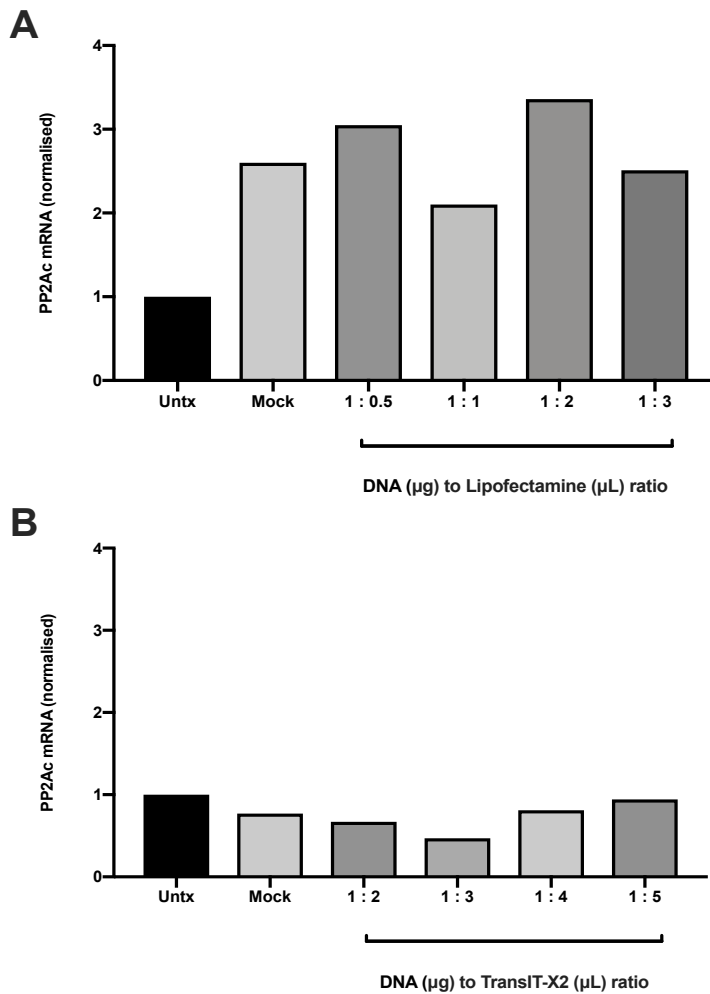


**Figure 23: Transfection of hCMEC/d3 cells with a PP2Ac plasmid (pcPP2ac) using Lipofectamine 2000 or TransIT-X2.**

hCMEC/d3 cells were treated with 0.5, 1, 2 or 3 μL of Lipofectamine 2000 (A) or 2, 3, 4 or 5 μL of TransIT-X2 (B) transfection reagents and 1 μg PP2Ac plasmid for 72 h. Relative mRNA expression was determined using semi quantitative RT-PCR-based SYBR green chemistry, normalised to the geometric mean of GAPDH and GPI (n-1).

Based on the above results, showing that the best transfection efficiency was achieved using PolyFect transfection reagent, the transfection protocol was further optimized by increasing the concentration of plasmid DNA used in the transfection mix. hCMEC/d3 cells were transfected using 2 or 4 μg of PP2Ac plasmid DNA and 5 or 10 μL of PolyFect transfection reagent. PP2Ac mRNA was increased by ~ 80 fold in



cells transfected using 2  $\mu\text{g}$  plasmid and 5  $\mu\text{L}$  PolyFect, while cells transfected using 10  $\mu\text{L}$  of PolyFect and 2 or 4  $\mu\text{g}$  plasmid DNA had increased PP2Ac mRNA by  $\sim 2000$  and  $\sim 1400$  fold, respectively (Figure 24). Importantly, mock transfected cells showed minimal increase in PP2Ac mRNA (0:5 and 0:10, Figure 24).

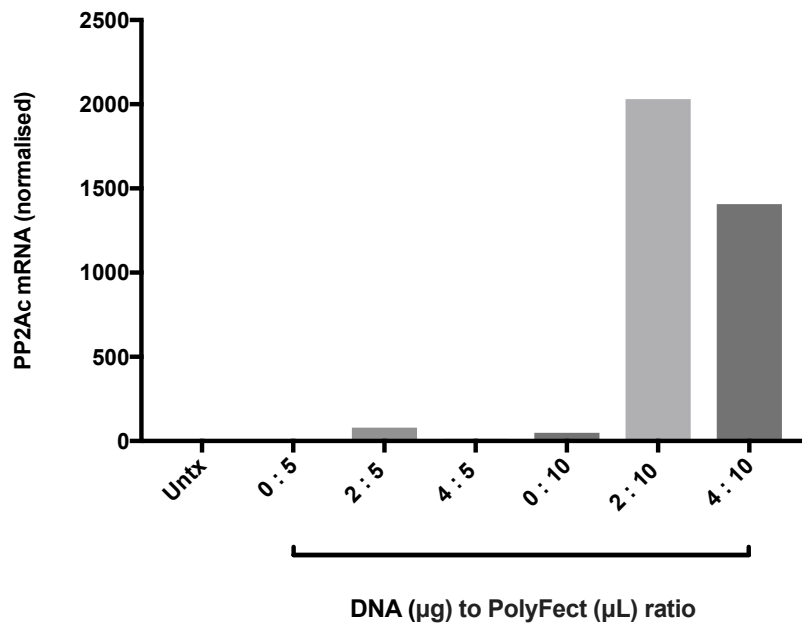


**Figure 24: Transfection using varying volumes of PP2Ac plasmid DNA and PolyFect Transfection Reagent.**

hCMEC/d3 cells were treated with 5 and 10  $\mu\text{L}$  of PolyFect transfection reagent alone (mock, 0:5 and 0:10 columns) or in combination with 2 or 4  $\mu\text{L}$  of PP2Ac plasmid for 72 h. Relative mRNA expression was determined using semi quantitative RT-PCR-based SYBR green chemistry, normalised to the geometric mean of GAPDH and GPI (n=1).

# Chapter 4

---

## 4. Discussion and Conclusion

Understanding the regulation of junctional proteins present in the blood-brain barrier and their association with barrier integrity is an essential component of designing novel treatment options for patients with diseases such as Alzheimer's and Parkinson's disease. To address this, the present study used human brain microvascular endothelial cells, which are a recognised model of the human BBB [371]. Tight and adherens junctions are a vital component of the BBB and are highly regulated through post-translational modifications, specifically phosphorylation. Protein kinases responsible for phosphorylating proteins have been studied much more extensively than the dephosphorylating phosphatases, especially in regards to drug development and human diseases [246]. However, protein phosphatases are starting to emerge as drug targets in cancer [247], cardiovascular disease [248] and neurodegenerative disease [249].

Endothelial cells present in the CNS microvasculature control the transport of molecules circulating in the blood to the brain and spinal cord. Opening and closing of adherens junctions regulates permeability of the CNS endothelium [118]. VE-cadherin is the most important protein of the adherens junctions, with a key role in junction formation, stability and regulation [372]. In the present study okadaic acid decreased both VE-cadherin mRNA expression and protein abundance in hCMEC/d3 cells (Figure 12 A, B). This is in agreement with previous work from our laboratory, which has shown okadaic acid to decrease VE-cadherin abundance, but is at variance with an increase in VE-cadherin mRNA expression reported before [373]. It is unclear why the effect of OA on VE-cadherin mRNA expression differs between studies, with previous data showing a ~ 2.7 fold increase and the current study reporting an 80 % decrease in mRNA abundance. Nevertheless, the data presented here is consistent with the observed decrease in VE-cadherin protein abundance noted in both studies. Functionally, the loss of VE-cadherin is consistent with okadaic acid-mediated cell rounding, loss of cell-cell

contacts, and disruption of the blood-brain barrier [374]. The down regulation of VE-cadherin expression and abundance is most likely a result of PP2A and not PP1 inhibition, as OA is relatively selective for PP2A at the concentration used [243]. It was interesting to note that the small molecule activators DBK-1154 and FTY-720 did not reverse the effects of OA at the concentrations used (Figure 12 A, B). This might simply reflect the dose limiting effect of DBK-1154 on cell viability or the possibility that the concentration of OA used is unsurmountable at this concentration of DBK-1154 (1  $\mu$ M). However, the role of PP2A in mediating these responses should be verified through siRNA silencing and over expression of PP2Ac.

Tight junctions are another type of cell-to-cell adhesion present in the brain endothelium, with an essential function in limiting paracellular permeability [146]. The main proteins localizing at tight junctions are claudins, and the most enriched tight junction protein at the blood-brain barrier is claudin-5 [375]. Interestingly, OA had no effect on the expression of claudin-5 mRNA in hCMEC/d3 cells (Figure 12 C). Although the effect of okadaic acid on claudin-5 has not been investigated before, a recent study which exposed human epithelial cells to okadaic acid showed that it increased mRNA expression of the channel forming claudins -2 and -4, as well as deregulating the tight junction network [336].

Although PP2A plays a role in inflammatory responses it remains to be established if inflammation modulates VE-cadherin and claudin-5 through PP2A [261]. In keeping with this, exposure of hCMEC/d3 cells to IFN $\gamma$ /TNF $\alpha$  decreased abundance of VE-cadherin mRNA and protein as well as decreased claudin-5 mRNA expression (Figure 13). This is further supported by previous studies showing decreased expression of VE-cadherin in BBB pathologies including ischemic stroke, and loss of claudin-5 from brain endothelial cells in neuroinflammatory conditions

such as multiple sclerosis and experimental autoimmune encephalomyelitis [227, 376, 377].

To test the hypothesis that this effect is mediated through PP2A, we treated hCMEC/d3 cells with IFN $\gamma$ /TNF $\alpha$  in combination with PP2A activators. The effect of IFN $\gamma$ /TNF $\alpha$  on VE-cadherin and claudin-5 was not reversed by DBK-1154 or FTY-720 at a concentration of 1  $\mu$ M (Figure 13), which is in accordance with the SMAPs' inability to prevent VE-cadherin downregulation mediated by OA. This data complements a study on FTY-720, where rat brain microvascular endothelial cells were exposed to IFN $\gamma$  and TNF $\alpha$  alone or in combination with FTY-720. While IFN $\gamma$  and TNF $\alpha$  caused a decrease in trans endothelial electrical resistance this was not altered by addition of FTY-720 up to a concentration of 100 nM [378].

Our lab has previously investigated the effect of OA on the post-transcriptional modifications of PP2Ac, showing that OA increases PP2Ac phosphorylation and demethylation, while also decreasing the abundance of LCMT-1, the protein which catalyses PP2Ac methylation [373]. PP2Ac phosphorylation and demethylation have been shown to lead to inactivation of phosphatase activity [274, 285], which is in accordance with the decrease in PP2Ac activity following okadaic acid treatment. In the present study we were interested to see if IFN $\gamma$ /TNF $\alpha$  have an effect similar to that of OA on PP2Ac abundance and its post-transcriptional modifications. There was no difference in the abundance of PP2Ac in hCMEC/d3 exposed to IFN $\gamma$ /TNF $\alpha$  (Figure 14 A), however, the expression of demethylated PP2Ac was downregulated (Figure 14 B), which would indicate an increase in phosphatase activity. Unexpectedly, this change was not accompanied by a change in the abundance of LCMT-1 or PME-1 (Figure 15). Since demethylated PP2Ac was decreased, it can be assumed that methylated PP2Ac is increased, which would be in keeping with a study on inflammatory bowel disease showing hyperosmolarity-induced inflammation is mediated through the

methylation of PP2Ac, which in turn activate NF- $\kappa$ B and lead to inflammatory cytokine secretion [379]. However, contrary to this, demethylated PP2A is increased and methylated PP2A decreased in Alzheimer's disease, a pathology which is characterised by a chronic neuroinflammation [380, 381].

Although we were not able to perform statistical analysis to examine whether phosphorylated PP2Ac is significantly increased in cells exposed to IFN $\gamma$ /TNF $\alpha$  compared to the untreated control group, pPP2Ac abundance appeared to be higher in the IFN $\gamma$ /TNF $\alpha$  group (Figure 16). Currently only two biological repeats of this experiment were conducted, and therefore it's possible that increasing this number and enabling analysis of the results will show their statistical significance. An increased pPP2Ac abundance following IFN $\gamma$ /TNF $\alpha$  treatment would be in keeping with the effect OA has on pPP2Ac [373]. However, PP2Ac phosphorylation leads to the deactivation of phosphatase activity [274], which is contrary to the increased PP2A methylation also found in this study, which is believed to indicate increased holoenzyme activity [285]. Therefore, the effect IFN $\gamma$ /TNF $\alpha$  on holoenzyme activity would need to be verified through a PP2A activity assay.

Due to PP2A's multi-faceted role in the regulation of cell cycle and signalling, re-activating this vital phosphatase is starting to emerge as a therapeutic approach for the treatment of human malignancies, including prostate and lung cancers, as well as inflammatory diseases, such as multiple sclerosis and Alzheimer's disease [261]. Our lab has previously shown that the overexpression of PP2Ac in hBMEC cells can reverse the loss of VE-cadherin abundance as well as attenuate increased permeability induced by a co-culture with pro-inflammatory macrophages. Additionally, overexpression of CIP2A and SET in hCMEC/d3 cells decreased VE-cadherin mRNA expression and protein abundance, while increasing paracellular permeability [373].

The current study aimed to examine whether overexpressing PP2Ac can reverse the loss of VE-cadherin mRNA and protein induced by exposing the cells to IFN $\gamma$ /TNF $\alpha$  and OA as well as the loss of claudin-5 mRNA caused by IFN $\gamma$ /TNF $\alpha$ . Unfortunately, optimization of the transfection protocol was quite challenging. While there was a significant increase in CIP2A and PP2Ac mRNA following 72 h transfection with CIP2A and PP2Ac plasmid DNA, respectively, there was no increase in protein concentration (Figures 21 and 22). The chemical methods of cell transfection that were availed of in this study work by inserting a gene encoding a protein of interest (the plasmid DNA) and a chemical (transfection reagent) into a cell. The transfection reagents used in this study are PolyFect which consists of activated-dendrimers, the polymer-based TransIT-X2 and the cationic lipid-based Lipofectamine 2000 transfection reagent. These positively charged chemicals interact with the negatively charged plasmid DNA, forming a positively charged complex, which can react with the cell membrane. The complex enters the cell by phagocytosis or endocytosis and the plasmid DNA is further transported into the nucleus, where it's transcribed into mRNA which is subsequently translated into protein [382, 383]. Many research groups rely on mRNA assays in their studies, as mRNA data is more easily available than protein data, and because they assume that differential mRNA expression correlates with differential expression of the corresponding protein [384]. However, the expression of mRNA and protein is often discordant, as is seen in the overexpression experiments in this study. Such effect can be caused by post-transcriptional regulation of the mRNA, translation repression by miRNAs, low rate of translation or protein degradation [385-387].

Although the expression level of mRNA doesn't always correlate with the protein expression within a cell, mRNA abundance can act as a proxy for the presence, or more precisely, the detectability, of the corresponding

protein. Vogel and Marcotte (2012) [388] have proposed a model, in which there's a stochastic 'on' and 'off' switch for transcription. According to this model, transcription is 'off' up to a certain level of mRNA concentration, and then when the mRNA concentration rises, the switch is flipped 'on' and protein production commences. We presumed this mechanism might be occurring during the CIP2A and PP2Ac overexpression study, as transfection with the respective plasmid DNA led to a ~ 7 fold CIP2A mRNA (Figure 21) and ~ 5 fold PP2Ac mRNA increase (Figure 22); however no change in the protein levels were detected. We expected to see an increase in protein expression once the mRNA levels reached the stochastic threshold, and for that reason we continued optimizing the transfection protocol. Finally, a profound overexpression of PP2Ac was achieved, with the mRNA level increasing by ~ 2,000 fold in the transfected group (Figure 24). While a corresponding differential expression in PP2Ac protein abundance was expected, this coincided with closure of the labs because of the SARS-CoV-2 pandemic which made it impossible to repeat the transfection experiment and extract the protein for a Western blot.

Post-transcriptional processes such as mRNA stability, translocation and translation are essential for cells to be able to rapidly respond to stimuli, such as inflammation [389]. mRNA stability is an important factor to consider when investigating mRNA and protein expression in a cell, as alterations in the half-life of mRNA can cause its abundance to fluctuate many fold [390]. Post-transcriptional regulation mediated by miRNAs and RNA-binding proteins can affect the mRNA stability of tight junction proteins, such as occludin, claudin-1 and -14 and JAM-1 [391]. A study by Ye *et al.*, (2011) [392] showed that TNF $\alpha$  increased expression of the miRNA miR-122a, which binds to occludin mRNA leading to its degradation as well as having a negative effect on intestinal tight junction permeability. To the best of our knowledge, no such studies have been conducted on the mRNA stability of VE-cadherin and claudin-5.



Investigating the effect of IFN $\gamma$ /TNF $\alpha$  on the half-life of VE-cadherin and claudin-5 would help to understand the mechanism which leads to the decrease in their mRNA expression. Since the half-life of VE-cadherin and claudin-5 mRNA was expected to decrease after exposure to IFN $\gamma$ /TNF $\alpha$ , this indicated that the assay needs further optimization (Figure 17). Unfortunately, due to closure of the laboratory, further optimization experiments were not conducted.

While this study aimed to investigate the effect of IFN $\gamma$ /TNF $\alpha$  on the mRNA stability of VE-cadherin and claudin-5, we decided to also look at the role that tristetraprolin plays in the regulation of the expression of these junctional proteins. TTP is a zinc finger mRNA-binding protein, which binds to the mRNA of pro-inflammatory mediators and cell-cycle progression regulators [259]. TTP catalyses the removal of mRNA's poly-(A) tail, decreasing the molecules' stability and enhancing the rate of its degradation [370]. Interestingly, phosphorylated TTP is inactive, and can be activated via dephosphorylation by PP2A [260, 393]. A study by Rahman *et al.*, [394] showed that inhibition of PP2A by okadaic acid leads to increased production of the pro-inflammatory cytokines IL-6 and IL-8 through a mechanism involving a build-up of inactive TTP. Moreover, the study demonstrated that this effect can be reversed by pre-treating cells with FTY-720 or by PP2Ac overexpression. The current study aimed to investigate the effect of TTP knockdown alone and in conjunction with OA or IFN $\gamma$ /TNF $\alpha$  treatment on the expression of VE-cadherin and claudin-5 (Figure 18). Furthermore, if the mRNA or protein abundance of VE-cadherin or claudin-5 was altered by TTP knockdown, it would be interesting to overexpress PP2Ac in the cells to definitively implicate PP2Ac in the process and ascertain if the effect can be reversed by SMAPs. Unfortunately, the lab was closed due to the coronavirus infectious disease 2019 pandemic before the TTP knockdown experiment was optimized.

In conclusion, this study shows that exposure of human microvascular endothelial cells to IFN $\gamma$ /TNF $\alpha$  decreased VE-cadherin mRNA and protein abundance as well as downregulated claudin-5 mRNA (Figure 13). Similarly, treating hCMEC/d3 cells with OA leads to a decrease in VE-cadherin mRNA and protein, although no alteration in claudin-5 mRNA was noted (Figure 12). Importantly, the novel PP2A activator DBK-1154 or FTY-720 were not able to prevent this effect. While the current study would indicate that PP2A may not be involved in the mechanism that leads to VE-cadherin and claudin-5 downregulation following exposure to IFN $\gamma$ /TNF $\alpha$  or VE-cadherin decrease mediated by OA, it could be a concentration dependent issue. Indeed, other groups investigating SMAPs as novel drug anti-cancer agents use concentrations between 5 and 30  $\mu$ M to achieve growth inhibitory effects [356, 395], whereas we used a concentration of 1 $\mu$ M to treat the cells, in order to minimise their effect on cell viability. The investigation of the mechanism through which IFN $\gamma$ /TNF $\alpha$  leads to a downregulation of VE-cadherin and claudin-5 mRNA was inconclusive, although the phosphorylation and methylation of PP2Ac might be involved.

#### 4.1 Future Directions

The current work will most likely be divided into two studies going forward; study one will concentrate on the effect of inflammation on junctional proteins and study two will look at the effect of okadaic acid. To establish the role of post-transcriptional modification of PP2Ac in the downregulation of VE-cadherin and claudin-5 caused by IFN $\gamma$ /TNF $\alpha$ , the involvement of phosphorylation of PP2Ac should be confirmed. The stability of VE-cadherin and claudin-5 mRNA following treatment with IFN $\gamma$ /TNF $\alpha$  will also be validated, as the protocol has not been optimized in the current study. Additionally, to get a better understanding of the mechanism involved in downregulation of junctional proteins expression,

it would be interesting to progress the siRNA approach to knockdown tristetraprolin.

As part of the second study, we would like to look at claudin-5 threonine phosphorylation in cells treated with OA alone or in combination with Rho kinase inhibitor. We would also like to use the TTP siRNA approach alone or in combination with OA to look at the expression of VE-cadherin and claudin-5. It will also be interesting to overexpress PP2Ac to investigate whether it can reverse the decrease in junctional proteins mediated by OA and by IFN $\gamma$  and TNF $\alpha$ . Furthermore, we are interested to employ immunofluorescence in order to visualize VE-cadherin internalization following OA and IFN $\gamma$ /TNF $\alpha$  treatment.

As part of the second study, or potentially a third study, it would be interesting to investigate the effect of the endogenous PP2A inhibitors CIP2A and SET on VE-cadherin and claudin-5. Preliminary results have shown that the transfection protocol has worked, successfully overexpressing PP2Ac in hCMEC/d3 cells with PolyFect transfection reagent. Once this result is validated using Western blotting, we can use the same method to overexpress CIP2A and SET, which will allow for an array of experiments on the effect of PP2A inhibition on junctional proteins to be conducted.

## References

### Uncategorized References

1. Abbott, N.J., et al., *Structure and function of the blood-brain barrier*. Neurobiol Dis, 2010. **37**(1): p. 13-25.
2. Ehrlich, P., *Das sauerstoff-bedarfnis des organismus*. Eine farbenanalytische studie, 1885.
3. Goldmann, E.E., *Die aussere und innere Sekretion des gesunden und kranken Organismus im Liche der" vitalen Farbung"*. Beitr. Klin. Chir., 1909. **64**: p. 192-265.
4. Abbott, N.J., *Evidence for bulk flow of brain interstitial fluid: significance for physiology and pathology*. Neurochem Int, 2004. **45**(4): p. 545-52.
5. Abbott, N.J., *Comparative physiology of the blood–brain barrier*, in *Physiology and Pharmacology of the Blood–Brain Barrier*. 1992, Bradbury, M.W.B. (Ed.) p. 371-396.
6. Abbott, N.J., L. Ronnback, and E. Hansson, *Astrocyte-endothelial interactions at the blood-brain barrier*. Nat Rev Neurosci, 2006. **7**(1): p. 41-53.
7. Muoio, V., P.B. Persson, and M.M. Sendeski, *The neurovascular unit - concept review*. Acta Physiol (Oxf), 2014. **210**(4): p. 790-8.
8. Hawkins, B.T. and T.P. Davis, *The blood-brain barrier/neurovascular unit in health and disease*. Pharmacol. Rev., 2005. **57**(2): p. 173-85.
9. Rennels, M.L., T.F. Gregory, and K. Fujimoto, *Innervation of capillaries by local neurons in the cat hypothalamus: a light microscopic study with horseradish peroxidase*. J Cereb Blood Flow Metab, 1983. **3**(4): p. 535-42.
10. Heye, A.K., et al., *Assessment of blood-brain barrier disruption using dynamic contrast-enhanced MRI. A systematic review*. Neuroimage Clin, 2014. **6**: p. 262-74.
11. Chesterman, C.N., *Vascular endothelium, haemostasis and thrombosis*. Blood Rev, 1988. **2**(2): p. 88-94.
12. Jaffe, E.A., et al., *Culture of human endothelial cells derived from umbilical veins. Identification by morphologic and immunologic criteria*. J Clin Invest, 1973. **52**(11): p. 2745-56.
13. Goncharov, N.V., et al., *Markers and Biomarkers of Endothelium: When Something Is Rotten in the State*. Oxid Med Cell Longev, 2017. **2017**: p. 9759735.
14. Yu, Q.J., et al., *Targeting brain microvascular endothelial cells: a therapeutic approach to neuroprotection against stroke*. Neural Regen Res, 2015. **10**(11): p. 1882-91.
15. McConnell, H.L., et al., *The Translational Significance of the Neurovascular Unit*. J Biol Chem, 2017. **292**(3): p. 762-770.
16. Jayadev, R. and D.R. Sherwood, *Basement membranes*. Curr Biol, 2017. **27**(6): p. R207-R211.

17. Tietz, S. and B. Engelhardt, *Brain barriers: Crosstalk between complex tight junctions and adherens junctions*. J Cell Biol, 2015. **209**(4): p. 493-506.
18. Stamatovic, S.M., R.F. Keep, and A.V. Andjelkovic, *Brain endothelial cell-cell junctions: how to "open" the blood brain barrier*. Curr Neuropharmacol, 2008. **6**(3): p. 179-92.
19. Betz, A.L., J.A. Firth, and G.W. Goldstein, *Polarity of the blood-brain barrier: distribution of enzymes between the luminal and antiluminal membranes of brain capillary endothelial cells*. Brain Res, 1980. **192**(1): p. 17-28.
20. Stokes, K.Y. and D.N. Granger, *Platelets: a critical link between inflammation and microvascular dysfunction*. J Physiol, 2012. **590**(5): p. 1023-34.
21. Shimizu, F., et al., *Pericyte-derived glial cell line-derived neurotrophic factor increase the expression of claudin-5 in the blood-brain barrier and the blood-nerve barrier*. Neurochem Res, 2012. **37**(2): p. 401-9.
22. Nowacka, M.M. and E. Obuchowicz, *Vascular endothelial growth factor (VEGF) and its role in the central nervous system: a new element in the neurotrophic hypothesis of antidepressant drug action*. Neuropeptides, 2012. **46**(1): p. 1-10.
23. Suliman, S., S.M. Hemmings, and S. Seedat, *Brain-Derived Neurotrophic Factor (BDNF) protein levels in anxiety disorders: systematic review and meta-regression analysis*. Front Integr Neurosci, 2013. **7**: p. 55.
24. Wang, J., et al., *Insulin-like growth factor-1 secreted by brain microvascular endothelial cells attenuates neuron injury upon ischemia*. Febs J, 2013. **280**(15): p. 3658-68.
25. Sims, D.E., *The pericyte--a review*. Tissue Cell, 1986. **18**(2): p. 153-74.
26. Armulik, A., A. Abramsson, and C. Betsholtz, *Endothelial/pericyte interactions*. Circ Res, 2005. **97**(6): p. 512-23.
27. Lindahl, P., et al., *Pericyte loss and microaneurysm formation in PDGF-B-deficient mice*. Science (N.Y.), 1997. **277**(5323): p. 242-5.
28. Ozerdem, U., et al., *NG2 proteoglycan is expressed exclusively by mural cells during vascular morphogenesis*. Dev Dyn, 2001. **222**(2): p. 218-27.
29. Nehls, V., K. Denzer, and D. Drenckhahn, *Pericyte involvement in capillary sprouting during angiogenesis in situ*. Cell Tissue Res, 1992. **270**(3): p. 469-74.
30. Mathiisen, T.M., et al., *The perivascular astroglial sheath provides a complete covering of the brain microvessels: an electron microscopic 3D reconstruction*. Glia, 2010. **58**(9): p. 1094-103.
31. Armulik, A., G. Genove, and C. Betsholtz, *Pericytes: developmental, physiological, and pathological perspectives, problems, and promises*. Dev Cell, 2011. **21**(2): p. 193-215.

32. Bell, R.D., et al., *Pericytes control key neurovascular functions and neuronal phenotype in the adult brain and during brain aging*. Neuron, 2010. **68**(3): p. 409-27.
33. Daneman, R., et al., *Pericytes are required for blood-brain barrier integrity during embryogenesis*. Nature, 2010. **468**(7323): p. 562-6.
34. Armulik, A., et al., *Pericytes regulate the blood-brain barrier*. Nature, 2010. **468**(7323): p. 557-61.
35. Dore-Duffy, P., et al., *CNS microvascular pericytes exhibit multipotential stem cell activity*. J Cereb Blood Flow Metab, 2006. **26**(5): p. 613-24.
36. Nakagomi, T., et al., *Brain vascular pericytes following ischemia have multipotential stem cell activity to differentiate into neural and vascular lineage cells*. Stem Cells, 2015. **33**(6): p. 1962-74.
37. Zheng, Y., et al., *Angiomotin like-1 is a novel component of the N-cadherin complex affecting endothelial/pericyte interaction in normal and tumor angiogenesis*. Sci Rep, 2016. **6**: p. 30622.
38. Choudhary, M., et al., *Tumor-induced loss of mural Connexin 43 gap junction activity promotes endothelial proliferation*. BMC Cancer, 2015. **15**: p. 427.
39. Gaengel, K., et al., *Endothelial-mural cell signaling in vascular development and angiogenesis*. Arterioscler Thromb Vasc Biol, 2009. **29**(5): p. 630-8.
40. Volterra, A. and J. Meldolesi, *Astrocytes, from brain glue to communication elements: the revolution continues*. Nat Rev Neurosci, 2005. **6**(8): p. 626-40.
41. Zhang, Z., et al., *The Appropriate Marker for Astrocytes: Comparing the Distribution and Expression of Three Astrocytic Markers in Different Mouse Cerebral Regions*. Biomed Res Int, 2019. **2019**: p. 9605265.
42. Ramón y Cajal, S., *Histologie du système nerveux de l'homme & des vertébrés*. Ed. française rev. & mise à jour par l'auteur, tr. de l'espagnol par L. Azoulay. ed. Vol. v. 1. 1909, Paris :: Maloine.
43. Sofroniew, M.V. and H.V. Vinters, *Astrocytes: biology and pathology*. Acta Neuropathol, 2010. **119**(1): p. 7-35.
44. Bushong, E.A., et al., *Protoplasmic astrocytes in CA1 stratum radiatum occupy separate anatomical domains*. J Neurosci, 2002. **22**(1): p. 183-92.
45. Peters, P., Webster, *The fine structure of the nervous system* Vol. Third edn. 1991, New York Oxford University Press.
46. Filosa, J.A., et al., *Beyond neurovascular coupling, role of astrocytes in the regulation of vascular tone*. Neuroscience, 2016. **323**: p. 96-109.
47. Nakagawa, S., et al., *A new blood-brain barrier model using primary rat brain endothelial cells, pericytes and astrocytes*. Neurochem Int, 2009. **54**(3-4): p. 253-63.

48. Bell, R.D., et al., *Apolipoprotein E controls cerebrovascular integrity via cyclophilin A*. *Nature*, 2012. **485**(7399): p. 512-6.
49. Gordon, G.R., S.J. Mulligan, and B.A. MacVicar, *Astrocyte control of the cerebrovasculature*. *Glia*, 2007. **55**(12): p. 1214-21.
50. Abbott, N.J., *Astrocyte-endothelial interactions and blood-brain barrier permeability*. *J Anat*, 2002. **200**(6): p. 629-38.
51. Liddelow, S.A. and B.A. Barres, *Reactive Astrocytes: Production, Function, and Therapeutic Potential*. *Immunity*, 2017. **46**(6): p. 957-967.
52. Anderson, M.A., et al., *Astrocyte scar formation aids central nervous system axon regeneration*. *Nature*, 2016. **532**(7598): p. 195-200.
53. Zamanian, J.L., et al., *Genomic analysis of reactive astrogliosis*. *J Neurosci*, 2012. **32**(18): p. 6391-410.
54. Greter, M., I. Lelios, and A.L. Croxford, *Microglia Versus Myeloid Cell Nomenclature during Brain Inflammation*. *Front Immunol*, 2015. **6**: p. 249.
55. Hristovska, I. and O. Pascual, *Deciphering Resting Microglial Morphology and Process Motility from a Synaptic Prospect*. *Front Integr Neurosci*, 2015. **9**: p. 73.
56. Dudvarski Stankovic, N., et al., *Microglia-blood vessel interactions: a double-edged sword in brain pathologies*. *Acta Neuropathol*, 2016. **131**(3): p. 347-63.
57. Gordon, S., *Alternative activation of macrophages*. *Nat. Rev. Immunol.*, 2003. **3**(1): p. 23-35.
58. Wolburg, H. and A. Lippoldt, *Tight junctions of the blood-brain barrier: development, composition and regulation*. *Vascul Pharmacol*, 2002. **38**(6): p. 323-37.
59. Findley, M.K. and M. Koval, *Regulation and roles for claudin-family tight junction proteins*. *IUBMB life*, 2009. **61**(4): p. 431-7.
60. Stamatovic, S.M., et al., *Junctional proteins of the blood-brain barrier: New insights into function and dysfunction*. *Tissue Barriers*, 2016. **4**(1): p. e1154641.
61. Balda, M.S. and K. Matter, *Tight junctions and the regulation of gene expression*. *Biochim Biophys Acta*, 2009. **1788**(4): p. 761-7.
62. Matter, K., et al., *Mammalian tight junctions in the regulation of epithelial differentiation and proliferation*. *Curr Opin Cell Biol*, 2005. **17**(5): p. 453-8.
63. Steed, E., M.S. Balda, and K. Matter, *Dynamics and functions of tight junctions*. *Trends Cell Biol*, 2010. **20**(3): p. 142-9.
64. Forster, C., *Tight junctions and the modulation of barrier function in disease*. *Histochem Cell Biol*, 2008. **130**(1): p. 55-70.
65. Furuse, M., et al., *Occludin: a novel integral membrane protein localizing at tight junctions*. *J Cell Biol*, 1993. **123**(6 Pt 2): p. 1777-88.

66. Furuse, M., et al., *Claudin-1 and -2: novel integral membrane proteins localizing at tight junctions with no sequence similarity to occludin*. J Cell Biol, 1998. **141**(7): p. 1539-50.
67. Martin-Padura, I., et al., *Junctional adhesion molecule, a novel member of the immunoglobulin superfamily that distributes at intercellular junctions and modulates monocyte transmigration*. J Cell Biol, 1998. **142**(1): p. 117-27.
68. Guillemot, L., et al., *The cytoplasmic plaque of tight junctions: a scaffolding and signalling center*. Biochim Biophys Acta, 2008. **1778**(3): p. 601-13.
69. Tsukita, S., M. Furuse, and M. Itoh, *Multifunctional strands in tight junctions*. Nat Rev Mol Cell Biol, 2001. **2**(4): p. 285-93.
70. Butt, A.M., H.C. Jones, and N.J. Abbott, *Electrical resistance across the blood-brain barrier in anaesthetized rats: a developmental study*. J Physiol, 1990. **429**: p. 47-62.
71. Staehelin, L.A., *Further observations on the fine structure of freeze-cleaved tight junctions*. J Cell Sci, 1973. **13**(3): p. 763-86.
72. Angelow, S., R. Ahlstrom, and A.S. Yu, *Biology of claudins*. Am J Physiol Renal Physiol, 2008. **295**(4): p. F867-76.
73. Morita, K., et al., *Claudin multigene family encoding four-transmembrane domain protein components of tight junction strands*. Proc Natl Acad Sci U S A, 1999. **96**(2): p. 511-6.
74. Umeda, K., et al., *ZO-1 and ZO-2 independently determine where claudins are polymerized in tight-junction strand formation*. Cell, 2006. **126**(4): p. 741-54.
75. Furuse, M. and S. Tsukita, *Claudins in occluding junctions of humans and flies*. Trends Cell Biol, 2006. **16**(4): p. 181-8.
76. Gunzel, D. and M. Fromm, *Claudins and other tight junction proteins*. Compr Physiol, 2012. **2**(3): p. 1819-52.
77. Morita, K., et al., *Endothelial claudin: claudin-5/TMVCF constitutes tight junction strands in endothelial cells*. J Cell Biol, 1999. **147**(1): p. 185-94.
78. Tsukita, S. and M. Furuse, *Occludin and claudins in tight-junction strands: leading or supporting players?* Trends Cell Biol, 1999. **9**(7): p. 268-73.
79. Wolburg, H., et al., *Localization of claudin-3 in tight junctions of the blood-brain barrier is selectively lost during experimental autoimmune encephalomyelitis and human glioblastoma multiforme*. Acta Neuropathol, 2003. **105**(6): p. 586-92.
80. Nitta, T., et al., *Size-selective loosening of the blood-brain barrier in claudin-5-deficient mice*. J Cell Biol, 2003. **161**(3): p. 653-60.
81. Hamm, S., et al., *Astrocyte mediated modulation of blood-brain barrier permeability does not correlate with a loss of tight junction proteins from the cellular contacts*. Cell Tissue Res, 2004. **315**(2): p. 157-66.



82. Ikari, A., et al., *Phosphorylation of paracellin-1 at Ser217 by protein kinase A is essential for localization in tight junctions*. J Cell Sci, 2006. **119**(Pt 9): p. 1781-9.
83. D'Souza, T., R. Agarwal, and P.J. Morin, *Phosphorylation of claudin-3 at threonine 192 by cAMP-dependent protein kinase regulates tight junction barrier function in ovarian cancer cells*. J Biol Chem, 2005. **280**(28): p. 26233-40.
84. Yamamoto, M., et al., *Phosphorylation of claudin-5 and occludin by rho kinase in brain endothelial cells*. Am J Pathol, 2008. **172**(2): p. 521-33.
85. Fujibe, M., et al., *Thr203 of claudin-1, a putative phosphorylation site for MAP kinase, is required to promote the barrier function of tight junctions*. Exp Cell Res, 2004. **295**(1): p. 36-47.
86. Feldman, G.J., J.M. Mullin, and M.P. Ryan, *Occludin: structure, function and regulation*. Adv Drug Deliv Rev, 2005. **57**(6): p. 883-917.
87. Moroi, S., et al., *Occludin is concentrated at tight junctions of mouse/rat but not human/guinea pig Sertoli cells in testes*. Am J Physiol, 1998. **274**(6): p. C1708-17.
88. Saitou, M., et al., *Complex phenotype of mice lacking occludin, a component of tight junction strands*. Molecular biology of the cell, 2000. **11**(12): p. 4131-42.
89. Saitou, M., et al., *Occludin-deficient embryonic stem cells can differentiate into polarized epithelial cells bearing tight junctions*. J Cell Biol, 1998. **141**(2): p. 397-408.
90. Balda, M.S., et al., *Functional dissociation of paracellular permeability and transepithelial electrical resistance and disruption of the apical-basolateral intramembrane diffusion barrier by expression of a mutant tight junction membrane protein*. J Cell Biol, 1996. **134**(4): p. 1031-49.
91. Sakakibara, A., et al., *Possible involvement of phosphorylation of occludin in tight junction formation*. J Cell Biol, 1997. **137**(6): p. 1393-401.
92. Morgan, L., et al., *Inflammation and dephosphorylation of the tight junction protein occludin in an experimental model of multiple sclerosis*. Neuroscience, 2007. **147**(3): p. 664-73.
93. Antonetti, D.A., et al., *Vascular endothelial growth factor induces rapid phosphorylation of tight junction proteins occludin and zonula occluden 1. A potential mechanism for vascular permeability in diabetic retinopathy and tumors*. J Biol Chem, 1999. **274**(33): p. 23463-7.
94. DeMaio, L., et al., *Oxidized phospholipids mediate occludin expression and phosphorylation in vascular endothelial cells*. Am J Physiol Heart Circ Physiol, 2006. **290**(2): p. H674-83.
95. Ebnet, K., *Junctional Adhesion Molecules (JAMs): Cell Adhesion Receptors With Pleiotropic Functions in Cell Physiology and Development*. Physiol Rev, 2017. **97**(4): p. 1529-1554.

96. Ebnet, K., et al., *Junctional adhesion molecules (JAMs): more molecules with dual functions?* J Cell Sci, 2004. **117**(Pt 1): p. 19-29.
97. Ebnet, K., et al., *Regulation of cell polarity by cell adhesion receptors.* Semin Cell Dev Biol, 2018. **81**: p. 2-12.
98. Steinbacher, T., D. Kummer, and K. Ebnet, *Junctional adhesion molecule-A: functional diversity through molecular promiscuity.* Cell Mol Life Sci, 2018. **75**(8): p. 1393-1409.
99. Weber, C., L. Fraemohs, and E. Dejana, *The role of junctional adhesion molecules in vascular inflammation.* Nat Rev Immunol, 2007. **7**(6): p. 467-77.
100. Ostermann, G., et al., *JAM-1 is a ligand of the beta(2) integrin LFA-1 involved in transendothelial migration of leukocytes.* Nat Immunol, 2002. **3**(2): p. 151-8.
101. Vorbodt, A.W. and D.H. Dobrogowska, *Molecular anatomy of intercellular junctions in brain endothelial and epithelial barriers: electron microscopist's view.* Brain Res Rev, 2003. **42**(3): p. 221-42.
102. Seibel, M., S. Robins, and J. Bilezikian, *Dynamics of Bone and Cartilage Metabolism: Principles and Clinical Applications.* 2006: Elsevier.
103. Navarro, P., L. Ruco, and E. Dejana, *Differential localization of VE- and N-cadherins in human endothelial cells: VE-cadherin competes with N-cadherin for junctional localization.* J. Cell Biol., 1998. **140**(6): p. 1475-84.
104. Vestweber, D., et al., *Cell adhesion dynamics at endothelial junctions: VE-cadherin as a major player.* Trends Cell Biol., 2009. **19**(1): p. 8-15.
105. Patel, S.D., et al., *Type II cadherin ectodomain structures: implications for classical cadherin specificity.* Cell, 2006. **124**(6): p. 1255-68.
106. Baumgartner, W., et al., *Cadherin interaction probed by atomic force microscopy.* Proc Natl Acad Sci U S A, 2000. **97**(8): p. 4005-10.
107. Dejana, E. and D. Vestweber, *The role of VE-cadherin in vascular morphogenesis and permeability control.* Prog Mol Biol Transl Sci, 2013. **116**: p. 119-44.
108. Giannotta, M., M. Trani, and E. Dejana, *VE-cadherin and endothelial adherens junctions: active guardians of vascular integrity.* Dev Cell, 2013. **26**(5): p. 441-54.
109. Breier, G., et al., *Molecular cloning and expression of murine vascular endothelial-cadherin in early stage development of cardiovascular system.* Blood, 1996. **87**(2): p. 630-41.
110. Carmeliet, P., et al., *Targeted deficiency or cytosolic truncation of the VE-cadherin gene in mice impairs VEGF-mediated endothelial survival and angiogenesis.* Cell, 1999. **98**(2): p. 147-57.

111. Corada, M., et al., *Vascular endothelial-cadherin is an important determinant of microvascular integrity in vivo*. Proc. Natl. Acad. Sci. U. S. A., 1999. **96**(17): p. 9815-20.
112. Gory-Faure, S., et al., *Role of vascular endothelial-cadherin in vascular morphogenesis*. Development, 1999. **126**(10): p. 2093-102.
113. Luo, Y. and G.L. Radice, *N-cadherin acts upstream of VE-cadherin in controlling vascular morphogenesis*. J Cell Biol, 2005. **169**(1): p. 29-34.
114. Murakami, M., et al., *The FGF system has a key role in regulating vascular integrity*. J Clin Invest, 2008. **118**(10): p. 3355-66.
115. Yang, X., et al., *Fibroblast growth factor signaling in the vasculature*. Curr Atheroscler Rep, 2015. **17**(6): p. 509.
116. Taddei, A., et al., *Endothelial adherens junctions control tight junctions by VE-cadherin-mediated upregulation of claudin-5*. Nat Cell Biol, 2008. **10**(8): p. 923-34.
117. Nawroth, R., et al., *VE-PTP and VE-cadherin ectodomains interact to facilitate regulation of phosphorylation and cell contacts*. EMBO J, 2002. **21**(18): p. 4885-95.
118. Dejana, E., F. Orsenigo, and M.G. Lampugnani, *The role of adherens junctions and VE-cadherin in the control of vascular permeability*. J Cell Sci, 2008. **121**(Pt 13): p. 2115-22.
119. Angelini, D.J., et al., *TNF-alpha increases tyrosine phosphorylation of vascular endothelial cadherin and opens the paracellular pathway through fyn activation in human lung endothelia*. Am J Physiol Lung Cell Mol Physiol, 2006. **291**(6): p. L1232-45.
120. Turowski, P., et al., *Phosphorylation of vascular endothelial cadherin controls lymphocyte emigration*. J. Cell Sci., 2008. **121**(Pt 1): p. 29-37.
121. Yan, J., et al., *Role of SCH79797 in maintaining vascular integrity in rat model of subarachnoid hemorrhage*. Stroke, 2013. **44**(5): p. 1410-7.
122. Dbouk, H.A., et al., *Connexins: a myriad of functions extending beyond assembly of gap junction channels*. Cell Commun Signal, 2009. **7**(1): p. 4.
123. Barbe, M.T., H. Monyer, and R. Bruzzone, *Cell-cell communication beyond connexins: the pannexin channels*. Physiol, 2006. **21**: p. 103-14.
124. Inai, T. and Y. Shibata, *Heterogeneous expression of endothelial connexin (Cx) 37, Cx40, and Cx43 in rat large veins*. Anat Sci Int, 2009. **84**(3): p. 237-45.
125. Revel, J.P. and M.J. Karnovsky, *Hexagonal array of subunits in intercellular junctions of the mouse heart and liver*. J Cell Biol, 1967. **33**(3): p. C7-C12.
126. Mathias, R.T., T.W. White, and X. Gong, *Lens gap junctions in growth, differentiation, and homeostasis*. Physiol Rev, 2010. **90**(1): p. 179-206.

127. White, T.W. and D.L. Paul, *Genetic diseases and gene knockouts reveal diverse connexin functions*. *Annu Rev Physiol*, 1999. **61**: p. 283-310.
128. Pappenheimer, J.R., E.M. Renkin, and L.M. Borrero, *Filtration, diffusion and molecular sieving through peripheral capillary membranes; a contribution to the pore theory of capillary permeability*. *Am J Physiol*, 1951. **167**(1): p. 13-46.
129. Ghitescu, L., et al., *Specific binding sites for albumin restricted to plasmalemmal vesicles of continuous capillary endothelium: receptor-mediated transcytosis*. *J Cell Biol*, 1986. **102**(4): p. 1304-11.
130. De Bock, M., et al., *Into rather unexplored terrain-transcellular transport across the blood-brain barrier*. *Glia*, 2016. **64**(7): p. 1097-123.
131. Mayor, S. and R.E. Pagano, *Pathways of clathrin-independent endocytosis*. *Nat Rev Mol Cell Biol*, 2007. **8**(8): p. 603-12.
132. Xiao, G. and L.S. Gan, *Receptor-mediated endocytosis and brain delivery of therapeutic biologics*. *Int J Cell Biol*, 2013. **2013**: p. 703545.
133. Lu, W., *Adsorptive-mediated brain delivery systems*. *Curr Pharm Biotechnol*, 2012. **13**(12): p. 2340-8.
134. Kumagai, A.K., J.B. Eisenberg, and W.M. Pardridge, *Absorptive-mediated endocytosis of cationized albumin and a beta-endorphin-cationized albumin chimeric peptide by isolated brain capillaries*. *J Biol Chem*, 1987. **262**(31): p. 15214-9.
135. Kaur, I.P., et al., *Potential of solid lipid nanoparticles in brain targeting*. *J Control Release*, 2008. **127**(2): p. 97-109.
136. Stewart, P.A., *Endothelial vesicles in the blood-brain barrier: are they related to permeability?* *Cell Mol Neurobiol*, 2000. **20**(2): p. 149-63.
137. Sweeney, M.D., et al., *Blood-Brain Barrier: From Physiology to Disease and Back*. *Physiol Rev*, 2019. **99**(1): p. 21-78.
138. Jurcovicova, J., *Glucose transport in brain - effect of inflammation*. *Endocr Regul*, 2014. **48**(1): p. 35-48.
139. Loscher, W. and H. Potschka, *Blood-brain barrier active efflux transporters: ATP-binding cassette gene family*. *NeuroRx*, 2005. **2**(1): p. 86-98.
140. Qosa, H., et al., *Regulation of ABC efflux transporters at blood-brain barrier in health and neurological disorders*. *Brain Res*, 2015. **1628**(Pt B): p. 298-316.
141. Hartz, A.M. and B. Bauer, *ABC transporters in the CNS - an inventory*. *Curr Pharm Biotechnol*, 2011. **12**(4): p. 656-73.
142. Wang, W., A.M. Bodles-Brakhop, and S.W. Barger, *A Role for P-Glycoprotein in Clearance of Alzheimer Amyloid beta -Peptide from the Brain*. *Curr Alzheimer Res*, 2016. **13**(6): p. 615-20.

143. Cirrito, J.R., et al., *P-glycoprotein deficiency at the blood-brain barrier increases amyloid-beta deposition in an Alzheimer disease mouse model*. J Clin Invest, 2005. **115**(11): p. 3285-90.
144. Georgieva, J.V., D. Hoekstra, and I.S. Zuhorn, *Smuggling Drugs into the Brain: An Overview of Ligands Targeting Transcytosis for Drug Delivery across the Blood-Brain Barrier*. Pharmaceutics, 2014. **6**(4): p. 557-83.
145. Mehta, D. and A.B. Malik, *Signaling mechanisms regulating endothelial permeability*. Physiol Rev, 2006. **86**(1): p. 279-367.
146. Dejana, E., et al., *Organization and signaling of endothelial cell-to-cell junctions in various regions of the blood and lymphatic vascular trees*. Cell Tissue Res, 2009. **335**(1): p. 17-25.
147. Gonzalez-Mariscal, L., R. Tapia, and D. Chamorro, *Crosstalk of tight junction components with signaling pathways*. Biochim Biophys Acta, 2008. **1778**(3): p. 729-56.
148. Wallez, Y. and P. Huber, *Endothelial adherens and tight junctions in vascular homeostasis, inflammation and angiogenesis*. Biochim Biophys Acta, 2008. **1778**(3): p. 794-809.
149. Dejana, E. and F. Orsenigo, *Endothelial adherens junctions at a glance*. J. Cell Sci., 2013. **126**(Pt 12): p. 2545-9.
150. Komarova, Y. and A.B. Malik, *Regulation of endothelial permeability via paracellular and transcellular transport pathways*. Annu Rev Physiol, 2010. **72**: p. 463-93.
151. Muller, W.A., *Leukocyte-endothelial-cell interactions in leukocyte transmigration and the inflammatory response*. Trends Immunol, 2003. **24**(6): p. 327-34.
152. Schulte, D., et al., *Stabilizing the VE-cadherin-catenin complex blocks leukocyte extravasation and vascular permeability*. EMBO J, 2011. **30**(20): p. 4157-70.
153. Filippi, M.D., *Mechanism of Diapedesis: Importance of the Transcellular Route*. Adv Immunol, 2016. **129**: p. 25-53.
154. Carman, C.V., et al., *Transcellular diapedesis is initiated by invasive podosomes*. Immunity, 2007. **26**(6): p. 784-97.
155. Gotsch, U., et al., *VE-cadherin antibody accelerates neutrophil recruitment in vivo*. J Cell Sci, 1997. **110** ( Pt 5): p. 583-8.
156. Fortin, D., *Altering the properties of the blood-brain barrier: disruption and permeabilization*. Prog Drug Res, 2003. **61**: p. 125-54.
157. Fenstermacher, J., et al., *Structural and functional variations in capillary systems within the brain*. Ann N Y Acad Sci, 1988. **529**: p. 21-30.
158. Kroll, R.A. and E.A. Neuwelt, *Outwitting the blood-brain barrier for therapeutic purposes: osmotic opening and other means*. Neurosurgery, 1998. **42**(5): p. 1083-99; discussion 1099-100.
159. Pardridge, W.M., *The blood-brain barrier: bottleneck in brain drug development*. NeuroRx, 2005. **2**(1): p. 3-14.

160. Kemper, E.M., et al., *Modulation of the blood-brain barrier in oncology: therapeutic opportunities for the treatment of brain tumours?* *Cancer Treat Rev*, 2004. **30**(5): p. 415-23.
161. Lipinski, C.A., *Drug-like properties and the causes of poor solubility and poor permeability.* *J Pharmacol Toxicol Methods*, 2000. **44**(1): p. 235-49.
162. Cordon-Cardo, C., et al., *Expression of the multidrug resistance gene product (P-glycoprotein) in human normal and tumor tissues.* *J Histochem Cytochem*, 1990. **38**(9): p. 1277-87.
163. Pardridge, W.M., *Blood-brain barrier delivery.* *Drug Discov Today*, 2007. **12**(1-2): p. 54-61.
164. Bellavance, M.A., M. Blanchette, and D. Fortin, *Recent advances in blood-brain barrier disruption as a CNS delivery strategy.* *AAPS J*, 2008. **10**(1): p. 166-77.
165. Rapoport, S.I., M. Hori, and I. Klatzo, *Testing of a hypothesis for osmotic opening of the blood-brain barrier.* *Am J Physiol*, 1972. **223**(2): p. 323-31.
166. Brightman, M.W., et al., *Osmotic opening of tight junctions in cerebral endothelium.* *J Comp Neurol*, 1973. **152**(4): p. 317-25.
167. Rodriguez, A., S.B. Tatter, and W. Debinski, *Neurosurgical Techniques for Disruption of the Blood-Brain Barrier for Glioblastoma Treatment.* *Pharmaceutics*, 2015. **7**(3): p. 175-87.
168. Miller, G., *Drug targeting. Breaking down barriers.* *Science (N.Y.)*, 2002. **297**(5584): p. 1116-8.
169. Doolittle, N.D., et al., *Safety and efficacy of a multicenter study using intraarterial chemotherapy in conjunction with osmotic opening of the blood-brain barrier for the treatment of patients with malignant brain tumors.* *Cancer*, 2000. **88**(3): p. 637-47.
170. Pulgar, V.M., *Transcytosis to Cross the Blood Brain Barrier, New Advancements and Challenges.* *Front Neurosci*, 2018. **12**: p. 1019.
171. Lajoie, J.M. and E.V. Shusta, *Targeting receptor-mediated transport for delivery of biologics across the blood-brain barrier.* *Annu Rev Pharmacol Toxicol*, 2015. **55**: p. 613-31.
172. Gregori, M., et al., *Novel Antitransferrin Receptor Antibodies Improve the Blood-Brain Barrier Crossing Efficacy of Immunoliposomes.* *J Pharm Sci*, 2016. **105**(1): p. 276-83.
173. Sonali, et al., *Transferrin liposomes of docetaxel for brain-targeted cancer applications: formulation and brain theranostics.* *Drug Deliv*, 2016. **23**(4): p. 1261-71.
174. Loureiro, J.A., et al., *Cellular uptake of PLGA nanoparticles targeted with anti-amyloid and anti-transferrin receptor antibodies for Alzheimer's disease treatment.* *Colloids Surf B Biointerfaces*, 2016. **145**: p. 8-13.
175. Pardridge, W.M., et al., *Plasma Pharmacokinetics of Valanafusp Alpha, a Human Insulin Receptor Antibody-Iduronidase Fusion Protein, in Patients with Mucopolysaccharidosis Type I.* *BioDrugs*, 2018. **32**(2): p. 169-176.

176. Giugliani, R., et al., *Neurocognitive and somatic stabilization in pediatric patients with severe Mucopolysaccharidosis Type I after 52 weeks of intravenous brain-penetrating insulin receptor antibody-iduronidase fusion protein (valanafusp alpha): an open label phase 1-2 trial*. Orphanet J Rare Dis, 2018. **13**(1): p. 110.
177. Gao, H. and X. Gao, *Brain Targeted Drug Delivery Systems: A Focus on Nanotechnology and Nanoparticulates* 1st ed. 2018, Academic Press: . 499.
178. Li, L., et al., *Large amino acid transporter 1 mediated glutamate modified docetaxel-loaded liposomes for glioma targeting*. Colloids Surf B Biointerfaces, 2016. **141**: p. 260-267.
179. Bhunia, S., et al., *Large Amino Acid Transporter 1 Selective Liposomes of L-DOPA Functionalized Amphiphile for Combating Glioblastoma*. Mol Pharm, 2017. **14**(11): p. 3834-3847.
180. Banks, W.A., *Characteristics of compounds that cross the blood-brain barrier*. BMC Neurol, 2009. **9 Suppl 1**: p. S3.
181. Lawther, B.K., S. Kumar, and H. Krovvidi, *Blood–brain barrier*. CEACCP, 2011. **11**(4): p. 128-132.
182. DiSabato, D.J., N. Quan, and J.P. Godbout, *Neuroinflammation: the devil is in the details*. J Neurochem, 2016. **139 Suppl 2**: p. 136-153.
183. Norden, D.M., et al., *Sequential activation of microglia and astrocyte cytokine expression precedes increased Iba-1 or GFAP immunoreactivity following systemic immune challenge*. Glia, 2016. **64**(2): p. 300-16.
184. Monahan, A.J., M. Warren, and P.M. Carvey, *Neuroinflammation and peripheral immune infiltration in Parkinson's disease: an autoimmune hypothesis*. Cell Transplant, 2008. **17**(4): p. 363-72.
185. Lee, B., K.M. Moon, and C.Y. Kim, *Tight Junction in the Intestinal Epithelium: Its Association with Diseases and Regulation by Phytochemicals*. J Immunol Res, 2018. **2018**: p. 2645465.
186. Roberts, T.K., et al., *CCL2 disrupts the adherens junction: implications for neuroinflammation*. Lab. Invest., 2012. **92**(8): p. 1213-33.
187. Beard, R.S., Jr., et al., *Non-muscle Mlck is required for beta-catenin- and FoxO1-dependent downregulation of Cldn5 in IL-1beta-mediated barrier dysfunction in brain endothelial cells*. J Cell Sci, 2014. **127**(Pt 8): p. 1840-53.
188. Bruewer, M., et al., *Proinflammatory cytokines disrupt epithelial barrier function by apoptosis-independent mechanisms*. J Immunol, 2003. **171**(11): p. 6164-72.
189. Wang, F., et al., *Interferon-gamma and tumor necrosis factor-alpha synergize to induce intestinal epithelial barrier dysfunction by up-regulating myosin light chain kinase expression*. Am J Pathol, 2005. **166**(2): p. 409-19.

190. Huber, J.D., et al., *Inflammatory pain alters blood-brain barrier permeability and tight junctional protein expression*. Am J Physiol Heart Circ Physiol, 2001. **280**(3): p. H1241-8.
191. McCaffrey, G. and T.P. Davis, *Physiology and pathophysiology of the blood-brain barrier: P-glycoprotein and occludin trafficking as therapeutic targets to optimize central nervous system drug delivery*. J Investig Med, 2012. **60**(8): p. 1131-40.
192. Sokolova, A., et al., *Monocyte chemoattractant protein-1 plays a dominant role in the chronic inflammation observed in Alzheimer's disease*. Brain Pathol, 2009. **19**(3): p. 392-8.
193. Cramer, S.P., et al., *Abnormal blood-brain barrier permeability in normal appearing white matter in multiple sclerosis investigated by MRI*. Neurolmage. Clinical, 2014. **4**: p. 182-9.
194. Gray, M.T. and J.M. Woulfe, *Striatal blood-brain barrier permeability in Parkinson's disease*. J Cereb Blood Flow Metab, 2015. **35**(5): p. 747-50.
195. Remy, S. and H. Beck, *Molecular and cellular mechanisms of pharmacoresistance in epilepsy*. Brain, 2006. **129**(Pt 1): p. 18-35.
196. Renia, L., et al., *Cerebral malaria: mysteries at the blood-brain barrier*. Virulence, 2012. **3**(2): p. 193-201.
197. Rosenberg, G.A., *Neurological diseases in relation to the blood-brain barrier*. J Cereb Blood Flow Metab, 2012. **32**(7): p. 1139-51.
198. Profaci, C.P., et al., *The blood-brain barrier in health and disease: Important unanswered questions*. J Exp Med, 2020. **217**(4).
199. HSE. *Multiple Sclerosis*. 2011 13/07/2011; Available from: <https://www.hse.ie/eng/health/az/m/ms/causes-of-multiple-sclerosis.html>.
200. Uzunkopru, C., *Invasive Therapies in Multiple Sclerosis*. Noro Psikiyatrs Ars, 2018. **55**(Suppl 1): p. S21-S25.
201. Plumb, J., et al., *Abnormal endothelial tight junctions in active lesions and normal-appearing white matter in multiple sclerosis*. Brain Pathol, 2002. **12**(2): p. 154-69.
202. Shimizu, F., et al., *Sera from remitting and secondary progressive multiple sclerosis patients disrupt the blood-brain barrier*. PLoS One, 2014. **9**(3): p. e92872.
203. Minagar, A. and J.S. Alexander, *Blood-brain barrier disruption in multiple sclerosis*. Mult. Scler., 2003. **9**(6): p. 540-9.
204. Song, L. and J.S. Pachter, *Monocyte chemoattractant protein-1 alters expression of tight junction-associated proteins in brain microvascular endothelial cells*. Microvasc Res, 2004. **67**(1): p. 78-89.
205. Weller, J. and A. Budson, *Current understanding of Alzheimer's disease diagnosis and treatment*. F1000Res, 2018. **7**: p. F1000 Faculty Rev-1161.
206. Dos Santos Picanco, L.C., et al., *Alzheimer's Disease: A Review from the Pathophysiology to Diagnosis, New Perspectives for*



- Pharmacological Treatment*. *Curr Med Chem*, 2018. **25**(26): p. 3141-3159.
207. Alonso Adel, C., et al., *Polymerization of hyperphosphorylated tau into filaments eliminates its inhibitory activity*. *Proc Natl Acad Sci U S A*, 2006. **103**(23): p. 8864-9.
208. Kinney, J.W., et al., *Inflammation as a central mechanism in Alzheimer's disease*. *Alzheimers Dement (N Y)*, 2018. **4**: p. 575-590.
209. Cai, Z., et al., *Role of Blood-Brain Barrier in Alzheimer's Disease*. *J Alzheimers Dis*, 2018. **63**(4): p. 1223-1234.
210. Wu, Z., et al., *Role of the MEOX2 homeobox gene in neurovascular dysfunction in Alzheimer disease*. *Nat Med*, 2005. **11**(9): p. 959-65.
211. Choi, B.R., et al., *Increased expression of the receptor for advanced glycation end products in neurons and astrocytes in a triple transgenic mouse model of Alzheimer's disease*. *Exp Mol Med*, 2014. **46**(2): p. e75.
212. Yamazaki, Y., et al., *Selective loss of cortical endothelial tight junction proteins during Alzheimer's disease progression*. *Brain*, 2019. **142**(4): p. 1077-1092.
213. Armstrong, M.J. and M.S. Okun, *Diagnosis and Treatment of Parkinson Disease: A Review*. *JAMA*, 2020. **323**(6): p. 548-560.
214. Dickson, D.W., et al., *Neuropathological assessment of Parkinson's disease: refining the diagnostic criteria*. *Lancet Neurol*, 2009. **8**(12): p. 1150-7.
215. Pan, Y. and J.A. Nicolazzo, *Impact of aging, Alzheimer's disease and Parkinson's disease on the blood-brain barrier transport of therapeutics*. *Adv Drug Deliv Rev*, 2018. **135**: p. 62-74.
216. Sawada, M., K. Imamura, and T. Nagatsu, *Role of cytokines in inflammatory process in Parkinson's disease*. *J Neural Transm Suppl*, 2006(70): p. 373-81.
217. Joers, V., et al., *Microglial phenotypes in Parkinson's disease and animal models of the disease*. *Prog Neurobiol*, 2017. **155**: p. 57-75.
218. Pisanu, A., et al., *Dynamic changes in pro- and anti-inflammatory cytokines in microglia after PPAR-gamma agonist neuroprotective treatment in the MPTPp mouse model of progressive Parkinson's disease*. *Neurobiol Dis*, 2014. **71**: p. 280-91.
219. Booth, H.D.E., W.D. Hirst, and R. Wade-Martins, *The Role of Astrocyte Dysfunction in Parkinson's Disease Pathogenesis*. *Trends Neurosci*, 2017. **40**(6): p. 358-370.
220. Brochard, V., et al., *Infiltration of CD4+ lymphocytes into the brain contributes to neurodegeneration in a mouse model of Parkinson disease*. *J Clin Invest*, 2009. **119**(1): p. 182-92.
221. Gattlinger, T., et al., *Predicting Early Mortality of Acute Ischemic Stroke*. *Stroke*, 2019. **50**(2): p. 349-356.

222. Benjamin, E.J., et al., *Heart Disease and Stroke Statistics-2017 Update: A Report From the American Heart Association*. Circulation, 2017. **135**(10): p. e146-e603.
223. Ojaghihaghighi, S., et al., *Comparison of neurological clinical manifestation in patients with hemorrhagic and ischemic stroke*. World J Emerg Med, 2017. **8**(1): p. 34-38.
224. Liu, S., S.R. Levine, and H.R. Winn, *Targeting ischemic penumbra: part I - from pathophysiology to therapeutic strategy*. J Exp Stroke Transl Med, 2010. **3**(1): p. 47-55.
225. Abdullahi, W., D. Tripathi, and P.T. Ronaldson, *Blood-brain barrier dysfunction in ischemic stroke: targeting tight junctions and transporters for vascular protection*. Am J Physiol Cell Physiol, 2018. **315**(3): p. C343-C356.
226. Liu, J., et al., *Matrix metalloproteinase-2-mediated occludin degradation and caveolin-1-mediated claudin-5 redistribution contribute to blood-brain barrier damage in early ischemic stroke stage*. J Neurosci, 2012. **32**(9): p. 3044-57.
227. Wacker, B.K., et al., *Junctional protein regulation by sphingosine kinase 2 contributes to blood-brain barrier protection in hypoxic preconditioning-induced cerebral ischemic tolerance*. J Cereb Blood Flow Metab, 2012. **32**(6): p. 1014-23.
228. Jiao, H., et al., *Specific role of tight junction proteins claudin-5, occludin, and ZO-1 of the blood-brain barrier in a focal cerebral ischemic insult*. J Mol Neurosci, 2011. **44**(2): p. 130-9.
229. Gralinski, L.E., et al., *Mouse adenovirus type 1-induced breakdown of the blood-brain barrier*. J Virol, 2009. **83**(18): p. 9398-410.
230. Xu, Z., et al., *West Nile virus infection causes endocytosis of a specific subset of tight junction membrane proteins*. PLoS One, 2012. **7**(5): p. e37886.
231. Afonso, P.V., et al., *Alteration of blood-brain barrier integrity by retroviral infection*. PLoS Pathog, 2008. **4**(11): p. e1000205.
232. Ng, S.C. and H. Tilg, *COVID-19 and the gastrointestinal tract: more than meets the eye*. Gut, 2020. **69**(6): p. 973-974.
233. Mao, L., et al., *Neurologic Manifestations of Hospitalized Patients With Coronavirus Disease 2019 in Wuhan, China*. JAMA Neurol, 2020. **77**(6): p. 683-690.
234. Bostanciklioglu, M., *Temporal Correlation Between Neurological and Gastrointestinal Symptoms of SARS-CoV-2*. Inflamm Bowel Dis, 2020. **26**(8): p. e89-e91.
235. Hepburn, M., et al., *Acute Symptomatic Seizures in Critically Ill Patients with COVID-19: Is There an Association?* Neurocrit Care, 2020.
236. Arbour, N., et al., *Neuroinvasion by human respiratory coronaviruses*. J Virol, 2000. **74**(19): p. 8913-21.
237. Bonavia, A., et al., *Infection of primary cultures of human neural cells by human coronaviruses 229E and OC43*. J Virol, 1997. **71**(1): p. 800-6.

238. Espinosa, P.S., et al., *Neurological Complications of Coronavirus Disease (COVID-19): Encephalopathy, MRI Brain and Cerebrospinal Fluid Findings: Case 2*. *Cureus*, 2020. **12**(5): p. e7930.
239. Maaroufi, H., *The Spike Protein S1 Subunit of SARS-CoV-2 Contains an LxxlxE-like Motif that is Known to Recruit the Host PP2A-B56 Phosphatase*. *bioRxiv*, 2020: p. 2020.04.01.020941.
240. Seshacharyulu, P., et al., *Phosphatase: PP2A structural importance, regulation and its aberrant expression in cancer*. *Cancer Lett.*, 2013. **335**(1): p. 9-18.
241. Manning, G., et al., *The protein kinase complement of the human genome*. *Science*, 2002. **298**(5600): p. 1912-34.
242. Damle, N.P. and M. Kohn, *The human DEPhOsphorylation Database DEPOD: 2019 update*. *Database (Oxford)*, 2019. **2019**.
243. Cohen, P., *The structure and regulation of protein phosphatases*. *Annu Rev Biochem*, 1989. **58**: p. 453-508.
244. Olsen, J.V., et al., *Global, in vivo, and site-specific phosphorylation dynamics in signaling networks*. *Cell*, 2006. **127**(3): p. 635-48.
245. Elgenaidi, I.S. and J.P. Spiers, *Regulation of the phosphoprotein phosphatase 2A system and its modulation during oxidative stress: A potential therapeutic target?* *Pharmacol Ther*, 2019. **198**: p. 68-89.
246. Ruvolo, P.P., *The broken "Off" switch in cancer signaling: PP2A as a regulator of tumorigenesis, drug resistance, and immune surveillance*. *BBA Clin*, 2016. **6**: p. 87-99.
247. Ruvolo, P.P., *Role of protein phosphatases in the cancer microenvironment*. *Biochim Biophys Acta Mol Cell Res*, 2019. **1866**(1): p. 144-152.
248. Lubbers, E.R. and P.J. Mohler, *Roles and regulation of protein phosphatase 2A (PP2A) in the heart*. *J Mol Cell Cardiol*, 2016. **101**: p. 127-133.
249. Javadpour, P., et al., *To be or not to be: PP2A as a dual player in CNS functions, its role in neurodegeneration, and its interaction with brain insulin signaling*. *Cell Mol Life Sci*, 2019. **76**(12): p. 2277-2297.
250. Shenolikar, S., *A SMAP in the face for cancer*. *J Clin Invest*, 2017. **127**(6): p. 2048-2050.
251. Shi, Y., *Serine/threonine phosphatases: mechanism through structure*. *Cell*, 2009. **139**(3): p. 468-84.
252. Dai, S., D.D. Hall, and J.W. Hell, *Supramolecular assemblies and localized regulation of voltage-gated ion channels*. *Physiol Rev*, 2009. **89**(2): p. 411-52.
253. Sents, W., et al., *The biogenesis of active protein phosphatase 2A holoenzymes: a tightly regulated process creating phosphatase specificity*. *Febs J*, 2013. **280**(2): p. 644-61.

254. Virshup, D.M. and S. Shenolikar, *From promiscuity to precision: protein phosphatases get a makeover*. *Molecular cell*, 2009. **33**(5): p. 537-45.
255. Sontag, J.M. and E. Sontag, *Protein phosphatase 2A dysfunction in Alzheimer's disease*. *Front Mol Neurosci*, 2014. **7**: p. 16.
256. Kobayashi, Y., et al., *Defects of protein phosphatase 2A causes corticosteroid insensitivity in severe asthma*. *PLoS ONE*, 2011. **6**(12): p. e27627.
257. Eichhorn, P.J., M.P. Creighton, and R. Bernards, *Protein phosphatase 2A regulatory subunits and cancer*. *Biochim Biophys Acta*, 2009. **1795**(1): p. 1-15.
258. Kowluru, A. and A. Matti, *Hyperactivation of protein phosphatase 2A in models of glucolipotoxicity and diabetes: potential mechanisms and functional consequences*. *Biochem. Pharmacol.*, 2012. **84**(5): p. 591-7.
259. Brooks, S.A. and P.J. Blackshear, *Tristetraprolin (TTP): interactions with mRNA and proteins, and current thoughts on mechanisms of action*. *Biochim Biophys Acta*, 2013. **1829**(6-7): p. 666-79.
260. Clark, A.R. and J.L. Dean, *The control of inflammation via the phosphorylation and dephosphorylation of tristetraprolin: a tale of two phosphatases*. *Biochem. Soc. Trans.*, 2016. **44**(5): p. 1321-1337.
261. Clark, A.R. and M. Ohlmeyer, *Protein phosphatase 2A as a therapeutic target in inflammation and neurodegeneration*. *Pharmacol Ther*, 2019. **201**: p. 181-201.
262. Kremmer, E., et al., *Separation of PP2A core enzyme and holoenzyme with monoclonal antibodies against the regulatory A subunit: abundant expression of both forms in cells*. *Mol. Cell. Biol.*, 1997. **17**(3): p. 1692-701.
263. Khew-Goodall, Y. and B.A. Hemmings, *Tissue-specific expression of mRNAs encoding alpha- and beta-catalytic subunits of protein phosphatase 2A*. *FEBS Lett.*, 1988. **238**(2): p. 265-8.
264. Stone, S.R., J. Hofsteenge, and B.A. Hemmings, *Molecular cloning of cDNAs encoding two isoforms of the catalytic subunit of protein phosphatase 2A*. *Biochemistry (Mosc.)*, 1987. **26**(23): p. 7215-20.
265. Janssens, V., S. Longin, and J. Goris, *PP2A holoenzyme assembly: in cauda venenum (the sting is in the tail)*. *Trends Biochem. Sci.*, 2008. **33**(3): p. 113-21.
266. Cho, U.S. and W. Xu, *Crystal structure of a protein phosphatase 2A heterotrimeric holoenzyme*. *Nature*, 2007. **445**(7123): p. 53-7.
267. Zhou, J., et al., *Characterization of the Aalpha and Abeta subunit isoforms of protein phosphatase 2A: differences in expression, subunit interaction, and evolution*. *Biochem. J.*, 2003. **369**(Pt 2): p. 387-98.
268. Hemmings, B.A., et al., *alpha- and beta-forms of the 65-kDa subunit of protein phosphatase 2A have a similar 39 amino acid*

- repeating structure*. *Biochemistry (Mosc.)*, 1990. **29**(13): p. 3166-73.
269. McCright, B. and D.M. Virshup, *Identification of a new family of protein phosphatase 2A regulatory subunits*. *J. Biol. Chem.*, 1995. **270**(44): p. 26123-8.
270. Janssens, V. and J. Goris, *Protein phosphatase 2A: a highly regulated family of serine/threonine phosphatases implicated in cell growth and signalling*. *Biochem. J.*, 2001. **353**(Pt 3): p. 417-39.
271. Thompson, J.J. and C.S. Williams, *Protein Phosphatase 2A in the Regulation of Wnt Signaling, Stem Cells, and Cancer*. *Genes (Basel)*, 2018. **9**(3).
272. Sontag, E., *Protein phosphatase 2A: the Trojan Horse of cellular signaling*. *Cell Signal*, 2001. **13**(1): p. 7-16.
273. Chen, J., B.L. Martin, and D.L. Brautigan, *Regulation of protein serine-threonine phosphatase type-2A by tyrosine phosphorylation*. *Science*, 1992. **257**(5074): p. 1261-4.
274. Lucas, C.M., et al., *Cancerous inhibitor of PP2A (CIP2A) at diagnosis of chronic myeloid leukemia is a critical determinant of disease progression*. *Blood*, 2011. **117**(24): p. 6660-8.
275. Guo, H. and Z. Damuni, *Autophosphorylation-activated protein kinase phosphorylates and inactivates protein phosphatase 2A*. *Proc. Natl. Acad. Sci. U. S. A.*, 1993. **90**(6): p. 2500-4.
276. Damuni, Z., H. Xiong, and M. Li, *Autophosphorylation-activated protein kinase inactivates the protein tyrosine phosphatase activity of protein phosphatase 2A*. *FEBS Lett*, 1994. **352**(3): p. 311-4.
277. Longin, S., et al., *Selection of protein phosphatase 2A regulatory subunits is mediated by the C terminus of the catalytic Subunit*. *J. Biol. Chem.*, 2007. **282**(37): p. 26971-80.
278. Chen, J., S. Parsons, and D.L. Brautigan, *Tyrosine phosphorylation of protein phosphatase 2A in response to growth stimulation and v-src transformation of fibroblasts*. *J. Biol. Chem.*, 1994. **269**(11): p. 7957-62.
279. Swingle, M., L. Ni, and R.E. Honkanen, *Small-molecule inhibitors of ser/thr protein phosphatases: specificity, use and common forms of abuse*. *Methods Mol. Biol.*, 2007. **365**: p. 23-38.
280. Kotlo, K., et al., *PR65A phosphorylation regulates PP2A complex signaling*. *PLoS ONE*, 2014. **9**(1): p. e85000.
281. Xu, Z. and B.R. Williams, *The B56alpha regulatory subunit of protein phosphatase 2A is a target for regulation by double-stranded RNA-dependent protein kinase PKR*. *Mol Cell Biol*, 2000. **20**(14): p. 5285-99.
282. Ahn, J.H., et al., *Protein kinase A activates protein phosphatase 2A by phosphorylation of the B56delta subunit*. *Proc. Natl. Acad. Sci. U. S. A.*, 2007. **104**(8): p. 2979-84.
283. Usui, H., et al., *Activation of protein phosphatase 2A by cAMP-dependent protein kinase-catalyzed phosphorylation of the 74-*

- kDa B'' (delta) regulatory subunit in vitro and identification of the phosphorylation sites.* FEBS Lett, 1998. **430**(3): p. 312-6.
284. Tolstykh, T., et al., *Carboxyl methylation regulates phosphoprotein phosphatase 2A by controlling the association of regulatory B subunits.* EMBO J., 2000. **19**(21): p. 5682-91.
285. Guenin, S., et al., *PP2A activity is controlled by methylation and regulates oncoprotein expression in melanoma cells: a mechanism which participates in growth inhibition induced by chloroethylnitrosourea treatment.* Int. J. Oncol., 2008. **32**(1): p. 49-57.
286. De Baere, I., et al., *Purification of porcine brain protein phosphatase 2A leucine carboxyl methyltransferase and cloning of the human homologue.* Biochemistry, 1999. **38**(50): p. 16539-47.
287. Lee, J., et al., *A specific protein carboxyl methyltransferase that demethylates phosphoprotein phosphatase 2A in bovine brain.* Proc Natl Acad Sci U S A, 1996. **93**(12): p. 6043-7.
288. Sontag, E., et al., *Downregulation of protein phosphatase 2A carboxyl methylation and methyltransferase may contribute to Alzheimer disease pathogenesis.* J Neuropathol Exp Neurol, 2004. **63**(10): p. 1080-91.
289. Xing, Y., et al., *Structural mechanism of demethylation and inactivation of protein phosphatase 2A.* Cell, 2008. **133**(1): p. 154-63.
290. Longin, S., et al., *An inactive protein phosphatase 2A population is associated with methyltransferase and can be re-activated by the phosphotyrosyl phosphatase activator.* Biochem J, 2004. **380**(Pt 1): p. 111-9.
291. Guo, F., et al., *Structural basis of PP2A activation by PTPA, an ATP-dependent activation chaperone.* Cell Res., 2014. **24**(2): p. 190-203.
292. Luo, Y., et al., *PTPA activates protein phosphatase-2A through reducing its phosphorylation at tyrosine-307 with upregulation of protein tyrosine phosphatase 1B.* Biochim. Biophys. Acta, 2013. **1833**(5): p. 1235-43.
293. Hombauer, H., et al., *Generation of active protein phosphatase 2A is coupled to holoenzyme assembly.* PLoS Biol, 2007. **5**(6): p. e155.
294. Stanevich, V., et al., *The structural basis for tight control of PP2A methylation and function by LCMT-1.* Mol. Cell, 2011. **41**(3): p. 331-42.
295. Bai, J., et al., *Tumor suppression and potentiation by manipulation of pp32 expression.* Oncogene, 2001. **20**(17): p. 2153-60.
296. Sangodkar, J., et al., *All roads lead to PP2A: exploiting the therapeutic potential of this phosphatase.* Febs J, 2016. **283**(6): p. 1004-24.
297. Adachi, Y., G.N. Pavlakis, and T.D. Copeland, *Identification of in vivo phosphorylation sites of SET, a nuclear phosphoprotein*

- encoded by the translocation breakpoint in acute undifferentiated leukemia.* FEBS Lett, 1994. **340**(3): p. 231-5.
298. Christensen, D.J., et al., *SET oncoprotein overexpression in B-cell chronic lymphocytic leukemia and non-Hodgkin lymphoma: a predictor of aggressive disease and a new treatment target.* Blood, 2011. **118**(15): p. 4150-8.
299. Leopoldino, A.M., et al., *SET protein accumulates in HNSCC and contributes to cell survival: antioxidant defense, Akt phosphorylation and AVOs acidification.* Oral Oncol, 2012. **48**(11): p. 1106-13.
300. Cristobal, I., et al., *Deregulation of the PP2A inhibitor SET shows promising therapeutic implications and determines poor clinical outcome in patients with metastatic colorectal cancer.* Clin Cancer Res, 2015. **21**(2): p. 347-56.
301. Almeida, L.O., et al., *Accumulated SET protein up-regulates and interacts with hnRNPK, increasing its binding to nucleic acids, the Bcl-xS repression, and cellular proliferation.* Biochem Biophys Res Commun, 2014. **445**(1): p. 196-202.
302. Kandilci, A., E. Mientjes, and G. Grosveld, *Effects of SET and SET-CAN on the differentiation of the human promonocytic cell line U937.* Leukemia, 2004. **18**(2): p. 337-40.
303. Li, M., H. Guo, and Z. Damuni, *Purification and characterization of two potent heat-stable protein inhibitors of protein phosphatase 2A from bovine kidney.* Biochemistry, 1995. **34**(6): p. 1988-96.
304. Arnaud, L., et al., *Mechanism of inhibition of PP2A activity and abnormal hyperphosphorylation of tau by I2(PP2A)/SET.* FEBS Lett, 2011. **585**(17): p. 2653-9.
305. Zhou, X., et al., *PROTOCADHERIN 7 Acts through SET and PP2A to Potentiate MAPK Signaling by EGFR and KRAS during Lung Tumorigenesis.* Cancer Res, 2017. **77**(1): p. 187-197.
306. Irie, A., et al., *Phosphorylation of SET protein at Ser171 by protein kinase D2 diminishes its inhibitory effect on protein phosphatase 2A.* PLoS ONE, 2012. **7**(12): p. e51242.
307. Takasaki, T., et al., *More than Just an Immunosuppressant: The Emerging Role of FTY720 as a Novel Inducer of ROS and Apoptosis.* Oxid Med Cell Longev, 2018. **2018**: p. 4397159.
308. De Palma, R.M., et al., *The NMR-based characterization of the FTY720-SET complex reveals an alternative mechanism for the attenuation of the inhibitory SET-PP2A interaction.* FASEB J, 2019. **33**(6): p. 7647-7666.
309. Kauko, O., et al., *Phosphoproteome and drug-response effects mediated by the three protein phosphatase 2A inhibitor proteins CIP2A, SET, and PME-1.* J. Biol. Chem., 2020. **295**(13): p. 4194-4211.
310. Come, C., et al., *CIP2A is associated with human breast cancer aggressivity.* Clin. Cancer Res., 2009. **15**(16): p. 5092-100.

311. Dong, Q.Z., et al., *CIP2A is overexpressed in non-small cell lung cancer and correlates with poor prognosis*. *Ann Surg Oncol*, 2011. **18**(3): p. 857-65.
312. Khanna, A., et al., *MYC-dependent regulation and prognostic role of CIP2A in gastric cancer*. *J Natl Cancer Inst*, 2009. **101**(11): p. 793-805.
313. Wang, J., et al., *Oncoprotein CIP2A is stabilized via interaction with tumor suppressor PP2A/B56*. *EMBO Rep.*, 2017. **18**(3): p. 437-450.
314. Junttila, M.R., et al., *CIP2A inhibits PP2A in human malignancies*. *Cell*, 2007. **130**(1): p. 51-62.
315. Puustinen, P., et al., *CIP2A oncoprotein controls cell growth and autophagy through mTORC1 activation*. *J. Cell Biol.*, 2014. **204**(5): p. 713-27.
316. Puustinen, P. and M. Jaattela, *KIAA1524/CIP2A promotes cancer growth by coordinating the activities of MTORC1 and MYC*. *Autophagy*, 2014. **10**(7): p. 1352-4.
317. Liu, C.Y., et al., *Targeting SET to restore PP2A activity disrupts an oncogenic CIP2A-feedforward loop and impairs triple negative breast cancer progression*. *EBioMedicine*, 2019. **40**: p. 263-275.
318. Inui, S., et al., *Molecular cloning of a cDNA clone encoding a phosphoprotein component related to the Ig receptor-mediated signal transduction*. *J. Immunol.*, 1995. **154**(6): p. 2714-23.
319. Inui, S., et al., *Ig receptor binding protein 1 (alpha4) is associated with a rapamycin-sensitive signal transduction in lymphocytes through direct binding to the catalytic subunit of protein phosphatase 2A*. *Blood*, 1998. **92**(2): p. 539-46.
320. Nanahoshi, M., et al., *Regulation of protein phosphatase 2A catalytic activity by alpha4 protein and its yeast homolog Tap42*. *Biochem Biophys Res Commun*, 1998. **251**(2): p. 520-6.
321. Nien, W.L., et al., *Overexpression of the mTOR alpha4 phosphoprotein activates protein phosphatase 2A and increases Stat1alpha binding to PIAS1*. *Mol. Cell. Endocrinol.*, 2007. **263**(1-2): p. 10-7.
322. Kong, M., et al., *Alpha4 is an essential regulator of PP2A phosphatase activity*. *Mol. Cell*, 2009. **36**(1): p. 51-60.
323. Hornbeck, P.V., et al., *PhosphoSitePlus, 2014: mutations, PTMs and recalibrations*. *Nucleic Acids Res.*, 2015. **43**(Database issue): p. D512-20.
324. Beresford, P.J., et al., *Recombinant human granzyme A binds to two putative HLA-associated proteins and cleaves one of them*. *Proc Natl Acad Sci U S A*, 1997. **94**(17): p. 9285-90.
325. Vaesen, M., et al., *Purification and characterization of two putative HLA class II associated proteins: PHAPI and PHAPII*. *Biol. Chem. Hoppe. Seyler*, 1994. **375**(2): p. 113-26.
326. Bialojan, C. and A. Takai, *Inhibitory effect of a marine-sponge toxin, okadaic acid, on protein phosphatases. Specificity and kinetics*. *Biochem. J.*, 1988. **256**(1): p. 283-90.



327. Louzao, M.C., M.R. Vieytes, and L.M. Botana, *Effect of okadaic acid on glucose regulation*. *Mini Rev Med Chem*, 2005. **5**(2): p. 207-15.
328. Tachibana, K., et al., *Okadaic acid, a cytotoxic polyether from two marine sponges of the genus Halichondria*. *J Am Chem Soc*, 1981. **103**(9): p. 2469-2471.
329. Murakami, Y., Y. Oshima, and T. Yasumoto, *Identification of okadaic acid as a toxic component of a marine dinoflagellate *Prorocentrum lima**. *Nippon Suisan Gakkaishi*, 1982. **48**(1): p. 69-72.
330. Valdíglesias, V., et al., *Okadaic acid: more than a diarrheic toxin*. *Mar Drugs*, 2013. **11**(11): p. 4328-49.
331. Vilarino, N., et al., *Human Poisoning from Marine Toxins: Unknowns for Optimal Consumer Protection*. *Toxins (Basel)*, 2018. **10**(8): p. 324.
332. Vieira, A.C., et al., *Oral toxicity of okadaic acid in mice: study of lethality, organ damage, distribution and effects on detoxifying gene expression*. *Toxins (Basel)*, 2013. **5**(11): p. 2093-108.
333. Fujiki, H., et al., *Mechanisms of action of okadaic acid class tumor promoters on mouse skin*. *Environ Health Perspect*, 1991. **93**: p. 211-4.
334. Valdíglesias, V., et al., *Okadaic acid induces morphological changes, apoptosis and cell cycle alterations in different human cell types*. *J Environ Monit*, 2011. **13**(6): p. 1831-40.
335. Hanana, H., et al., *Effect of okadaic acid on cultured clam heart cells: involvement of MAPkinase pathways*. *Biol Open*, 2012. **1**(12): p. 1192-9.
336. Dietrich, J., et al., *The marine biotoxin okadaic acid affects intestinal tight junction proteins in human intestinal cells*. *Toxicol In Vitro*, 2019. **58**: p. 150-160.
337. Takahashi, K., E. Nakajima, and K. Suzuki, *Involvement of protein phosphatase 2A in the maintenance of E-cadherin-mediated cell-cell adhesion through recruitment of IQGAP1*. *J. Cell. Physiol.*, 2006. **206**(3): p. 814-20.
338. Nunbhakdi-Craig, V., et al., *Protein phosphatase 2A associates with and regulates atypical PKC and the epithelial tight junction complex*. *J. Cell Biol.*, 2002. **158**(5): p. 967-78.
339. Hong, C.S., et al., *LB100, a small molecule inhibitor of PP2A with potent chemo- and radio-sensitizing potential*. *Cancer Biol Ther*, 2015. **16**(6): p. 821-33.
340. Lee, M. and J.S. Lee, *Exploiting tumor cell senescence in anticancer therapy*. *BMB Rep*, 2014. **47**(2): p. 51-9.
341. Chung, V., et al., *Safety, Tolerability, and Preliminary Activity of LB-100, an Inhibitor of Protein Phosphatase 2A, in Patients with Relapsed Solid Tumors: An Open-Label, Dose Escalation, First-in-Human, Phase I Trial*. *Clin Cancer Res*, 2017. **23**(13): p. 3277-3284.

342. Ho, W.S., et al., *Pharmacologic inhibition of protein phosphatase-2A achieves durable immune-mediated antitumor activity when combined with PD-1 blockade*. Nat. Commun., 2018. **9**(1): p. 2126.
343. Gordon, I.K., et al., *Protein Phosphatase 2A Inhibition with LB100 Enhances Radiation-Induced Mitotic Catastrophe and Tumor Growth Delay in Glioblastoma*. Mol. Cancer Ther., 2015. **14**(7): p. 1540-1547.
344. Farrington, C.C., et al., *Protein phosphatase 2A activation as a therapeutic strategy for managing MYC-driven cancers*. J Biol Chem, 2020. **295**(3): p. 757-770.
345. Fujita, T., et al., *Fungal metabolites. Part 11. A potent immunosuppressive activity found in Isaria sinclairii metabolite*. J Antibiot (Tokyo), 1994. **47**(2): p. 208-15.
346. Kahan, B.D., *FTY720: from bench to bedside*. Transplant Proc, 2004. **36**(2 Suppl): p. 531S-543S.
347. Kharel, Y., et al., *Sphingosine kinase 2 is required for modulation of lymphocyte traffic by FTY720*. J Biol Chem, 2005. **280**(44): p. 36865-72.
348. Payne, S.G., et al., *The immunosuppressant drug FTY720 inhibits cytosolic phospholipase A2 independently of sphingosine-1-phosphate receptors*. Blood, 2007. **109**(3): p. 1077-85.
349. Ingwersen, J., et al., *Fingolimod in multiple sclerosis: mechanisms of action and clinical efficacy*. Clin Immunol, 2012. **142**(1): p. 15-24.
350. Perrotti, D. and P. Neviani, *Protein phosphatase 2A: a target for anticancer therapy*. Lancet Oncol, 2013. **14**(6): p. e229-38.
351. Neviani, P., et al., *FTY720, a new alternative for treating blast crisis chronic myelogenous leukemia and Philadelphia chromosome-positive acute lymphocytic leukemia*. J. Clin. Invest., 2007. **117**(9): p. 2408-21.
352. Kastrinsky, D.B., et al., *Reengineered tricyclic anti-cancer agents*. Bioorg Med Chem, 2015. **23**(19): p. 6528-34.
353. Jaszczyszyn, A., et al., *Chemical structure of phenothiazines and their biological activity*. Pharmacol Rep, 2012. **64**(1): p. 16-23.
354. Gutierrez, A., et al., *Phenothiazines induce PP2A-mediated apoptosis in T cell acute lymphoblastic leukemia*. J. Clin. Invest., 2014. **124**(2): p. 644-55.
355. Sangodkar, J., et al., *Activation of tumor suppressor protein PP2A inhibits KRAS-driven tumor growth*. J Clin Invest, 2017. **127**(6): p. 2081-2090.
356. McClinch, K., et al., *Small-Molecule Activators of Protein Phosphatase 2A for the Treatment of Castration-Resistant Prostate Cancer*. Cancer Res, 2018. **78**(8): p. 2065-2080.
357. Yang, C.S., et al., *Ligand binding to the androgen receptor induces conformational changes that regulate phosphatase interactions*. Mol Cell Biol, 2007. **27**(9): p. 3390-404.

358. Pateraki, I., et al., *Total biosynthesis of the cyclic AMP booster forskolin from Coleus forskohlii*. *Elife*, 2017. **6**.
359. Insel, P.A. and R.S. Ostrom, *Forskolin as a tool for examining adenylyl cyclase expression, regulation, and G protein signaling*. *Cell Mol Neurobiol*, 2003. **23**(3): p. 305-14.
360. Cristobal, I., et al., *Activation of the Tumor Suppressor PP2A Emerges as a Potential Therapeutic Strategy for Treating Prostate Cancer*. *Mar Drugs*, 2015. **13**(6): p. 3276-86.
361. Neviani, P., et al., *The tumor suppressor PP2A is functionally inactivated in blast crisis CML through the inhibitory activity of the BCR/ABL-regulated SET protein*. *Cancer Cell*, 2005. **8**(5): p. 355-68.
362. Carter, J. and P. Tadi, *Erlotinib*. 2020, StatPearls Publishing : Treasure Island (FL).
363. Yu, H.C., et al., *Inhibition of CIP2A determines erlotinib-induced apoptosis in hepatocellular carcinoma*. *Biochem. Pharmacol.*, 2013. **85**(3): p. 356-66.
364. Huether, A., et al., *Erlotinib induces cell cycle arrest and apoptosis in hepatocellular cancer cells and enhances chemosensitivity towards cytostatics*. *J Hepatol*, 2005. **43**(4): p. 661-9.
365. Bradford, M.M., *A rapid and sensitive method for the quantitation of microgram quantities of protein utilizing the principle of protein-dye binding*. *Anal Biochem*, 1976. **72**: p. 248-54.
366. Sun, L., et al., *Tristetraprolin (TTP)-14-3-3 complex formation protects TTP from dephosphorylation by protein phosphatase 2a and stabilizes tumor necrosis factor-alpha mRNA*. *J Biol Chem*, 2007. **282**(6): p. 3766-77.
367. Sharma, A., et al., *Trichostatin-A modulates claudin-1 mRNA stability through the modulation of Hu antigen R and tristetraprolin in colon cancer cells*. *Carcinogenesis*, 2013. **34**(11): p. 2610-21.
368. Ogilvie, R.L., et al., *Tristetraprolin mediates interferon-gamma mRNA decay*. *J Biol Chem*, 2009. **284**(17): p. 11216-23.
369. Deleault, K.M., S.J. Skinner, and S.A. Brooks, *Tristetraprolin regulates TNF TNF-alpha mRNA stability via a proteasome dependent mechanism involving the combined action of the ERK and p38 pathways*. *Mol Immunol*, 2008. **45**(1): p. 13-24.
370. Newman, R., J. McHugh, and M. Turner, *RNA binding proteins as regulators of immune cell biology*. *Clin Exp Immunol*, 2016. **183**(1): p. 37-49.
371. Weksler, B., I.A. Romero, and P.O. Couraud, *The hCMEC/D3 cell line as a model of the human blood brain barrier*. *Fluids Barriers CNS*, 2013. **10**(1): p. 16.
372. Duong, C.N. and D. Vestweber, *Mechanisms Ensuring Endothelial Junction Integrity Beyond VE-Cadherin*. *Front Physiol*, 2020. **11**: p. 519.

373. Casey, G., *Association of PP2A and VE-cadherin in a mono and co-culture with implications on brain microvascular permeability*, in *School of Medicine 2019*, Trinity College Dublin.
374. Gabel, S., et al., *Protein phosphatases 1 and 2A maintain endothelial cells in a resting state, limiting the motility that is needed for the morphogenic process of angiogenesis*. *Otolaryngol Head Neck Surg*, 1999. **121**(4): p. 463-8.
375. Greene, C., et al., *Dose-dependent expression of claudin-5 is a modifying factor in schizophrenia*. *Mol Psychiatry*, 2018. **23**(11): p. 2156-2166.
376. Argaw, A.T., et al., *VEGF-mediated disruption of endothelial CLN-5 promotes blood-brain barrier breakdown*. *Proc Natl Acad Sci U S A*, 2009. **106**(6): p. 1977-82.
377. Blecharz, K.G., et al., *Glucocorticoid effects on endothelial barrier function in the murine brain endothelial cell line cEND incubated with sera from patients with multiple sclerosis*. *Mult Scler*, 2010. **16**(3): p. 293-302.
378. Schuhmann, M.K., et al., *Fingolimod (FTY720-P) Does Not Stabilize the Blood-Brain Barrier under Inflammatory Conditions in an in Vitro Model*. *Int. J. Mol. Sci.*, 2015. **16**(12): p. 29454-66.
379. Schwartz, L., et al., *Hyperosmotic stress contributes to mouse colonic inflammation through the methylation of protein phosphatase 2A*. *Am J Physiol Gastrointest Liver Physiol*, 2008. **295**(5): p. G934-41.
380. Heneka, M.T., et al., *Neuroinflammation in Alzheimer's disease*. *Lancet Neurol*, 2015. **14**(4): p. 388-405.
381. Park, H.J., et al., *Protein Phosphatase 2A and Its Methylation Modulating Enzymes LCMT-1 and PME-1 Are Dysregulated in Tauopathies of Progressive Supranuclear Palsy and Alzheimer Disease*. *J Neuropathol Exp Neurol*, 2018. **77**(2): p. 139-148.
382. Clancy, S. and W. Brown, *Translation: DNA to mRNA to Protein* Nature Education 2008: p. 101.
383. Hunter, M., et al., *Optimization of Protein Expression in Mammalian Cells*. *Curr Protoc Protein Sci*, 2019. **95**(1): p. e77.
384. Koussounadis, A., et al., *Relationship between differentially expressed mRNA and mRNA-protein correlations in a xenograft model system*. *Sci Rep*, 2015. **5**(1): p. 10775.
385. Perl, K., et al., *Reduced changes in protein compared to mRNA levels across non-proliferating tissues*. *BMC Genomics*, 2017. **18**(1): p. 305.
386. Maier, T., M. Guell, and L. Serrano, *Correlation of mRNA and protein in complex biological samples*. *FEBS Lett*, 2009. **583**(24): p. 3966-73.
387. Gu, S. and M.A. Kay, *How do miRNAs mediate translational repression?* *Silence*, 2010. **1**(1): p. 11.

388. Vogel, C. and E.M. Marcotte, *Insights into the regulation of protein abundance from proteomic and transcriptomic analyses*. Nat Rev Genet, 2012. **13**(4): p. 227-32.
389. Herman, A.B. and M.V. Autieri, *Inflammation-regulated mRNA stability and the progression of vascular inflammatory diseases*. Clin Sci (Lond), 2017. **131**(22): p. 2687-2699.
390. Ross, J., *mRNA stability in mammalian cells*. Microbiol Rev, 1995. **59**(3): p. 423-50.
391. Yang, H., J.N. Rao, and J.Y. Wang, *Posttranscriptional Regulation of Intestinal Epithelial Tight Junction Barrier by RNA-binding Proteins and microRNAs*. Tissue Barriers, 2014. **2**(1): p. e28320.
392. Ye, D., et al., *MicroRNA regulation of intestinal epithelial tight junction permeability*. Gastroenterology, 2011. **141**(4): p. 1323-33.
393. Mahtani, K.R., et al., *Mitogen-activated protein kinase p38 controls the expression and posttranslational modification of tristetraprolin, a regulator of tumor necrosis factor alpha mRNA stability*. Mol Cell Biol, 2001. **21**(19): p. 6461-9.
394. Rahman, M.M., et al., *Basal protein phosphatase 2A activity restrains cytokine expression: role for MAPKs and tristetraprolin*. Sci Rep, 2015. **5**: p. 10063.
395. Tohme, R., et al., *Direct activation of PP2A for the treatment of tyrosine kinase inhibitor-resistant lung adenocarcinoma*. JCI insight, 2019. **4**(4).